Aerodynamic Test Platform for Human Powered Vehicle (HPV)

Dr. Kim Shollenberger

Cal Poly Human Powered Vehicle Club

Dr. John Ridgely, Advisor

TEAM ANEMOI

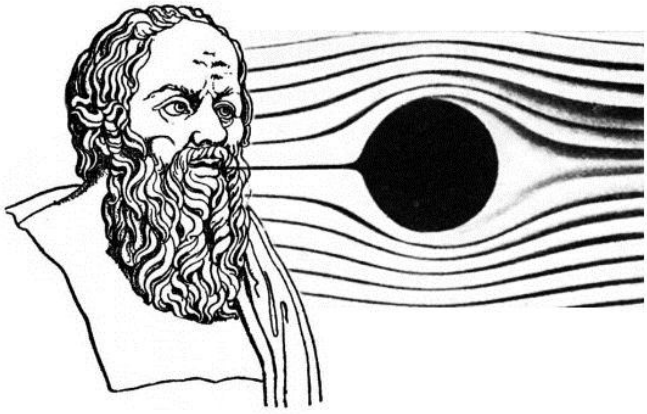

Spencer Wangerin
swangeri@calpoly.edu
206-612-7782

Spencer Lillywhite
slillywh@calpoly.edu
916-337-7850

Colburn Davis
cdavis07@calpoly.edu
360-951-1025

Statement of Disclaimer

This project is a result of a class assignment; therefore it has been graded and accepted as fulfillment of the course requirements. Acceptance does not imply technical accuracy or reliability. Any use of the information in this report is done at the risk of the user. These risks may include catastrophic failure of the device or infringement of patent or copyright laws. California Polytechnic State University at San Luis Obispo and its staff cannot be held liable for any use or misuse of the project.

Table of Contents

List of Tables

List of Figures

Executive Summary

The Aerodynamic Test Platform (ATP) for the Cal Poly HPV Club is a system that was designed by Cal Poly mechanical engineering students to measure aerodynamic characteristics of a human-powered vehicle (HPV). The HPV team desired a system that could quantify the lift, drag, and other aerodynamic qualities of a full scale HPV at various orientations in oncoming airflow. Established methods for determining aerodynamic characteristics include computational fluid dynamics (CFD) and wind tunnel testing of scaled models. The ATP was devised to simulate the test results given by a full-scale wind tunnel without requiring a wind tunnel large enough to test a full-size HPV. The basic premise was that the HPV could be mounted to the ATP and located on the roof of a motor vehicle and driven through still air to approximate the oncoming airflow present in the wind tunnel.

The project sponsor and design team agreed upon a list of full specifications including size, function, durability, and usability. The primary goal of the system was to safely attach an HPV to the roof of the van and measure lift and drag. A budget of $2000.00 was specified for the project. The vehicle was chosen to be the Cal Poly ME department van. Many different concepts and designs were developed in parallel with preliminary testing and calculation of the distortion of the airflow field around the van. A small scale model was made out of wood to better understand the geometry of the structure and its eventual ability to resist vibration. Ultimately an ATP design was determined which could provide the different orientations specified by the sponsor and reasonably obtain the desired results. The system would draw primarily on load cells fitted with strain gauges to measure the aerodynamic forces.

With the design of ATP established, components were sized relative to a worst-case loading condition, in part associated with a 30 mph crosswind. Each part was meticulously considered in sizing calculations due to the dangers posed to other drivers in the event of a system failure. Hand calculations of simplified loading cases and large factors of safety led to initial sizes of parts. Next, finite element analysis was performed critical system components to further verify the hand analysis. The effects of noise due to road vibrations (pot holes, uneven road, etc.) vibrations (pot holes, uneven road, etc.) in the lift and drag signals was investigated. An accelerometer was attached to the roof of the van and the recorded accelerations were used as inputs into a transient finite element analysis. The analysis suggested that road noise would not noticeably distort the strains being measured in the load cells.

With the parts satisfactorily sized, they were purchased from various suppliers including local steel suppliers, hardware stores, and some specialty online business. Manufacturing was split up according to familiarity with design and manufacturing capability of each team member. Most of the manufacturing processes consisted of cutting to raw materials to length, machining assorted holes and notches, and welding. The system was completely built in a few weeks of fabrication. Previously established safety tests, such as verifying that the system could handle the worst-case design loads without failure, were implemented. Strain gauges were attached at the necessary locations of the load cells. Due to a lack of access to a more sophisticated circuit board, a crude data acquisition system was employed with a spring scale to measure the output signal of individual strain gauge bridges over a drag force range of 0 to 30 N. The data acquisition system clearly measured a change in the signal under the test loads, proving strain could be accurately measured in the load cells. The system was delivered to the HPV club and once calibrated, will be ready for use.

Chapter 1 — Introduction

The Aerodynamic Test Platform (ATP) for the Cal Poly Human Powered Vehicle (HPV) project will support experimentation and implementation of future HPV designs. The HPV Club enters their latest fully-faired bicycle design in the annual American Society of Mechanical Engineers (ASME) HPV competition, competing in the design, drag, utility, and speed endurance events. Cal Poly students have built a reputation of outstanding performance and established themselves as one of the teams to beat at the competition.

Sponsor Background

The HPV Club advisor, Dr. Kim Shollenberger, has proposed this project to obtain full-scale aerodynamic test results of different HPV designs without the use of a large-scale wind tunnel (which is not available on the Cal Poly campus). The ATP will offer final testing of a vehicle, including lift and drag measurements of the entire assembly. As a substitute to wind tunnel testing, this device will mount to a car roof rack such that lift and drag measurements can be taken at a variety of velocities and angles of attack. Additionally, the HPV Club requires provisions for flow visualization over the body of the entire assembly. With this data, the club will document past and current performance and design future HPVs.

Objectives and Problem Definition

We have accepted the challenges of designing, building, and testing the ATP for the Cal Poly HPV Club. Our goals include satisfying all needs of the club: providing a means for full-scale aerodynamic testing of different HPV designs without the use of a larger and externally contracted wind tunnel. We will provide a platform for the Cal Poly HPV club to accurately obtain lift and drag measurements of multiple fairing designs at a variety of spatial orientations, including a means of flow visualization with onboard cameras. Additionally, we hope to simulate ground effects, wheel pumping, and provide measures of side forces and 3-axis moments. Moreover, our goals for this design consist of mounting to the Cal Poly Mechanical Engineering Department's Ford E-350 van, and being easily assembled and transported by one or two club members.

Specification Development

The engineering specifications found in Table 1 were developed based on Quality Function Deployment (QFD) analysis, shown in Appendix A. Instructions for interpreting the QFD results follow in the same appendix.

There are several distinct benefits arising from our QFD analysis. First and foremost, we were able to generate engineering specifications with a high correlation to each of the Cal Poly HPV Club's expressed needs. By identifying these specific targets, we also developed additional specifications that relate to both the customer needs and initial specifications. Furthermore, constructing a House of Quality led us to fully consider our competition's ability to satisfy HPV club needs. In this way, we have a much better idea of what concepts to combine and implement on the ATP.

The table of engineering requirements for the ATP is included in Table 1. The "Risk" column describes the difficulty in meeting each of the targets listed. High (H), Medium (M), or Low (L) designations are included for each specification. Also, a summary of how each target is met is included in the "Compliance" column. In order to evaluate the effectiveness of the ATP, each specification may require Analysis (A), Testing (T), a comparison or Similarity to Existing Design (S), and/or mere Inspection (I). Finally, to better understand how the engineering specifications were developed, each individual specification's source is described with a series of symbols in the rightmost column.

Table 1. Aerodynamic Test Platform for Cal Poly HPV Club list of engineering requirements.

Specification #	Parameter Description	Requirement or Target	Tolerance	Risk	Compliance	Source
1	Vehicle speed	65 mph	Min	L	A, T	α
2	Measure lift force	100 lbf	Min	M	T	α
3	Measure drag force	100 lbf	Min	L	T	α
4	Pitch fairing	10°	Min	L	I	α
5	Roll fairing	45°	Min	L	I	α
6	Wheelbase compatibility range	36 to 60 in	Range	M	T, S, I	β
7	Frame/dropout compatibility range	3 to 6 in	Range	M	T, S, I	β
8	Minimum weight support	100 lbf	Min	M	A, T	δ
9	Height of system [with van]	14 ft	Max	M	I	γ
10	Width of system [with van]	8.5 ft	Max	M	I	γ
11	Length of system [with van]	40 ft	Max	L	I	γ
12	Total cost	$2000.00	Max	M	S, I	α
13	Flow visualizer density	1 units/sq. ft	Min	L	I	δ
14	Number of camera views	1 view	Min	L	S, I	β
16	Wheels touch ground	no	N/A	L	I	α
17	Total weight	200 lbf	Max	L	A, T, S	δ
18	Chip van paint	no	N/A	M	T, I	δ
19	Holes in van roof	no	N/A	L	S, I	δ
20	Withstand crosswind	30 mph	Min	M	A,T	δ
21	Mounts on Ford E-350 roof rack	yes	N/A	L	T, I	α
22	Model ground effects	yes	N/A	H	A, T, I	β
23	Model wheel pumping effects	yes	N/A	H	A, T, I	β
24	Measure side forces	100 lbf	Min	M	T, S	δ
25	Measure moments	100 ft-lbf	Max	H	T, S	δ
26	Packing volume	90 cu. ft	Max	M	A, I	δ
27	Time to install	30 min	Max	M	T, S	δ
28	Yaw fairing	30°	Min	L	I	α
29	Fatigue life	1000 hrs	Min	L	A	δ
$^{\alpha}$ Directly dictated customer requirement						
$^{\beta}$ Derived from HPV design reports or club recommendation						
$^{\gamma}$ Developed from CA-DOT laws and regulations						
$^{\delta}$ Estimated by team calculation and advisor recommendation (subject to change as design approaches completion)						

Chapter 2 — Background

This section details the results of literature searches and contextual research done by our team. In general, several areas of interest arise in the discussion of relevant background to the design of the ATP:

- Definition and description of an HPV design
- Existing aerodynamic testing procedure
- Measurement and calculation methods for aerodynamic loads
- Object pitch, yaw, and roll methods
- California state highway law

These are each discussed in more detail below.

Definition and Description of an HPV Design

The term "Human Powered Vehicle" is used frequently in this report, so it is important to understand exactly what is implied by its usage. In general, "HPV" refers to any means of transport that is driven by a human muscular input, without the use of other power sources. However, for the purposes of this report, HPV will be used to describe a fully-faired recumbent bicycle. An annotated schematic of a typical HPV frame with the fairing removed is shown in Figure 1. By lowering the bike's vertical profile and including a specially designed fairing, designers lower the overall drag acting on the vehicle, allowing for much higher speeds and efficiencies to be achieved over traditional bicycle designs. The fairing decreases overall drag by smoothing out the surface exposed to air flow (decreasing the magnitude of viscous shear forces associated with friction drag) and by gradually transitioning between leading and trailing frontal areas (decreasing the difference in pressure between leading and trailing surfaces associated with pressure drag). Figure 2 shows the Atlas fairing, one of Cal Poly's previous entries into the ASME competition.

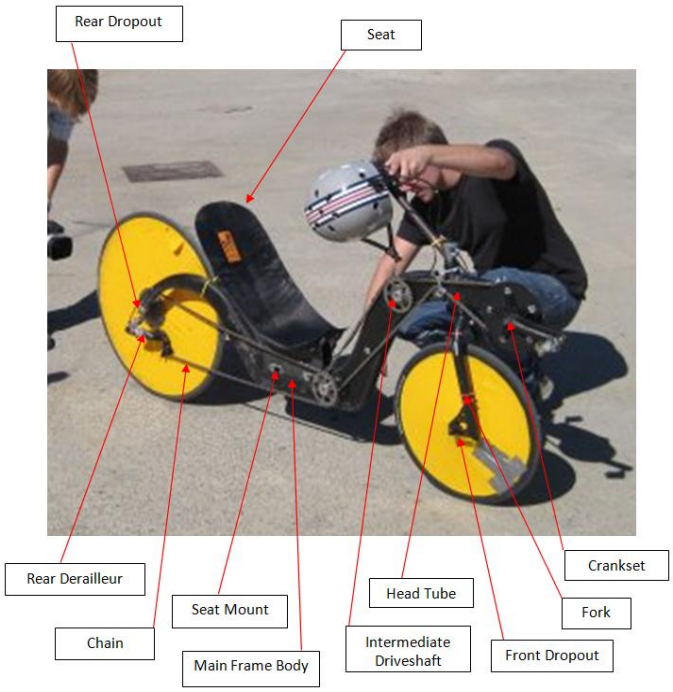

Figure 1. Schematic of typical HPV frame (Christensen et al, 2011).

Figure 2. Cal Poly's Atlas fairing with rider, mounted to the frame shown in Figure 1 (Christensen et al, 2011).

Existing Aerodynamic Testing Procedure

A number of established methods exist for the purpose of determining aerodynamic properties of a test object. This section briefly covers each type and its application to HPV design.

Wind Tunnel Testing

Wind tunnel testing represents the most commonly used and most accurate aerodynamic test procedure. The implementation of flow straighteners at the tunnel's entrance can create uniform flow with a very low (<1%) free stream turbulence intensity in the test section, allowing the flow over the model to accurately represent transitions from laminar to turbulent flow regimes. Lift, drag, and side forces, as well as pitch, roll, and yaw moments are generally measured with a wind tunnel balance, discussed in a later section. Full-scale wind tunnel testing would be the most accurate aerodynamic test method; however, wind tunnels large enough to test a full-size HPV are expensive to run. Additionally, the Cal Poly HPV Club does not have access to a large enough wind tunnel to accomplish the required testing. The HPV club's past designs have been up to 8 feet long, 5 feet tall, and 3 feet wide. According to Kyle & Weaver (2004), to accurately represent flow conditions of a full-scale aerodynamic test run, the wind tunnel would need to produce 60 mph free stream velocities in a test section 8 feet tall, 12 feet wide, and 10 feet long. Kirsten Wind Tunnel at the University of Washington Aeronautical Laboratory was used in Kyle and Weaver's investigation. For economic perspective, this wind tunnel cost $124,501 in 1934, which is equal to over $2 million today assuming an average 3.71% inflation per year.

The Cal Poly HPV team currently utilizes scaled wind tunnel testing on a 1/5 scale model. Using a wind tunnel balance, lift and drag on the model are measured and then scaled to yield approximations of the full-size vehicle. While this method seems to produce reasonable estimates, intricacies associated with full-scale fluid dynamics (including mountings between the fairing and the frame, the presence of wheels, etc.) and other errors in the scaling procedure produce significant sources of uncertainty. Specifically, Cal Poly's wind tunnel maxes out at 110 mph, which is the equivalent to only 22 mph relative to the full-scale fairing. This gives the HPV club access to only a small range of free stream velocities for lift and drag measurements, requiring extrapolation for a more complete picture, and limiting confidence in results. Furthermore, the surface of the scaled model is simply prepared with fine sanding. When applying a scaling factor, it is difficult to accurately capture a surface finish representative of the full-sized fairing's exterior, which could appreciably influence the local skin friction calculations.

Coast-down Testing

A coast down test involves bringing a vehicle up to a certain speed and letting it coast to a stop. The velocity of the vehicle is recorded throughout the test with onboard data-logging equipment. By analyzing the vehicle's deceleration over time, the rolling resistance and aerodynamic properties of the vehicle can be estimated. This is a good option because it is cheap, easy to set up, and operates in real-world conditions that may be hard to simulate with other tests, such as a moving ground plane and spinning wheels. Unfortunately, this method requires a functioning frame before a fairing can be tested. Also, running the entire system before significant aerodynamic analysis has occurred may result in unforeseen effects and/or damage to the fairing. Another issue with this method is that it is difficult to differentiate

between the effect of drag and other sources of friction on the vehicle's deceleration. Furthermore, this test provides no way to measure lift.

Captive-Carry Testing

Captive-carry testing refers to attaching a vehicle prototype to another proven vehicle in order to investigate aerodynamic and other operational properties in full-scale environments. Most commonly, this technique is used for final stage testing of air or spacecraft before attempting free flights. For example, NASA used a captive-carry technique by mounting the Enterprise space shuttle prototype to a Boeing 747 Shuttle Carrier Aircraft with all electronic systems active to rehearse crew procedures and perform some flutter analysis. However, captive-carry testing has also been applied to scaled aircraft prototypes and small unmanned aerial vehicles (UAVs) attached to the roof of a ground vehicle. In a study performed at Linköping University in Sweden, a car-top testing rig was designed and built to evaluate handling characteristics of a radio-controlled UAV (shown in Figure 3) which was used to model the Raven business jet. In this design, a calibrated aluminum frame fitted with a load cell holds up the aircraft and orients it using a 3-axis gimbal. Figure 4 shows a schematic diagram of the measurement system. This method of aerodynamic testing greatly resembles a possible solution to the HPV club's problem. However, one problem that the designers noted was a weakness to peak crosswinds in the aluminum frame. If this design of car top testing rig were modified to accommodate a full-scale HPV, it would require significant strengthening at attachment points. Furthermore, this design requires some modification to the test prototype to safely mount to the gimbal. Still, this design of car-top test rig could be reasonably modified to effectively test an HPV. It is important to note that the velocity field around a commercial motor vehicle could change the air stream velocity around the test object (HPV) if the model is

Figure 4. Captive-carry car-top test rig for Raven business jet radio-controlled model (Lundström, 2008).

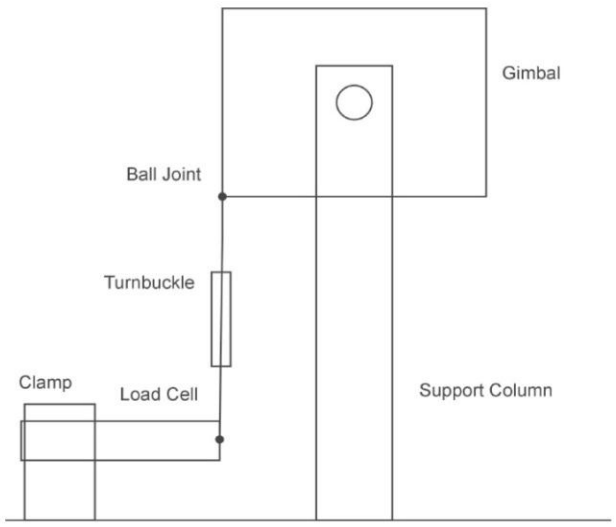

Figure 3. Schematic diagram of moment measurement system for Linköping University captive-carry test rig (Munro, 2002).

mounted too close to the vehicle's surfaces. Also, vibrations from the car can transmit through the mounting structure and create errors in the lift and drag force signals obtained experimentally with gauges. However, if these factors can be mitigated through careful and proper design, the result could approach equivalence to wind tunnel test measurements and flow quality.

Computational Fluid Dynamics (CFD)

Over the past 50 years, CFD has had an increasing role in aerodynamic testing and design. CFD uses numerical methods to obtain approximate solutions to the Navier-Stokes equations for velocity and pressure that are then used to calculate lift, drag, and other key parameters. Due to nonlinearity in the Navier-Stokes equations and imperfect turbulence models, CFD solutions may offer erroneous results in some cases. Ideally, CFD analysis should be accompanied by validation with experimental testing. The Cal Poly HPV team has used CFD analysis in past fairing design iterations, but has yet to acceptably validate the results experimentally.

Measurement and Calculation Methods for Aerodynamic Loads

A number of established methods exist for measuring and calculating aerodynamic loads. This section briefly covers each type and its application to HPV design.

Wind Tunnel Balances

Wind tunnel balances are the most commonly used method of measuring aerodynamic loads on a test object. The object is typically mounted to the balance by means of a sting or multiple struts. The aerodynamic loads on the model are transmitted to the balance, where they are measured with load cells; the most common load cells are calibrated flexures with strain gauges. A complete balance has the ability to measure lift, drag, and side forces, as well as pitch, roll, and yaw moments. There are two main types of balances; internal and external. Internal or sting balance instrumentation resides inside of the model or the balance itself, and external balance instrumentation resides outside of the wind tunnel test section and therefore can become quite large. As such, an internal balance would be most appropriate for the ATP. According to Pope and Rae's *Low Speed Wind Tunnel Testing*, many wind tunnel tests become delayed because of balance calibration or tuning. Still, despite their complexity and difficult instrumentation, wind tunnel balances provide the most accurate aerodynamic load information.

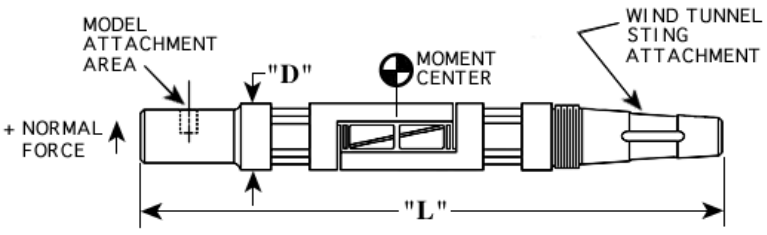

Figure 5. An internal "sting" balance schematic ("Strain Gage Wind Tunnel Balances", 2011).

On their website, the Modern Machine & Tool Company claims that their balances have accuracies between 0.1% and 0.5%. Wind tunnel balances are extremely expensive; a Triumph Aerospace Systems employee quoted an approximate price of $200,000 for their basic balance. The least expensive balance we found is produced by KineOpitics, and costs around $8,000 for the complete six component measurement capability.

Despite the complexities associated with balances, the concept of measuring aerodynamic loads directly from a model may be developed in a simplified fashion for the purposes of obtaining strictly lift and drag forces in the context of designing the ATP.

Pressure Taps

Aerodynamic loads can also be calculated by inserting pressure taps along the surface of the test object. The measured pressures at the various stream-wise tap locations are used to generate the pressure field around the object. These pressures then can be numerically integrated to produce quantities such as lift and drag. This technique is partially destructive to the test object. It requires the installation of pressure taps in the model, recording each pressure accurately during the experiment, and finally numerical calculations to obtain values for lift and drag. Drag measurements obtained using this technique may be inaccurate if the geometry of the pressure taps' orientation is insufficient to resolve the pressure field along the leading edge of the model. As such, this method is more suitable for two-dimensional (i.e. infinite wing) models.

Wake Integral Method

Aerodynamic drag on a test object within a wind tunnel is often calculated using a technique called the wake integral. Velocities at known downstream locations are measured typically using a Pitot tube in various locations including one free-stream region, through the wake region, and into the next free-stream region. By calculating the loss in momentum in the wake region, the drag on the object can be determined. Data collection and calculation of the momentum loss can be time consuming, as it is often necessary to slowly traverse pressure sensors across significant distances. While this technique does apply to both two and three-dimensional test object aerodynamic tests, a three-dimensional wake analysis is complex to conduct and difficult to accurately interpret due to the volume of data reduction. Again, this method provides no way to measure lift.

Preston Tubes

Local skin friction measurements are also worthy of note, despite the fact that they cannot measure total drag on a test object. Preston tubes, small Pitot tubes that are placed on the surface of the object, can be calibrated to yield measurements of local skin friction in a boundary layer. Also, oil film interferometry can produce equally accurate results when done in a controlled environment. These techniques are incapable of measuring total drag on a body (especially a blunt body with significant separation) and are ideally suited for applications where skin friction drag is a primary concern.

Object Pitch, Yaw, and Roll Methods

A number of designs exist which allow for changing the orientation of a specimen within a wind tunnel. Rather than seek to classify or explain all of the available designs, a single patent is described in this section for a quick reference.

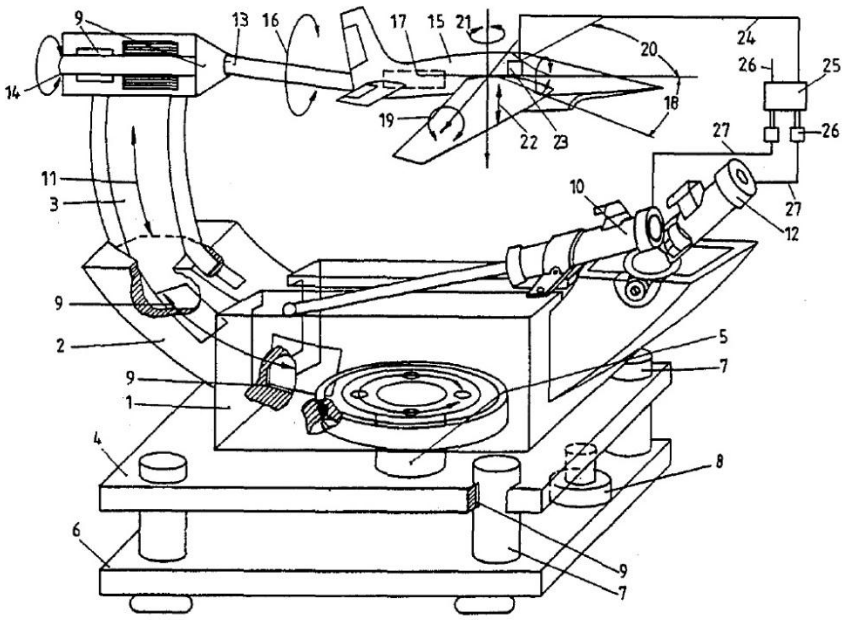

Figure 6. USP# 4,658,635 depicting a method for pitching, yawing, and rolling a test object in a wind tunnel.

United States Patent #4,658,635 issued on April 21, 1987 details a "Simulator for Aerodynamic Investigations of Models in a Wind Tunnel." According to the patent's abstract, "the simulator is equipped with a multipartite support comprising a part for the accommodation of a model. The parts of the support are arranged telescopically in the form of an approximate semicircle. Hydrostatic bearings are used as mountings." Due to the nature of the support bearings, the test object can be set at specific pitch, yaw, and roll angles while resisting oscillation resulting from the impinging air. One of the drawings associated with this patent is included in Figure 6. By investigating the methods outlined in this patent, we can adapt a similar system for orienting a HPV in the free stream regime of our ATP.

California State Highway Law

The ATP will be designed to operate within the existing highway system in the immediate vicinity of Cal Poly campus. As such, the entire setup, including the ATP and fully faired Cal Poly HPV, must conform to all California Department of Transportation vehicle codes. The most relevant for the ATP design are included in Appendix, and summarized below, taken from the California Department of Transportation website (www.dot.ca.gov).

- The total width of the vehicle may not exceed 102 inches (8.5 feet)
- The total height of the vehicle may not exceed 14 feet
- The total length of the vehicle may not exceed 40 feet
- The extension of any additional rigging may not exceed 3 inches on either side of the vehicle

Chapter 3 — Design Development

This section of the report details the results of our design process. We will discuss different aspects of the development of our final ATP design in more detail below, including a brief outline of several top concepts, and the top concept selection process.

Brief Outline of Several Top Concepts

Our team has developed several design concepts that we feel can meet and exceed the engineering specifications. Based on several design decisions resulting from analysis (described in more detail in the following section), we have selected the following promising concepts. The designs described in this section represent those that helped us arrive at our top concept. For the details of that design, refer to the "Detailed Description of Top Concept" section.

3-Axis Clamping Joint Gimbal

This design expands on the idea developed in our conceptual model (discussed in more detail later), using a pyramidal support structure to raise the HPV into an area of near-free stream airflow. The difference is that this design utilizes several threaded joints to pitch, roll, and yaw the HPV (shown in Figure 7 on the following page). The U-shaped clamps straddle a block with threaded holes, giving each the ability to tighten down in different orientations using nuts and bolts. The 3-Axis Clamping Joint Gimbal allows for a large amount of orientation freedom, but focuses all of the loads on a few critical locations and may be prone to detrimental vibration.

Discrete Pin-and-Hole Pitching Lifter

The design shown in Figure 8 on page 17 builds on the universal joint idea described above, but instead uses a discrete pin-and-hole system to pitch the HPV. Universal joints still provide the rolling motion as in the previous design, but square tubing with pinholes allow both the front and back wheels to be raised and lowered to change the HPV's pitch. Here, a quick-release pin holds the square tubes in the desired orientation and can be removed easily to make adjustments. The Discrete Pin-and-Hole Pitching Lifter loses the ability to yaw the HPV, but has the advantage of two robust supports to absorb a variety of loading conditions and limit vibration. Additionally, this design requires that orientation adjustments be made with the ATP either on the ground or by several operators lifted up to roof level.

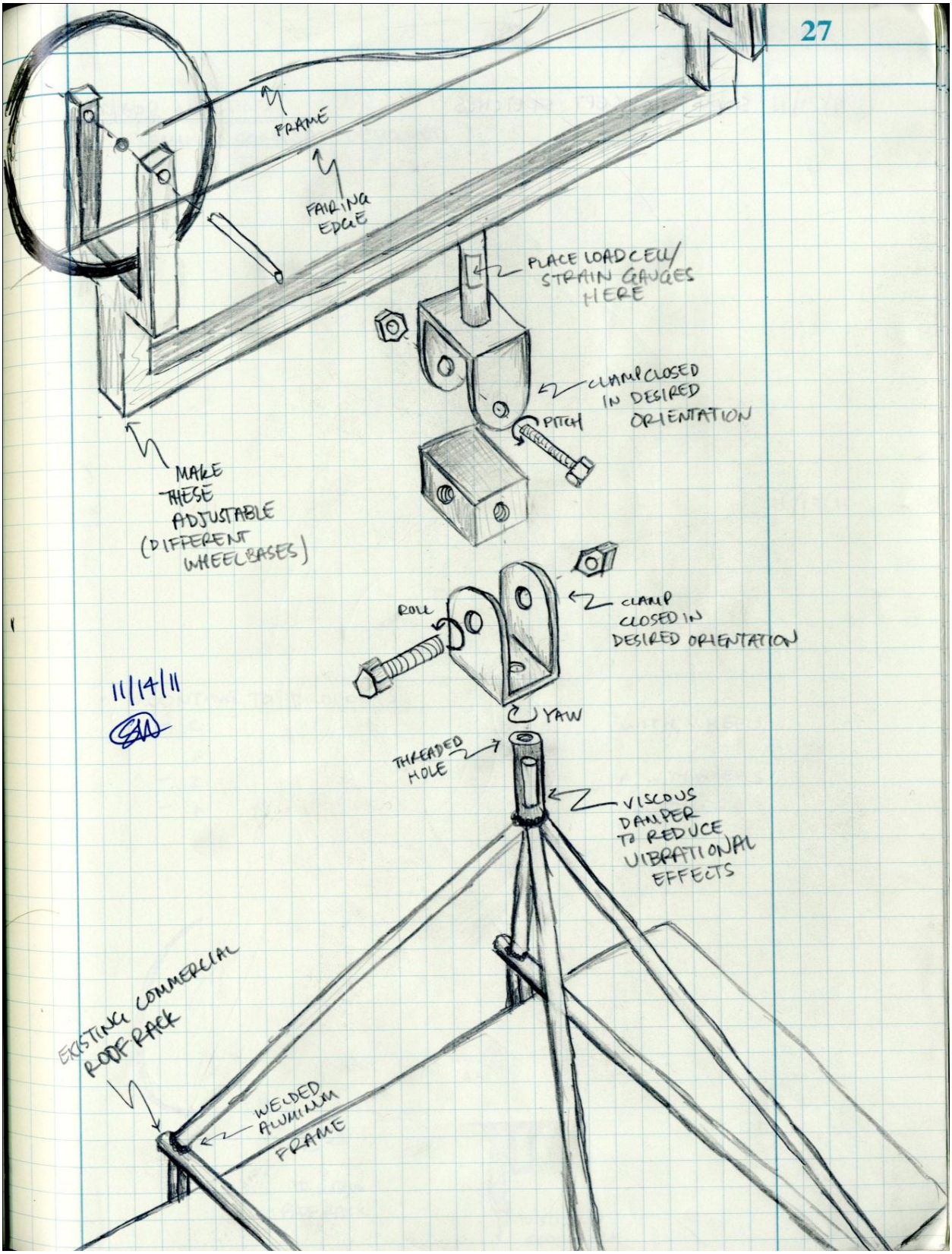

Figure 7. 3-Axis Universal Joint Gimbal design concept.

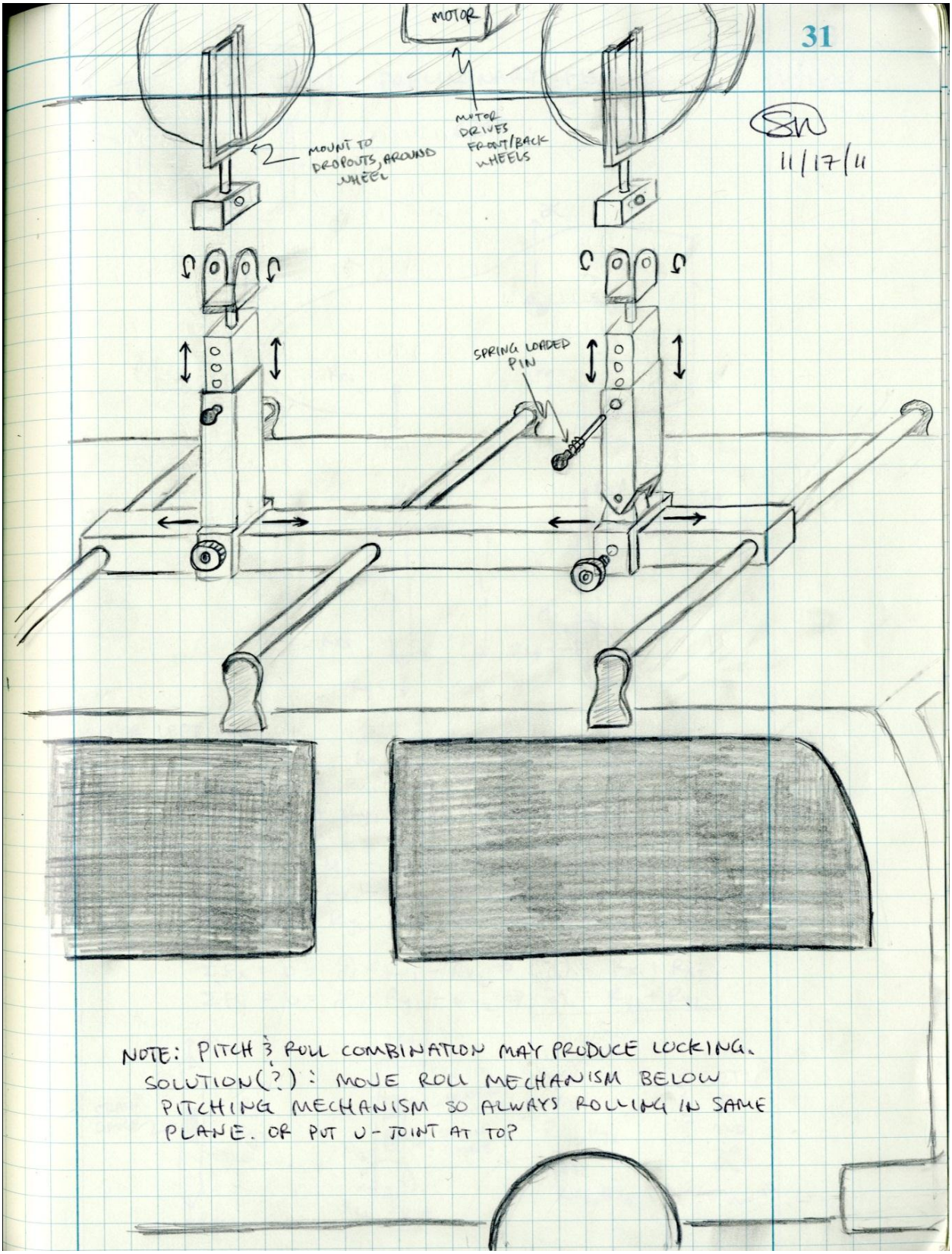

Figure 8. Discrete Pin-and-Hole Pitching Lifter design concept.

Turnbuckle Roll Support

The differentiating feature of this design is the adjustment of roll by the simultaneous adjustment of two turnbuckles attached to each support strut, as seen in Figure 10 on the following page. The turnbuckles allow for high rigidity to resist roll-wise vibration, but the adjustment process of different roll angles would be difficult with the HPV mounted. The rear support strut would have nesting square steel tubing that slides vertically and is set by either set screws or quick-release pins through holes for discrete angle adjustment. Both support struts are mounted to two horizontal rails and are free to slide allowing vehicles of different wheel bases to be mounted. Strain gauges along the support struts of the structure will provide data to determine the lift and drag on the HPV.

Top Concept Selection Process

Throughout the idea generation and concept selection process, we performed a number of experiments and engineering analyses to determine which concepts will best meet the specifications. This section provides a detailed description of these investigations, their results, and how those results were applied to selecting our top concepts.

Modeling, Experimentation, and Results

In addition to traditional pen-and-paper analysis, our team created several models and performed experiments to help guide and select our top designs. This section outlines these studies.

Conceptual Model

As a preliminary exercise to understanding scale, strength issues, and degrees of freedom in a possible ATP design similar to the 3-Axis Universal Joint Gimbal, our team built a 1/5th scale model out of basswood (shown in Figure 9). In this way, we could incorporate a rapid-prototyped model of an older HPV club fairing, and gain a more complete idea of the physical implications of their combination. One major advantage of creating this model was witnessing the problems associated with narrowing to a single support between the HPV and the van within the ATP. Without any detailed calculations, we could see that the qualitative stress in this member (associated with a large crosswind, for example) could result in a catastrophic failure without substantial strength provisions. Furthermore, we observed that this single support design allowed for multiple modes of vibration within the frame of the ATP. With the slightest perturbation, the model would oscillate for a considerable amount of time in a variety of directions. Thus, from the experience of building the con-

Figure 9. Conceptual model of one possible ATP design, constructed of basswood.

ceptual model, we were able to conclude that a two support system would limit the size and complexity of the ATP connections to the HPV, increase the ATP's robustness to crosswinds, and reduce vibration within the frame (which both improves the safety of the design and the clarity of lift and drag data).

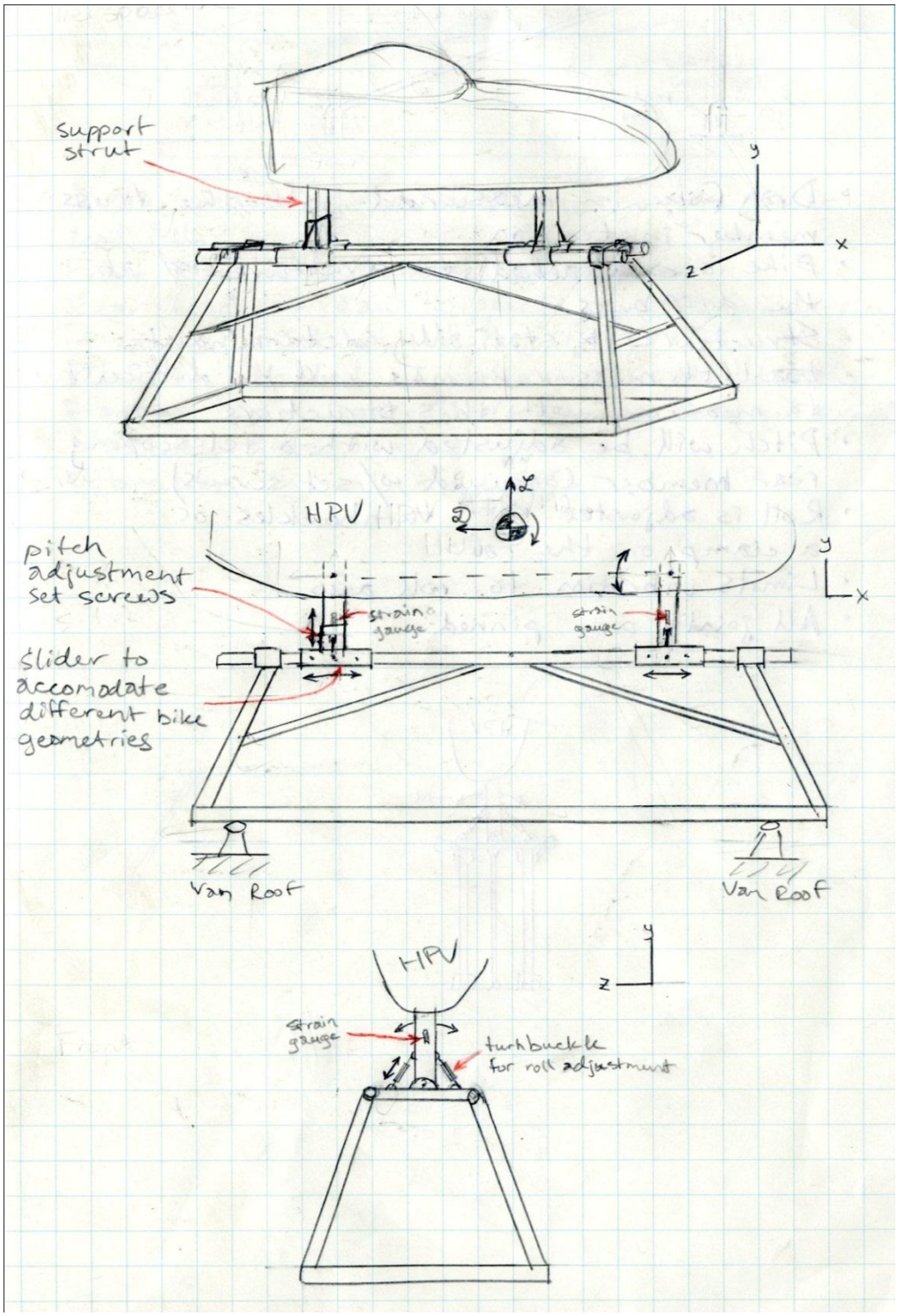

Figure 10. Turnbuckle Roll Support design concept.

Van CFD

Unfortunately, performing detailed CFD analysis on the van lies well beyond the scope of our team's abilities. However, using code obtained from the MATLAB file exchange (Jayaraman, 2006) and known dimensions of the Ford E-350 van, we were able to obtain a possible 2-D inviscid velocity vector plot of flow around the van, shown in Figure 11. Many aspects of this plot seem inaccurate, including the acceleration implied around the back of the body (this would probably be an area of separation in reality), and the non-parallel nature of the velocity vectors located well above the roof of the van (perhaps the result of 2-D solution simplification). What we can learn from these results is that the flow appears parallel and straight located close to the van's roof, especially in the middle of its length.

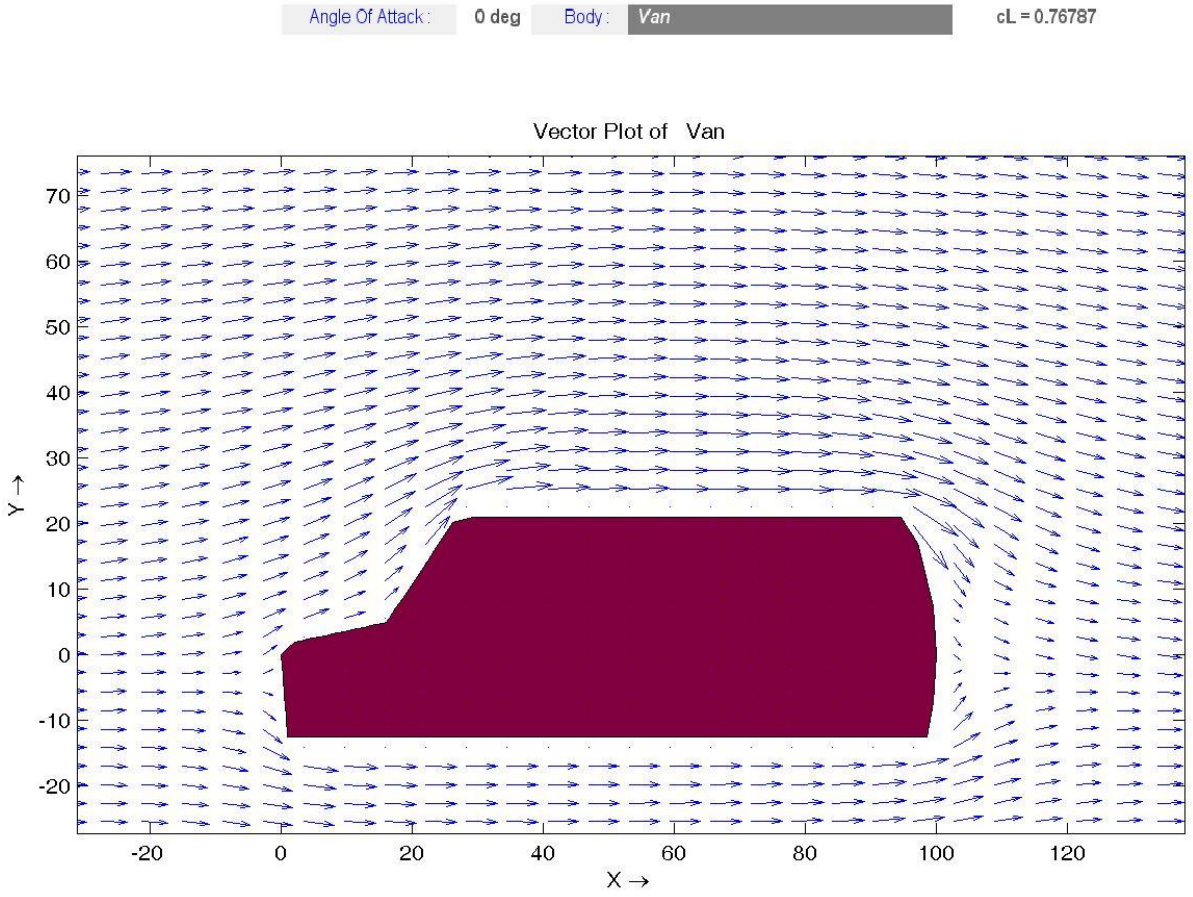

Figure 11. Panel method based 2-D inviscid potential flow velocity vector plot based on code developed by Divahar Jayaraman.

Van Flow Field Visualization

In an effort to verify the CFD analysis described above, we designed an experiment to qualitatively understand the flow field around the nose of the Ford E-350 van. By examining the behavior of flow visualization tufts above the van's roof, we sought to obtain heights at which streamlines became parallel, and therefore more closely represented free stream conditions.

The vertical tuft testing arm shown in Figure 13 consists of several metal rods welded onto a frame of square tubing. We fitted one long, vertical rod with an aerodynamic aluminum cover, which we in turn covered with 2 inch strands of string spaced 3 inches apart. The overall height of this rig is 59.5 inches. We secured the tuft array against severe vibration using fishing line connecting the top of the vertical rod with each of the four corners of the square base. We mounted this rig to the front roof of the van using nylon straps, shown in Figure 12. In order to gain a qualitative understanding of the flow field in this region, we took videos of the tuft behavior with multiple trials at several speeds including 45 and 60 mph. Some screenshots manipulated for clarity are shown in Figure 14.

Figure 13. Tuft testing apparatus, shown mounted to the van.

Figure 13. Qualitative tuft testing apparatus, shown in profile with all components visible.

Speed comparison results (shown in Figure 14) indicate that the lower streamlines may be parallel with the ones running through the top of the tuft testing rig (assumed to be within the free stream), at around the second or third tuft from the bottom. This indicates that the air flow quality may resemble the free stream at a height of around 24-30 inches (measured from the roof of the van) in this frontal location. Coupling these results with the CFD analysis, we may be able to achieve more steady flow conditions closer to the van's roof if we locate the ATP further back along the length of the van. In any case, we see that meeting the specification of total height restriction is feasible – a 4-foot-tall HPV mounted 2.5 feet above the 7-foot-tall van comes in at a total height of 13.5 feet.

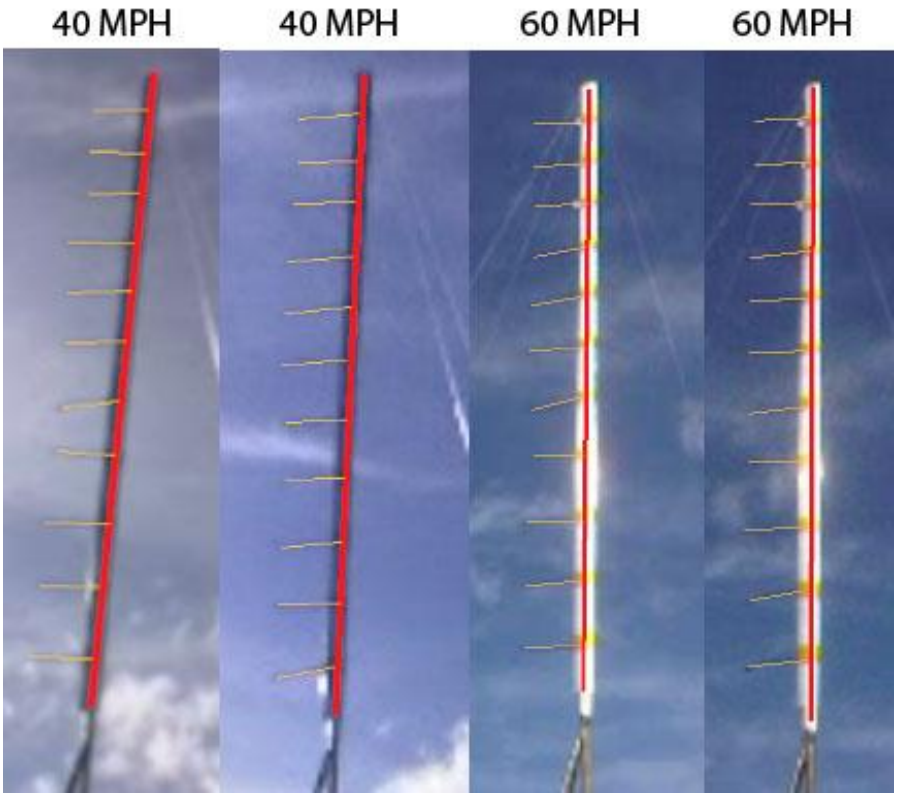

Figure 14. Speed comparison results obtained from frame captures of video data obtained during qualitative tuft experimentation.

Preliminary Van Vibrational Analysis

In conjunction with running the van flow field visualization experiment, we attached the Rocket Data Acquisition System (RDAS) two-axis accelerometer and data-logger to the tuft rig base to gain quantitative vibrational data for an object strapped to the van roof. A picture of the RDAS system is included in Figure 15. The results of this test represent van roof acceleration data sampled at 200 Hz for vehicle speeds of 30 and 60 mph. By using a Fast-Fourier Transform method, we obtained a preliminary understanding of the vibrational frequencies that are most prevalent during roof-top testing. With this data in hand, we can design the stiffness of our ATP such that its natural frequency lies well outside the ranges of these values. The raw acceleration data from this test can be found in Appendix D.

Figure 15. RDAS two-axis accelerometer mounted to base of tuft testing apparatus.

Dropout Strength Test

Since many of our ATP designs require attaching to the dropouts, we have designed a test to evaluate the safety of this connection in worst case loading conditions (a strong crosswind). Normally the dropouts of a bicycle are not designed to resist substantial moments in this plane. Thus, understanding the actual strength of this location under these specific loading conditions is critical. Our test apparatus (shown in Figures 16 and 17) consists of an arm that attaches to the dropout and holds the front fork of a bicycle horizontally such that it can be loaded with weights. The weights create the desired moment in the connection point of the dropouts, and indicate what sort of maximum moment this location can withstand. Figure 17 shows one trial of this test. With an approximate moment arm of 100 inches and a test load of 45 pounds, both forks we tested survived without failure. This demonstrates that a standard bike fork is capable of resisting a moment induced by a strong crosswind of up to 4500 inch-pounds. Hand analysis shown in Appendix E reveals that this is more than enough dropout strength to resist the sort of moments seen in the event of a 30 mph crosswind. Refer to Appendix G for a full testing procedure.

Figure 16. Dropout strength test apparatus, shown with bike fork mounted.

Figure 17. Bike fork loaded with 45 pounds at a center distance of approximately 100 inches from the connection point.

Preliminary Analysis

Through this stage of the design process, we had not started sizing components with pen-and-paper analysis. However, we did complete several hand calculations to determine the feasibility different aspects of our top concepts. In this section, we will summarize the results of these analyses. Refer to Appendix C for the details of the preliminary analysis.

Most importantly, we performed a free body analysis of the HPV and the ATP support to show that we could accurately measure lift and drag with strain gauges strategically positioned within the support. By

implementing two strain bridges on each of the two pinned-fixed supports (connecting the dropouts to the roll-bar of the ATP), the strain measured in each could be used together to calculate both lift and drag on the HPV.

Additionally, we estimated the typical drag force on an HPV travelling at 80 mph with an average rider output power of 1300 W. Assuming 80% of the rider's power goes into overcoming aerodynamic drag, this calculation indicates a drag force of 6.6 pounds. This result indicates drag forces that the ATP must be capable of measuring in the presence of air flow that is perfectly straight on to the direction of motion. We know measuring this force is well within the scope of strain gauges. Additionally in the more detailed design analysis we perform in subsequent sections of this report, we verify this number's accuracy.

We also estimated the side forces on the HPV, assuming a worst-case 30 mph crosswind gusts up directly perpendicular to the direction of the HPV's travel. By using a drag coefficient of a thin disk, we found that side forces on the HPV could range from 39.2 to 117.4 pounds. In conjunction with the dropout strength test described earlier, we think the ATP frame will be capable of withstanding these conditions if sized correctly.

Evolutionary Design

As we designed each of the promising concepts in the previous sections, we checked them against the relevant analysis that we had completed at that time. Through this process, we constantly improved and modified each concept throughout, without establishing a formal decision matrix weighing each against the other. Instead, we mixed aspects of all of our top concepts that best satisfied the specifications into what we consider our best concept. This design is described in the next section of this report.

Chapter 4 — Description of Final Design

This section of the report details our final ATP design. The following categories discuss different aspects the final design in more detail:

- Overall description/layout
- Detailed design description
- Analysis results (hand calculation and finite element method)
- Cost analysis
- Assembly schematics
- Manufacturing drawings
- Safety considerations
- Operational guide
- Preventative maintenance

Each of these items is discussed with accompanying figures and description below.

Overall Description/Layout

Our final ATP design is shown in Figure 18 below. This model utilizes a roll tube which is raised above the roof of the van. This is to decrease the stress in the supports and decrease the horizontal travel of the fairing when it is fully pitched. The supports above the roll tube are both fixed at the bottom and pinned at the top. This means the drag will be calculated by measuring the strain in both supports. Previous designs utilized one fixed/pin support and one pin/pin support and measured strain in only one place. We chose to make both supports rigid at the bottom in order to assure that they remain vertical at all times. This is to make certain that the geometry of the structure allows for simple and accurate strain measurements.

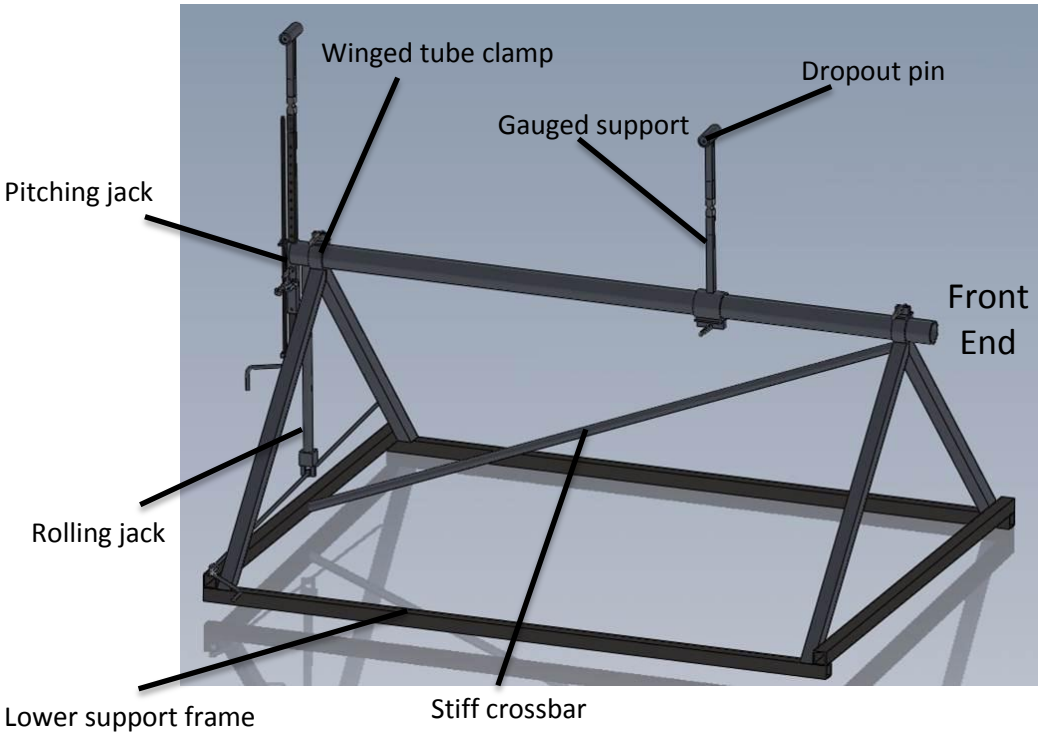

Figure 18. Annotated schematic diagram of final ATP design.

As opposed to previous models, our final design utilizes screw jacks to actuate both the roll and the pitch. This allows for the fairing to be positioned continuously, rather than discretely, as in some of our earlier concepts. However, discrete positioning options are available with a pin-and-hole positioning system in order to ensure reproducibility of tests. By utilizing a long crank arm, it is possible for operators to easily adjust the position of the fairing while standing on the ground, beside the van.

The front support of the platform clamps to the roll tube and can be slid back and forth to accommodate different wheelbases and different pitch angles. To configure pitch, the rear support is actuated vertically while the front support is unclamped and simultaneously allowed to slide horizontally. To actuate roll, the second screw jack raises and lowers a small horizontal arm which is fixed to the roll tube. The supports which hold that roll tube allow for the tube to rotate and can also clamp down to strengthen the structure and minimize vibration during testing.

Detailed Design Description

Our final ATP design is further broken down into several subsystems and components. In order to better understand each part's contribution to meeting the engineering specifications above, they are described below in more detail. Refer to the Analysis Results section for a description of supporting engineering analysis, the Manufacturing Drawings section for information about individual part drawings, and the detailed bill of materials in the Cost Analysis section for dimensions, part numbers, and pricing.

Dropout Pins

The dropout pins serve as the interface between the HPV's wheel dropouts and the gauged supports of the ATP. They consist of a standard dropout axle, a weldable steel tube, and some simple roller bearings. This assembly ensures that all past HPV frames are accommodated (by the standardized axle dimensions) and that the connection will act as a true pin throughout the range of pitching and rolling actuation.

Figure 19. Dropout pin assembly with front fork installed.

Gauged Supports

The gauged supports are 0.75×0.75-inch square tubing with a 0.065-inch wall thickness, made from 4130 alloy steel. We chose this specific size tubing because it satisfies the imposed strength requirements and reduces drag and airflow disturbances near the HPV compared to larger tube sections. The sections of the supports that house the strain gauges for lift and drag measurement are 0.75×0.75-inch solid 7075 alloy aluminum bar stock. The gauged supports are each fitted with two strain bridges in order to measure axial force and bending in each notched section (which in turn are used to calculate lift and drag acting on the HPV fairing). The aluminum load cells have 0.225-inch notches to provide the necessary stress concentration to obtain strain measureable by the gauges at typical operating loads (around 8 to 12 pounds). The load cells bolt into place within the upper and lower steel support sections.

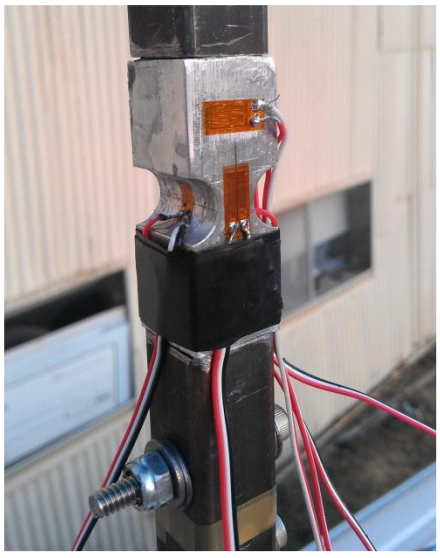

Figure 20. Detail view of gauged support.

Roll Tube

Very simply, the roll tube is a 2.5-inch diameter by 0.188-inch wall thickness steel tube that is 72 inches long. The front gauged support can clamp near the midpoint of the tube, which is supported from below by winged tube clamps welded to the accompanying support frame. The pitch screw assembly is welded onto the aft end of the roll tube, which is in turn what provides the rear support. When the clamps are loosened, the roll tube can pull com-

pletely out such that the HPV can be mounted separately from the remainder of the frame. This helps reduce the time it takes to prepare for an aerodynamic test and also reduces the weight of each component that needs to be lifted onto the van roof. During the pitching procedure, the gauged support clamp is loosened to allow the front contact point to slide freely as the horizontal distance between the two wheel dropout pins changes.

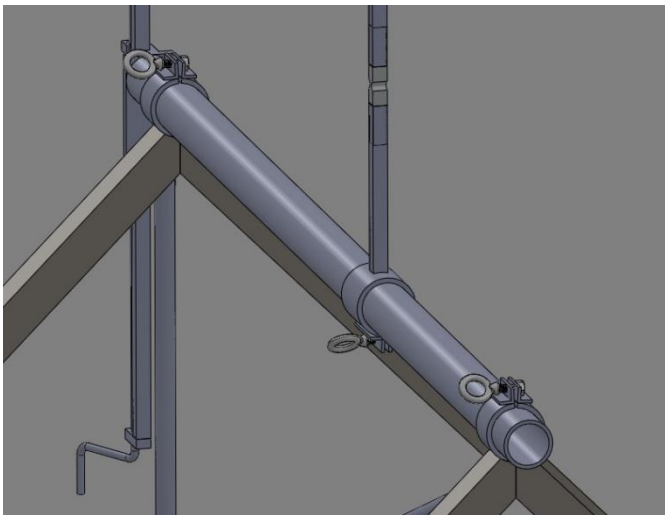

Figure 21. Detail view of roll tube mounted on support frame.

Winged Tube Clamps

These components are manufactured from nominal 2.5-inch diameter by 0.25-inch thick steel tubing and some 1 x 1 inch L-beams. By cutting a notch in the tubing and welding the L's onto either side of the notch, we created the clamping device shown in Figure 22, a variation of which is used on commercial bicycles. By tightening the bolt through the winged plates, the tube closes, reducing its diameter, and creating an interference clamp on the roll tube that runs through the center. The friction resulting from this interference resists the torque produced in worst-case loading conditions while the HPV is both pitched and rolled.

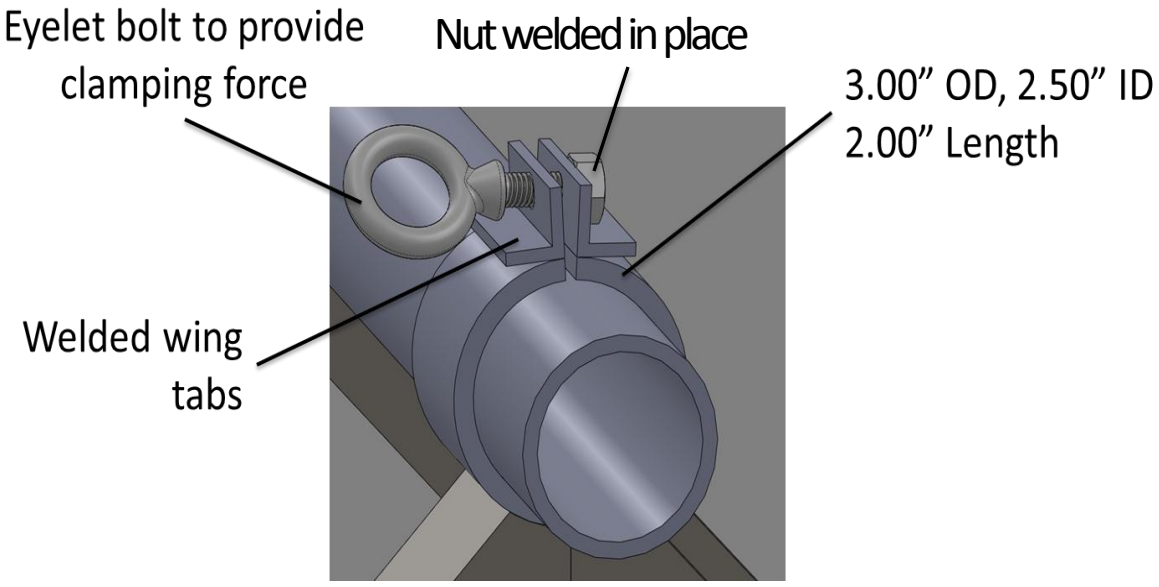

Figure 22. Detail view of winged tube clamp with some dimensions shown.

Pitching and Rolling Jacks

The pitching and rolling jack both utilize 3/8”-12 acme screws to produce linear motion. The acme screw has stronger and smoother threads compared with regular threaded rods, leading to more controlled actuation of the jacks. The rolling jack requires the translating acme nut be mounted on a pivot to account for changes in geometry. This pivot is mounted on the end of the roll arm as indicated in the figures below and at right. The opposing end of the screw will be mounted within a rod end to allow the acme screw to rotate, but not translate. With the test platform is mounted near the back of the van, both pitch and roll jacks are operable from the ground using a similar eyelet to those in the winged tube clamps.

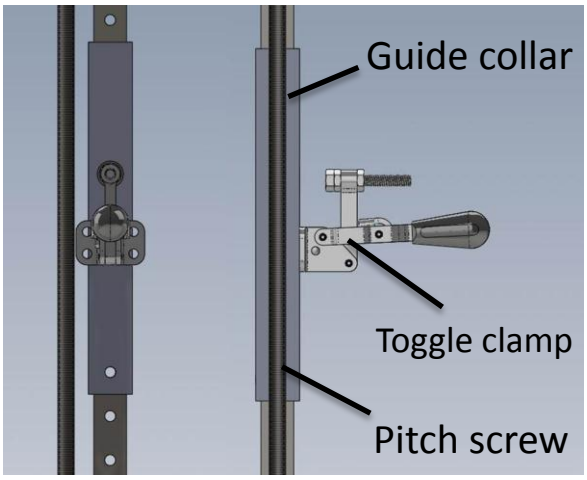

Figure 23. Detail view of pitching jack assembly.

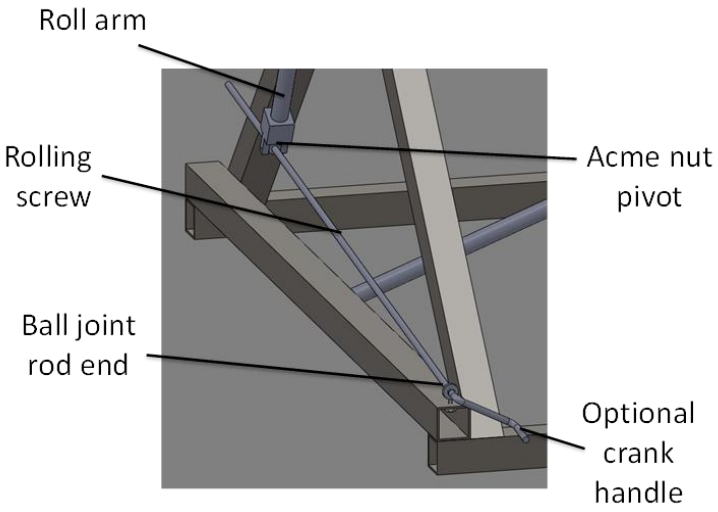

Figure 24. Detail view of rolling jack assembly.

Support Frame

The support frame (shown in Figure 25) is built from welded sections of 1.5”x1.5”x0.120” carbon steel square tubing. We have arranged the members such that the A-frame section meets at a 45° angle to ease the manufacturing process. The base members that run lengthwise along the roof of the van are spaced 56 inches apart to put the edge of the frame almost directly over the van’s roof gutter. This ensures that the tension in the nylon straps (described more in the following section) is focused vertically into the gutter system. Furthermore, these 66-inch-long, lateral sections sit below and support the sections running along the width of the van to accommodate the curvature of the van’s roof. In this configuration, the weld area of A-frame sections is maximized, adding to the stiffness of the structure. Finally, in an effort to further increase stiffness under heavy aerodynamic loading, a diagonal crossbar is included connecting the top of the front A-frame section to the lower-back section. We have ensured that the frame is well-overdesigned for normal loading conditions and worst-case loading. Refer to the Analysis Results section for more information.

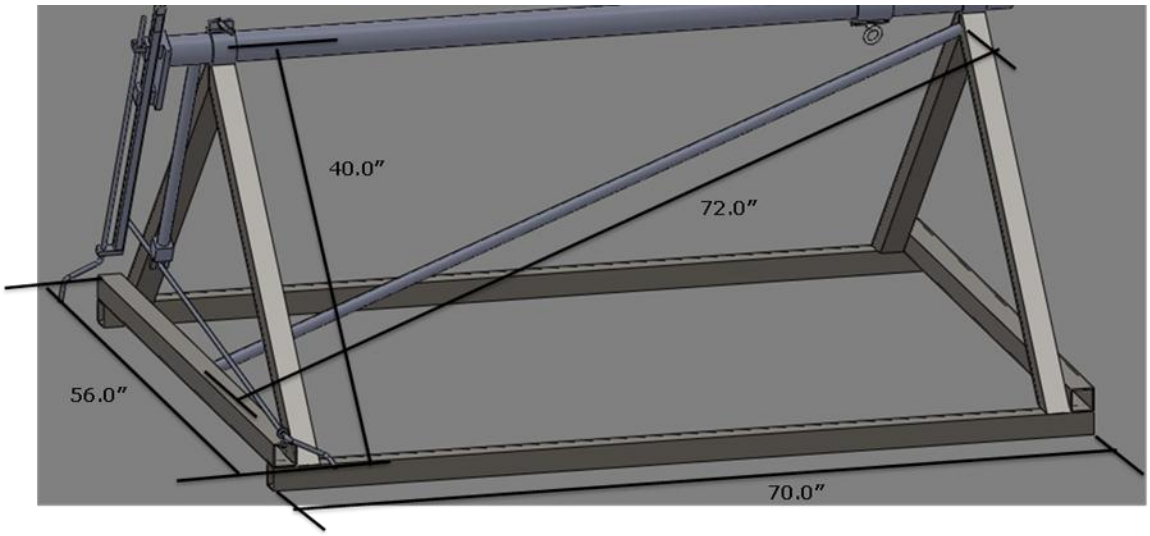

Figure 25. Support frame assembly shown with a few reference dimensions.

Frame/Van Interface

The frame interfaces with van roof via rubber L-strips running along the length of the lateral sections. The rubber feet serve two purposes: making sure that the van roof's paint job doesn't become chipped, and damping the vibration transferred from the roof to the support frame. Additionally, they have the added bonus of increasing the friction at the interface, thereby increasing safety against slippage. The frame attaches to the van with several 1-inch wide nylon straps that run across the width of the frame and attach to the roof gutter using standard flat hooks. The straps are tensioned by individual ratchets, cinching the structure down securely to the roof. Due to the geometry of the frame, a majority of this strap tension is concentrated in the vertical direction, ensuring a strong contact friction at the frame/van interface.

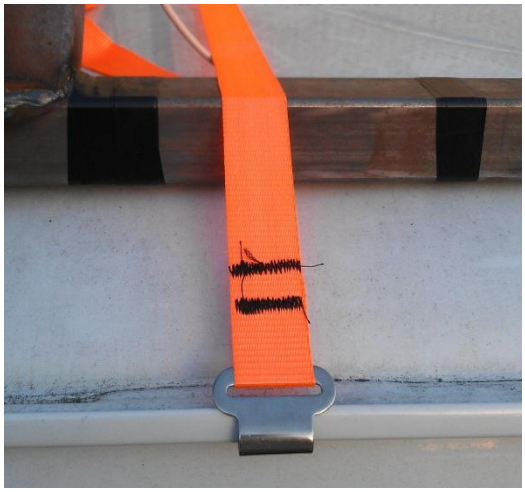

Figure 26. Detail view of frame/van interface.

Hand Analysis Results

We have sized each of the components described in the previous section such that they are safe against several predicted modes of failure and will remain robust throughout the lifetime use of the ATP. This section summarizes calculations used in this effort, their results, and physical implications resulting from the analysis. Copies of the raw hand calculations are included in Appendix E.

Worst Case Loading Condition

Most (if not all) of the analysis techniques we employed in designing the ATP are based on a worst-case loading condition that we predetermined to ensure that each component was overdesigned and safe. To this effect, we assumed a max HPV weight of 50 pounds, acting at a center of mass located 3 feet from the roll axis of the ATP. This weight was extrapolated from a past HPV club report (Christensen, 2011), and is conservative for past and future fairing designs. Additionally, we estimated the front and side drag forces on the HPV while pitched and/or rolled as acting on a 6'x4'x2' block with a conservative coefficient of drag (C_D = 1.0). For a vehicle speed of 70 mph and a 30 mph crosswind, we calculated a front and side drag of 150 and 80 pounds respectively. For simplicity, we assumed that these aerodynamic forces can be applied at the center of mass location, showing in Figure 27. This assumption orients the forces in a relatively conservative location for moment and torque calculations in design analyses. Under typical operation, the ATP will be used at lower speeds and without windy conditions, resulting on a frontal drag more on the order of 15 pounds. Thus, by designing to these worst-case conditions, we can safeguard against any type of failure, even those that may lie outside the scope of our initial perception.

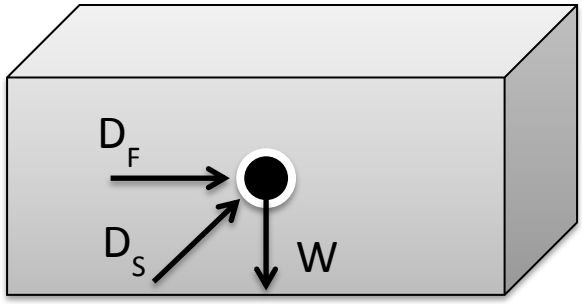

Figure 27. Frontal drag (D_F), side drag (D_S), and weight (W) acting on the center of mass of the HPV, modeled as a 6'x4'x2' block with C_d = 1.0.

Dropout Pins

To analyze the dropout pins, we resolved the worst-case loading on the HPV into the corresponding radial and thrust loads experienced by the bearings on each dropout. To do this, we summed moments around the center of dropout, including contributions from both the weight of the HPV and the load from the crosswind. Despite the loading, the bearings within the dropout pins resist shear failure with an acceptable safety factor of 6.8 against yielding.

Gauged Supports

The safety of the square tube section of the gauged supports subjected to bending moments was confirmed for the loading case described above. The notched section, however, required a completely different analysis to ensure that the proper strains would be achieved to register on the strain gauges. We determined the radius of the notch by comparing the drag force to cause yielding in the notched section and the micro-strain produced by the typical drag measurement load of 7 pounds for different radii varying from 0.075 to 0.275 inches. To register this type of drag force accurately, we chose the 0.225 inch radius notch to produce 410 micro-strain. Unfortunately, due to the reduced area of the notched aluminum section, this spot becomes critical and may experience plastic deformation when exposed to a frontal drag larger than 90 pounds according to hand analysis. However, we are willing to accept this condition, given that our loads are for the absolute worst-case. If the structure were to actually see this magnitude of frontal drag, it isn't unreasonable to require replacement of this small section. Further examination of this area can be found in the Finite Element Analysis section.

Roll Tube

We verified proper sizing for the roll tube by lumping the worst-case loads at a point with a perpendicular distance of 18 inches from the middle of the tube, perpendicular to the tube axis. This assumption approximates the stresses and deflections of the three-dimensional loading conditions on the actual structure. Using this model, the greatest bending stress in the tube was 2310.7 psi and resulted directly from the bending moments due to the weight of the HPV and the worst case side load. For this case, the maximum deflection is 0.0266 inches. Additionally, the worst-case loading when the HPV is rolled also creates a torque in the roll tube. This torque was calculated at 2002 inch-pounds, corresponding to a shear stress of 1362.4 psi and an angular deflection of 0.201 degrees. The more critical of these two deflections is the angular deflection, which we have kept significantly less than the target value of 0.5 degrees. In meeting these minimum deflection criteria, we are confident that the structure will not yield as the result of these loads either.

Winged Tube Clamps

The primary purpose of these clamps is resisting the torque produced by the HPV's weight and any side drag produced by a strong crosswind. To make sure these clamps could securely hold the roll tube with the HPV fully rolled at 45°, we performed two separate analyses. First, we implemented a shaft and hub interference pressure calculation. The pressure generated by closing the clamp completely around the shaft induces a friction, which in turn resists the torque in the shaft. We calculated the resisting torque resulting from fully closing the winged section and compared that to the moment associated with the entire weight and side drag. This calculation assumes all but one of the winged tube clamps are insufficiently tightened, and thus one must support the entire load. As shown in the previous section, these clamps can meet and exceed the required torque resistance with a factor of safety of 29.0 when fully closed. However, this high safety factor led us to question whether or not completely closing the clamp was reasonable. In order to back up the calculation, we performed a separate analysis that calculates the required bolt tension in the winged section to generate the necessary pressure to resist the load torque. The required tension we solved for was far less than that which would cause yielding in the bolt.

Pitch and Roll Jacks

The loads on the pitching jack are relatively small, as this part of the ATP is not designed to carry load during operation. The acme screw and nut must support only the weight of HPV. The 3/8" screw we selected has more than enough strength to support this load. The roll jack, on the other hand, was slightly more difficult to analyze because it needs share support of the worst-case moment at different geometries. By resolving this moment into a tension carried by the acme screw, we again found that the load was small compared to the tensile strength of the screw and corresponding strength of the acme nut. Since the roll jack only moves in one direction, the acme screw is kept in tension, and thus buckling does not pose a problem.

Support Frame

The welded square tubing that composes the lower support frame sees a variety of combined loading scenarios that we modeled to confirm the safety of the geometry. First, we determined axial loads in the members of the A-frame section using a truss analysis. This underestimates the stiffness of the structure in reality, and thus provides a conservative picture of axial forces in the beams. Then, we determined the bending moment seen by one of the A-legs, assuming that each one must support the entire load associated with weight and drag (again, consistent with an insufficient tightness in a few of the clamps above). Finally, by utilizing superposition we can combine these loads and solve for the resulting safety factor against failure for the square tube geometry described earlier. For this somewhat simplified loading condition, there is a safety factor of 3.8 against yielding, demonstrating that this geometry is more than strong enough to withstand any sort of ultimate failure during operation.

The crossbar running between the two A-frame structures also resists some of the bending in the front of the frame. This member is mostly loaded axially in compression, so we made sure that it was strong enough to resist both axial yielding and buckling. Since this crossbar also connects to the center of the A-frame base in the rear of the ATP, we checked that this beam wouldn't fail due to the resulting deflection. As we expected, both the loads in the crossbar and into the center of the A-frame base were far from inducing any degree of plastic deformation, let alone failure. Refer to the structural finite element analysis results in the following section for more detail.

Finite Element Analysis Results

In addition to the hand analysis described in the previous sections, we have completed some finite element analysis (FEA) for the ATP design. This analysis can be broken down into two main categories: an enquiry in structural strength, and an investigation of the system's vibrational characteristics.

Structural FEA

We have conducted preliminary finite element analysis of the ATP structure consistent with the worst-case loading conditions discussed in the previous section. Due to the complexity of the geometry and part interactions within the system, FEA is desirable for verifying that the individual components of the ATP have been sized appropriately. Specifically, it is useful to know that the stresses and deflections in different members fall well within the

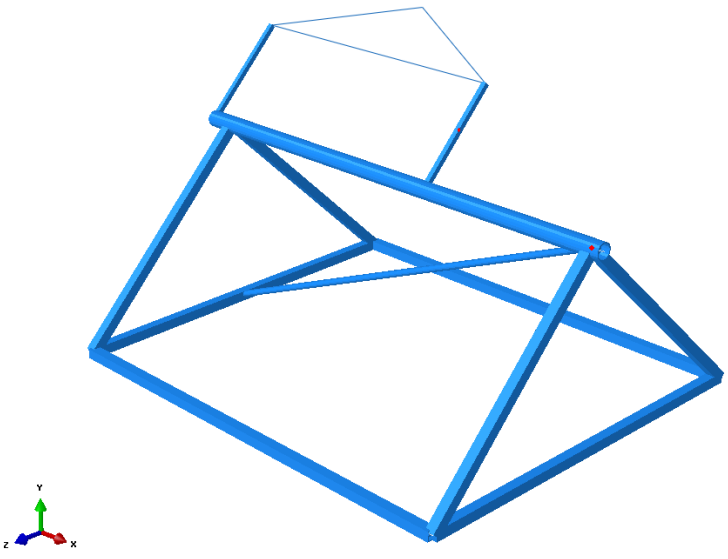

Figure 28. Rendered beam profiles of finite element ATP model.

elastic range of their respective materials. Since the hand analysis was specifically designed to produce a conservative estimate of stresses in the ATP, it is expected that all stresses within individual members due to worst-case aerodynamic loads transmitted from the exposed fairing will be well below the yield strength of the materials used. Holistically speaking, FEA on the test platform provides another medium of verification that the design meets weight, strength, and most importantly, safety design specifications.

Using beam elements with appropriate cross-sectional geometry, a first analysis examines the ATP in the rolled configuration shown in Figure 28. Applying a fixed boundary condition along the longitudinal lower support members and the worst-case loads at the top of the triangle representing the HPV's center of mass (with mass-properties consistent with the most recent design iteration), we obtained the invariant stress results shown in Figure 29. We have reasonably validated these results by hand in Appendix E.

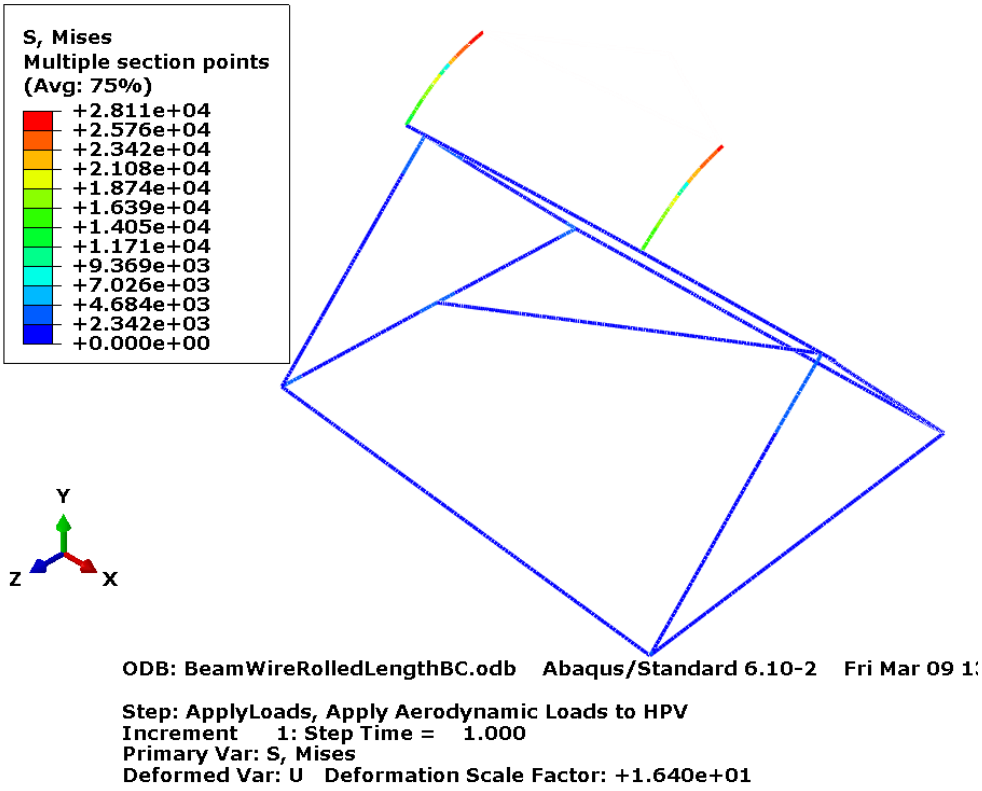

Figure 29. von Mises stress contour plot of ATP in rolled configuration subject to worst-case loading.

These results agree with hand analysis, and confirm that the stresses in the lower support structure are very low with respect to yield. Additionally, we see that the von Mises stress in the gauged supports (at least in this rough, preliminary analysis) falls well below the yield strength of the materials in this location as well.

We also performed a more detailed analysis of the notched aluminum sections to check this critical location against material yielding. A von Mises stress contour plot of the notched aluminum section result-

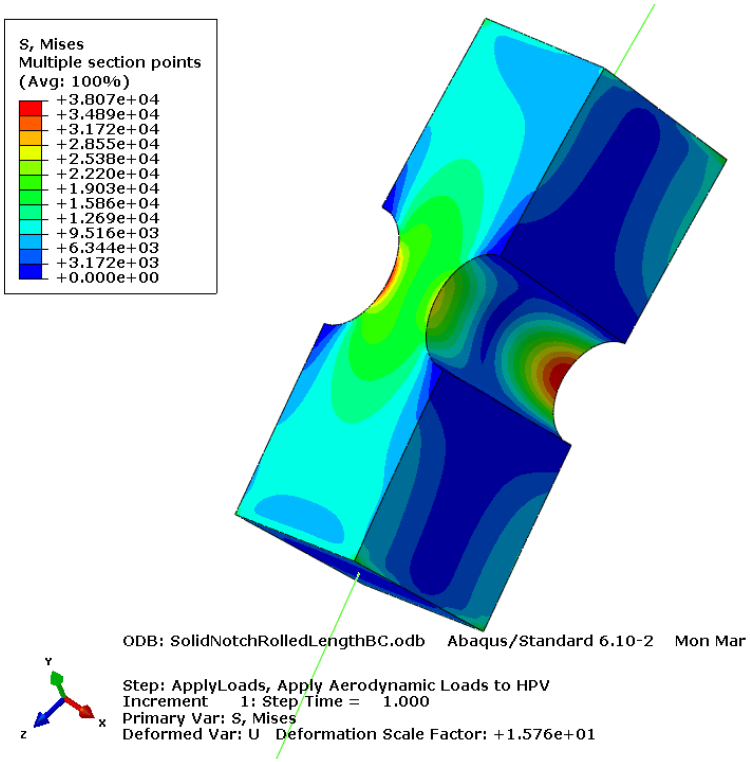

Figure 30. von Mises stress contour from detailed analysis of notched section.

ing from a more detailed analysis of this location is shown in Figure 30. The maximum von Mises stress predicted by the FE model subject to the worst-case loading condition is 38.1 ksi, giving a safety factor of at least 1.4 against yielding. Thus the design of the ATP and corresponding notched sections is acceptable with respect to material yielding.

Vibrational FEA

One of the main concerns in sizing the load cells with enough sensitivity to measure small lift and drag forces is that they may be influenced by road noise. The fluctuating strains, caused by road noise-induced vibration in the structure, could also be measured by the gauges and add significant noise to the steady strains caused by lift and drag. The goal of this vibrational FEA is to model the ATP under road loads by performing a dynamic, steady state analysis in order to determine the magnitude of the unsteady strains resulting from a variety of frequencies.

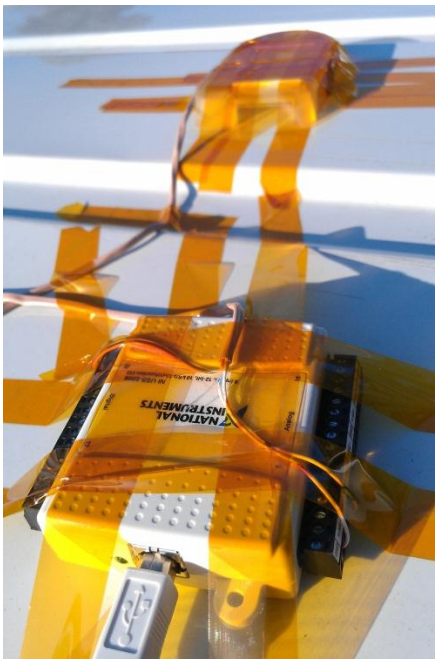

Figure 31. Road noise accelerometer and data acquisition system.

To determine the amplitudes and frequencies that should be applied to the FE model, road noise was measured with an accelerometer and data acquisition system (DAQ) mounted to the roof of the van at 30, 45, and 60 miles per hour. Data for accelerations in the x, y, and z-axis directions was recorded. The x, y, and z-directions are specified in Figure 38, which includes the coordinate system referred to in this section. The results of the vibrations test showed that the accelerations in the y-direction (vertical) were significant (see Figure 32), but accelerations in the x and z-directions (horizontal) were smaller than the accelerometer's resolution (see Figure 33). A fast Fourier transform (FFT) of the acceleration data was performed with MATLAB to determine the frequency content of the signals. This allows for greater accuracy in amplitudes of the vibration frequencies applied to the FE model if a steady-state modal FE analysis is performed in the future.

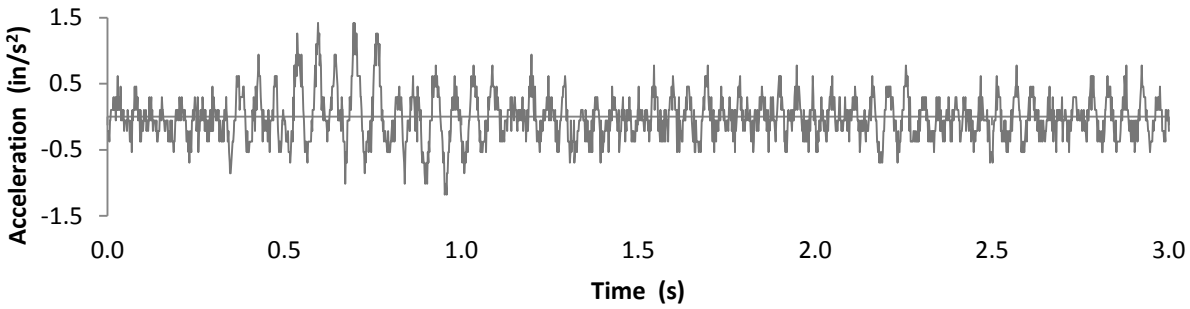

Figure 32. Recorded vertical acceleration signal, measured at the van roof at 60 mph.

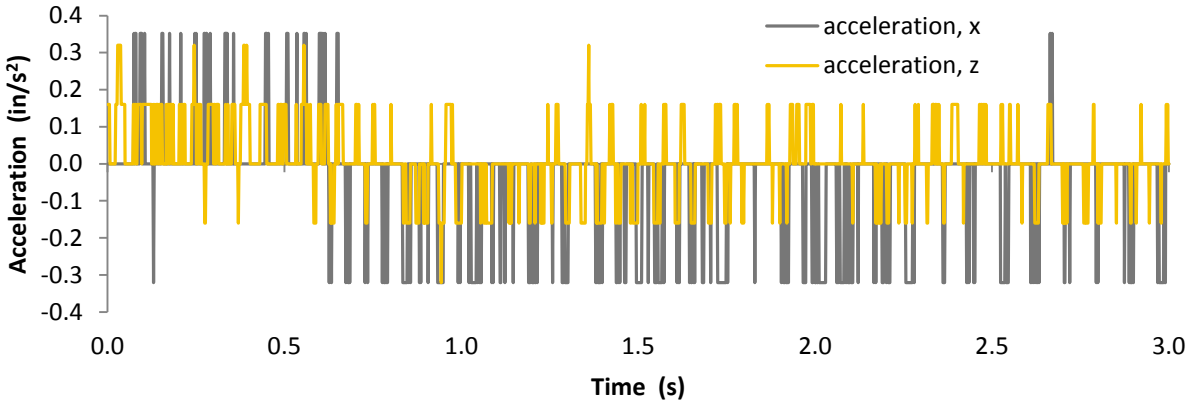

Figure 33. Recorded horizontal acceleration signal, measured at the van roof at 60 mph.

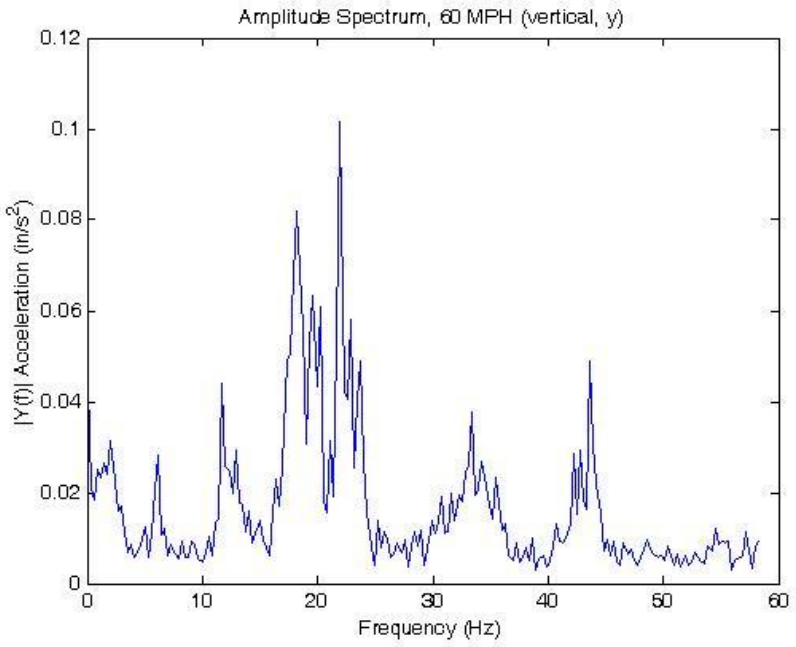

Figure 34. FFT of the vertical accelerations measured at 60 mph.

We chose to perform a “transient modal dynamics” analysis, a type of linear perturbation model, with the measured acceleration times the mass of the van as the forcing function. According to the online ABAQUS manual, “this type of analysis gives the response of the model as a function of time based on a given time-dependent loading. The structure’s response is based on a subset of the modes of the system, which must first be extracted using an eigenfrequency extraction procedure.” A simplified model of the ATP, consisting of the roll tube, gauged supports, aluminum notch, and rigid HPV was created and the first 30 eigenfrequncies extracted. The results were compared to the hand calculations to verify accuracy of the FEA model. The simplified FE model estimated 74.118 and 270.25 Hz for the first two “bounce-pitch” mode natural frequencies and the hand calculations produced values of 65.73 and 269.76 Hz; thus the FE model is in agreement with the hand calculations.

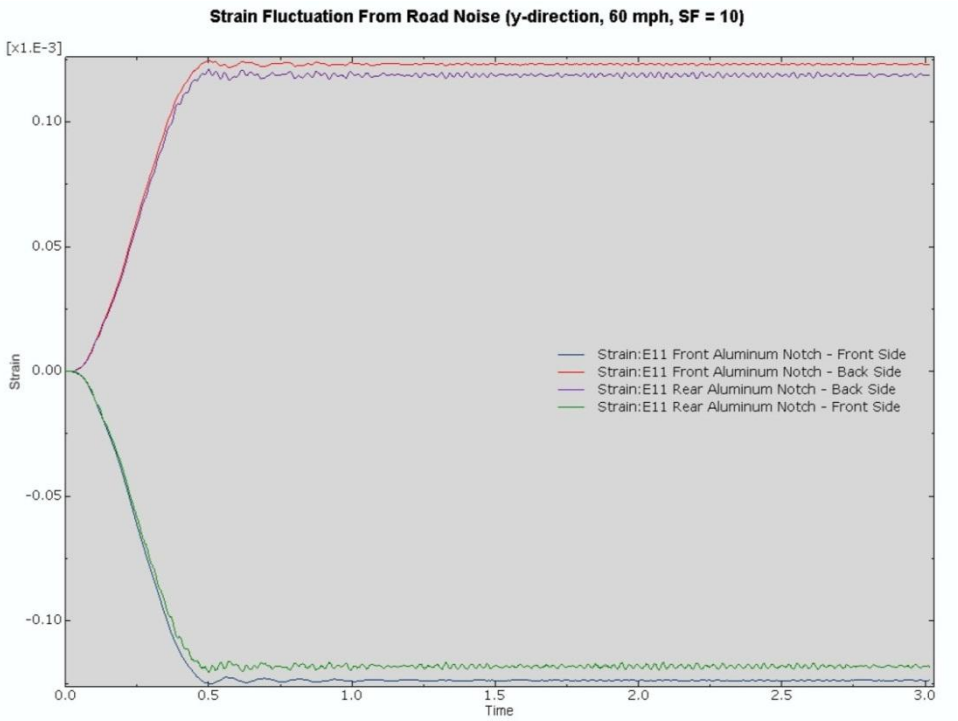

Figure 35. Strain fluctuation from road noise in the y-direction at 60 mph with a safety factor of 10.

The full 3-D model of the ATP was almost exclusively composed of beam sections with the only exception being the notched aluminum inserts in the upper supports used for strain measurement. These notched components were modeled with solid elements because of their irregular geometry. The welds and clamps used in the structure were simply modeled as the junctions of beam elements. Although a more accurate model of the system would account for the clamps, the nonlinearities due to contact and other interactions along with the increased number of parts in the model puts that level of analysis outside the scope of this class. The use of beam elements is a simplification but will make the model much more efficient to run while maintaining a reasonable level of accuracy for both static and dynamic analyses. The HPV was modeled as a rigid body with the inertial properties defined at the center of gravity. The forcing function applied to the ATP in the transient modal analysis, as stated above, was one representative acceleration signal directly measured with the DAQ at 60 mph (see Figure 32) multiplied by the

mass of the van (6940 lb_m). A drag force of 7 lb_f was slowly applied over a half second to the centroid of the HPV, creating a steady strain for comparison if the transient strains. The acceleration at 60 mph was the greatest and therefore was the only speed used in the analysis. In the vertical direction, the signal (see Figure 32) was multiplied by ten as a factor of safety. The results proved that, even with a safety factor of 10, the fluctuating strains were around 2 to 3 orders of magnitude smaller than the steady strain (see Figure 35). Because the of the accelerometer's inability to pick up acceleration in the horizontal directions, the measured 60 mph signal was divided by 5 and used as an estimate of those signals. The analysis of the system's response to acceleration in the x-direction (the structure's least stiff direction) produced fluctuating strains were still extremely small, despite a safety factor of 10 applied to the forcing function (see Figure 36). The system's response to excitation in the z-direction was ignored because the strain gauges will be located along the neutral axis of the load cell. A final analysis of the ATP's response to vertical excitation with the HPV rolled 45 degrees was performed per sponsor concern of failure in the load cells due to the moment created by cantilevering the HPV. In this analysis, the same factor of safety of 10 was applied to the input signal and an additional 43.697 lb_f load (weight of the HPV) was applied to the centroid of the HPV as a weight force. The resulting maximum von Mises stress in the load cell notch was around 15 ksi, and was a result of the loading due to the weight of the HPV (see Figure 37). It should be noted that the large scale harmonic oscillations in the stress plot in Figure 37 are due to the application of weight load to the HPV (and is therefore fictitious because gravity is constant); the smaller noisy fluctuations that become apparent around 1.25 seconds is the fluctuating stress caused by the road noise. This means that fatigue resulting from the road noise doesn't need to obe considered.

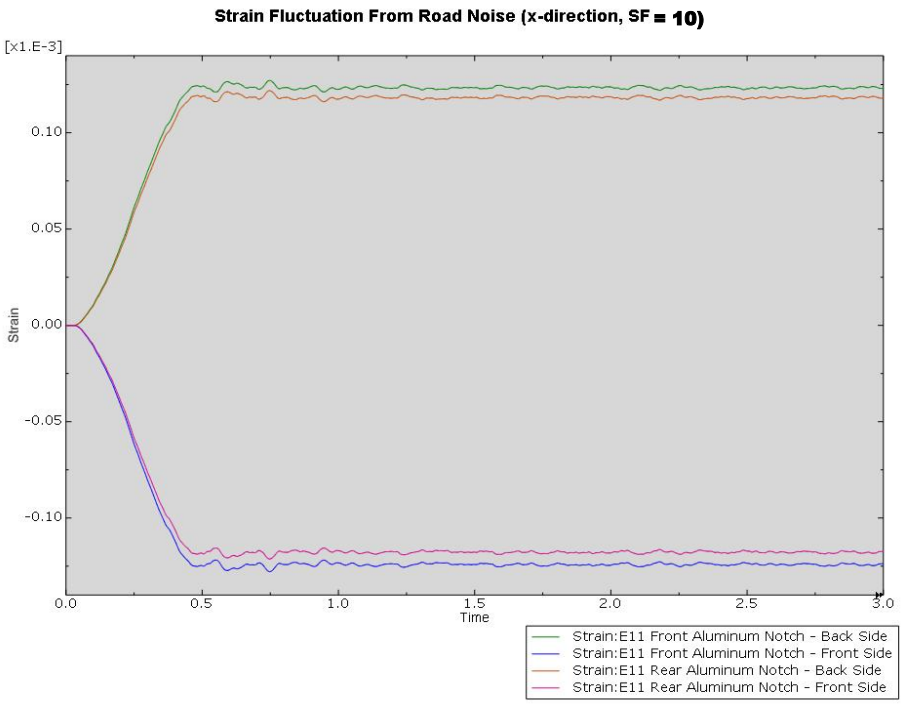

Figure 36. Strain fluctuation from road noise in the x-direction at 60 mph with a safety factor of 10.

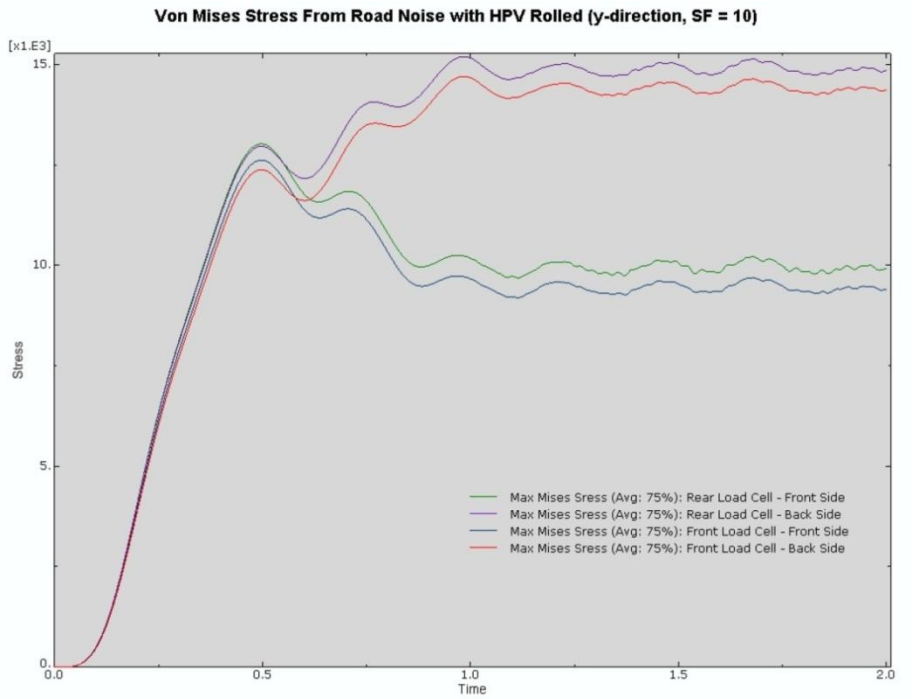

Figure 37. Fluctuating von Mises stress from road noise in the y-direction with the HPV rolled 45 degrees and a safety factor of 10.

Although it wasn't the main focus of this analysis, the transient stresses in the ATP structure from the FEA provided valuable information. According to the model results shown in the Figure 38, the maximum von Mises stress in the structure throughout the whole dynamics analysis (see the scale on the left of image) is around 38 psi; roughly 4 orders of magnitude below the endurance of the steel. This means that fatigue failure in the beams or any associated component is not a concern.

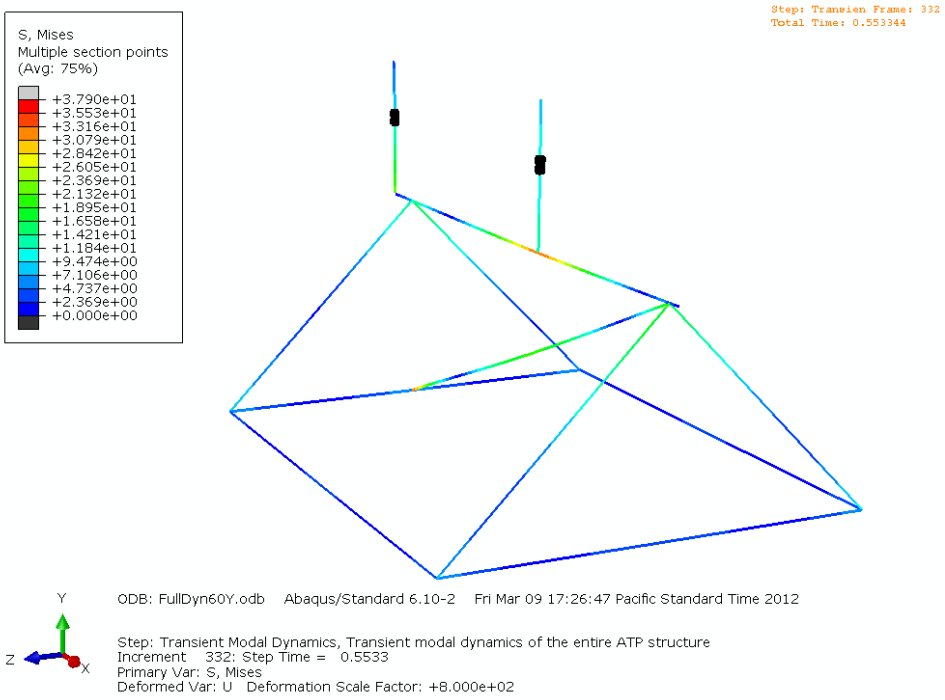

Figure 38. Von Mises stress in the ATP during an increment of the transient modal dynamic analysis showing areas of "high" stress.

Cost Analysis

The Bill of Materials shown in Table 2 gives a list of all of the components used in the construction of ATP, including a brief description. This table provides dimensions and description of the parts as they are applied in the ATP design. However, we have manufactured many of these components ourselves from steel stock tubes or other miscellaneous components. Table 3 links the content of Table 2 to actual suppliers and prices for raw materials.

Table 2. Component bill of materials listing parts and description as applied in the ATP assembly.

COMP. #	COMPONENT	DESCRIPTION	QTY.
1	Roll Tube	2.5"x2.124"x72" Tube - Steel	1
2	Gauged Support Top Section	0.75"x.065"x6.5" Steel Square Tube	2
3	Front Gauged Support Bottom	0.75"x.065"x8.5" Steel Square Tube	1
4	Aluminum Support Section	.75"x.75"x6" Aluminum Bar Stock	2
5	Hub	1.5"x3.51" Steel Round Stock	2
7	Clamp Tube (Long)	3.0"x0.25"x3.0" Steel Tube	1
8	Clamp Tab (Long)	1"x.1875"x3" 90 Degree - Steel	2
9	Clamp Bolt	3/8"-16 Eyebolt	3
10	Clamp Nut	3/8"-16 Nut	3
11	Roll Arm	1"x0.120"x72" Steel Tube	1
12	Acme Nut Pivot	1.5"x1.5"x2.78" Aluminum Stock	1
13	Rod End	Steel Ball Joint Rod End 3/8"-24 RH Male Shank, 3/8" Ball ID	1
15	Rolling Screw	3/8"- 8 tpi x 57"Acme Screw	1
16	Acme Nut	3/8"- 8 Acme Nut	2
17	Rod End Nut	3/8"-24 Nut	1
18	Width-Wise Base Members	1.5"x0.120"x56" Steel Square Tube	2
19	Lateral Base Members	1.5"x0.120"x70" Steel Square Tube	2
20	A-Frame Base Member	1.5"x0.120"x40" Steel Square Tube	4
21	Diagonal Base Support	1"x0.120"x72" Steel Tube	1
22	Clamp Tube (Short)	3"x0.25"x1.5" Steel Tube	2
23	Clamp Tab (Short)	1"x.1875"x1.5" 90 Degree Angle - Steel	4
24	Rear Clamp Tube	1"x.120"x8" Square Tube Steel	1
25	Toggle Clamp	Hold Down Toggle Clamp	1
26	Rear Support Bottom	0.75"x.065"x27" Steel Square Tube	1
27	Bottom Plate	0.75"x0.50"x1.75" Steel Stock	1
28	Pitching Acme Screw	3/8"-8 x 34" Acme Screw	1
29	Nut Cup	1"x.1875"x1" 90 Degree Angle Steel	1
30	Bearing	24 mm OD bearing	4
31	Strain Gauges	Strain Gauges, wire, mounting glue	1
32	Straps and Hardware	Polyester Straps, Ratchets, Flathooks	1
33	Hub Axle	9mm Threaded Rod	2
34	Hub Nuts	9mm Bicycle Nuts	1
35	Pulley	Pulley Used For Testing	1
36	Bearing Spacer	7/16" x 12" Stainless Steel Tube	1
37	Rubber Mounting Feet	12' Rubber L-Sheet	1

Table 3. Part and raw material ordering bill of materials. Refer to Table 2 for component descriptions.

COMP. #	DESCRIPTION	ORDER #	Source	QTY.	PRICE	TOTAL
1	2.5" x 2.124" x 6' 4130 Alloy Steel Tube	89955K7	McMaster	1	$140.13	$140.13
2,3,26,27	0.75" x 0.065" x 6' 4130 Alloy Steel Tube	6582K416	McMaster	1	$79.84	$79.84
4	0.75" x 0.75" x 3' 7075 Alloy Aluminum Bar Stock	9055K133	McMaster	1	$56.39	$56.39
13	Ball Joint Rod End	60645K141	McMaster	1	$3.86	$3.86
28	Acme Screw 3/8"- 8 tpi 3'	93410A607	McMaster	1	$17.07	$17.07
15	Acme Screw 3/8"- 8 tpi 6'	93410A310	McMaster	1	$27.76	$27.76
16	Acme Nut 3/8"-8 tpi	94815A011	McMaster	8	$2.82	$22.56
30	Bearings - 9mm shaft diameter, 22mm OD	6153K112	McMaster	4	$12.01	$48.04
37	Rubber L-Sheets, 1”x”1, 1/8” thick	3482K6	McMaster	12	$4.02	$48.24
25	Hold-Down Toggle Clamp	5126A52	McMaster	1	$10.94	$10.94
32	Stainles Steel Flat Hook	3648T18	McMaster	8	$2.48	$19.48
22,7	3" x 2.5" x 1' Low Carbon Steel Tube	7767T731	McMaster	1	$40.69	$40.69
8,23,29,18,19,20	1.5" x 1.5" x 20' Low Carbon Steel Bar Stock	N/A	B&B	4	$44.00	$176.00
24	1"x.120"x12" Steel Bar Stock	N/A	B&B	1	$11.40	$11.40
11,21	1" x 0.120" x 20' Low Carbon Steel Tube	N/A	B&B	1	$26.00	$26.00
5	1.5"x12" Steel Round Stock	N/A	B&B	1	$18.05	$18.05
35	Pulley	N/A	Miner's	1	$4.99	$4.99
36	7/16" x 12" Steel Tube	N/A	Miner's	1	$6.99	$6.99
9,10,17	Miscellaneous Hardware	N/A	Miner's	1	$20.00	$20.00
12	Hinge	N/A	Miner's	1	$3.99	$3.99
33	Hub Axles	N/A	Foothill Cyclery	2	$9.99	$19.98
34	Hub Nut Set	N/A	Foothill Cyclery	1	$7.99	$7.99
31	Strain Gauges	N/A	Cal Poly	4	$0.00	$0.00
32	Strap and Ratchet Set		Amazon	1	$21.54	$21.54
	Shipping Costs and Tax				$95.00	$95.00
					Total:	**$926.93**

The overall cost of the ATP prototype is $929.93, which is well under the specified $2000.00 budget. This prototype is designed specifically for end-user operation, and therefore will not need refinement to a “production model.” That said, the additional room in the budget allows ample funds for any improvements to the design after it is delivered to the HPV club, including a separate ground plane, pinplates for discrete rolling positions, flow visualization aids, an onboard anemometer, and a camera-mounting apparatus. Refer to the Recommendations section for more information about these pursuits.

Manufacturing Drawings

Manufacturing drawings of the ATP assembly can be found in Appendix F. These include exploded drawings depicting the general assembly process, detailed drawings of individual parts, and qualitative manufacturing drawings expressing special construction notes. Refer to this design packet for more information. Further description of the ATP’s construction can be found in the Product Realization section.

Safety Considerations

We have ensured the critical components of the ATP design are safe against worst-case loading and reasonable human error. However, we do still have some preliminary safety concerns associated with the manufacturing and implementation of the ATP.

Mounting the ATP

When loaded with an HPV frame and fairing, the entire assembly could weigh up to 200 pounds. When mounting the ATP on the roof of the van, it is important that no less than 3 people are present to help lift. This minimizes the risk associated with situating the ATP on the van roof.

Driving Under Overpasses

The vertical profile of the van, ATP, and HPV comes in at just under 14 feet when in the upright position. For this reason, the driver of the van during an aerodynamic test should take special precaution to avoid freeway overpasses or low hanging trees. Make sure to plan a test route accordingly to circumvent any associated danger.

Operating in Heavy Wind

While we have ensured that the ATP design is safe under worst-case loading conditions, including an 80 pound side load due to a 30 mph crosswind, it is still important both for the validity of results and for the safety of test engineers that the ATP not be operated in high winds. Avoiding operation in the worst-case loading conditions is appropriate for safety purposes.

Operational Guide

This section details the process for performing aerodynamic testing with the ATP. Each subsection refers to the operating method for a specific action of the ATP.

Calibrating the Gauges

Each HPV has its own specific geometry associated with it, and thus the data acquisition system (DAQ) must be recalibrated for each new HPV tested on the ATP. Drag and lift measurements must be calibrated separately. To calibrate drag, a cord must be attached to the frame/fairing in such a way that its line of action intersects the approximate location of the fairing's aerodynamic center. Once the cord has been attached, a fish-scale should be used to apply a force on the frame/fairing parallel to the direction of forward travel, and acting to the rear. By measuring the number of bits output by the DAQ, and using analytical equations (listed in Appendix E) that offer strain in terms of drag force, a calibration curve can be produced to convert bits on the drag strain bridges to drag force. Likewise, by pulling vertically on the frame/fairing from the cord attachment point, a similar calibration curve can be produced for measuring lift. Using these calibration curves, data outputted from the DAQ during testing can be translated into actual lift and drag values.

Mounting on the Van

First and foremost, to mount the HPV onto ATP itself, remove the wheels and lift the frame into position over the two dropout hubs. Adjust the position of the front support by loosening its corresponding clamp and sliding it the proper location to support the wheelbase of the frame. Once in position, lightly tighten the front support in place so that it remains within a few degrees of vertical during mounting. Place each dropout on the front and rear axles and tighten the nuts to secure the frame of the HPV to the platform's supports. Add additional washers on the front and rear axle as necessary to avoid overly compressing the frame when tightening the nuts.

Once the HPV is correctly mounted to the ATP, make sure all supports are vertical and that all three tube clamps are completely tightened. Lift the ATP onto the roof of the van from the rear, centering the platform between the left and right rails on the van's roof. Distribute the four tie-down straps evenly across the length of the frame and place each hook underneath the van's gutter as shown in Figure 39. Tighten the straps down as tight as possible without causing any noticeable deflection in the roof gutter.

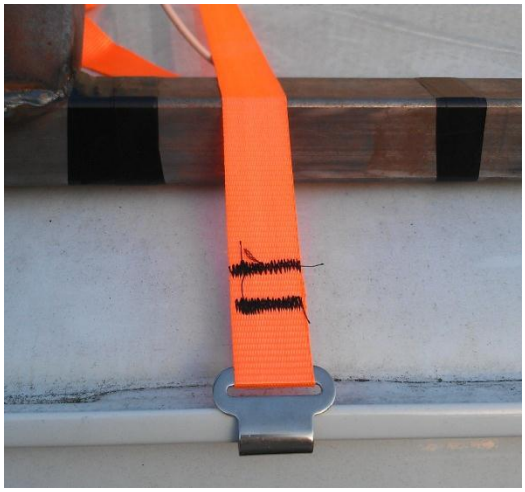

Figure 39. Strap and hook securely fastened to van roof gutter.

Rolling the HPV

To roll the HPV, the front and rear tube clamps must be loosened to allow the roll bar to rotate freely within the clamps. The clamp corresponding to the front support should be completely tightened at this time. Once the front and rear clamps are loosened, the HPV can be rolled by rotating the eyelet on the end of the rolling screw. Take care to stay within the intended range of 0^{o}- 45^{o}. Also note that the ATP can only roll the HPV to the right side. Rolling the incorrect side may damage the rolling screw. Once the desired roll angle has been achieved fully tighten down both tube clamps to secure the HPV before testing.

Pitching the HPV

Before pitching, the HPV must be rolled to the vertical, 0° position. Once positioned correctly, the front support clamp must be loosened to allow the front support to slide freely down the roll tube, as the horizontal distance between the supports changes as the wheelbase is pitched up to down. The pitch angle may now be set by opening the toggle clamp on the rear support collar and turning the eyelet on the bottom of the pitching screw. Do not attempt to actuate the screw when the translational limits of the rear support have been reached, as this may cause damage to the screw. While pitching, make sure that the front support is able to slide freely along the roll tube to accommodate changes in geometry. Once the desired pitch angle is achieved, clamp the front support to the roll tube and close the toggle clamp before testing.

Notes on Aerodynamic Testing

In order to properly perform aerodynamic tests on the HPV, follow the instructions in the previous sections to pitch and roll the fairing to the desired position and prepare the DAQ for data acquisition. Refer to the Safety Considerations section for a reminder on proper operating safety. On a flat, smooth surface, drive the vehicle to the desired speed and begin to log data. Be sure to record the speed of the vehicle to correlate it with the associated drag and lift data. Future improvements to the design may include an onboard anemometer to directly measure wind speed passing the exposed HPV. Refer to the Recommendations section for more information.

Preventative Maintenance

The ATP's design is relatively robust to degradation over time, but a little preventative maintenance can keep the ATP operating smoothly throughout its lifetime.

Unbinding Moving Surfaces

Before using the ATP, all moving surfaces should move freely without binding. Grease should be applied on a regular basis to both the hub bearings and to the ends of both power screws, especially if they begin to bind or are difficult to rotate. The tube clamps should not be greased under any circumstances, but users should check the mating surfaces for rust before each aerodynamic test. If there rust has accumulated on the clamping surfaces, it should be scrubbed with a wire brush until the roll tube can rotate freely. Additionally, the ATP should be stored in a dry area to avoid preventable rusting. If the steel frame is exposed to water, it should be dried off immediately.

Care for the Strain Gauges

The aluminum load cell sections of the supports should be treated with care, since the gauges are especially fragile. To this effect, all leads from gauges should be secured with electrical tape and checked for any areas where snagging may occur. Additionally, the support bolts that clamp the aluminum sections in place should be fully tightened before every aerodynamic test to minimize vibration and ensure safety.

Chapter 5 — Product Realization

This section of the report details the manufacturing processes we employed in the construction of the ATP. This includes specific procedures for fabricating critical components, differences in implementation of parts described in the design packet, and recommendations for future reproduction.

Component Manufacture

Each subsystem of the ATP was constructed in the Cal Poly Mechanical Engineering machine shops, without the use of especially sophisticated machinery. The following subsections discuss the processes employed on each subsystem in detail.

Dropout Pins

The first step in assembling the dropout pins was clamping the 1.5-inch steel round stock in the lathe and cutting two sections to length. Next, we bored out the axle hole using a 0.50-inch drill bit. Finally, using a boring bar, we produced the countersink that matched the depth of each roller bearing. Using a steel tube with an inner diameter just wider than the bearing hole (found in a scrap pile), we fashioned a bearing spacer to press between the inner races of each bearing. By fitting the spacer in the axle hole, sandwiched between the two bearings, the only step that remained was to feed through the 9 mm axle and apply the appropriate number of washers and the two axle nuts.

Figure 40. Dropout pin shown assembled with front fork attached.

Gauged Supports

The gauged supports were produced almost entirely on a hand mill. First, each aluminum section was faced and squared to the larger dimensions of the notched section. Then, 2-inch long sections on either end were milled down to fit within then steel supports. Next, we cut the two notches by plunging through a 0.225-inch end mill. Finally, with the steel square tubes in place over either end of the aluminum sections, we drilled bolt holes to accommodate the #10 socket-head cap screws used to clamp the gauged supports together.

A total of 12 strain gauges are mounted on the ATP. Each support has six gauges, which in turn comprise two Wheatstone bridges – one for measuring bending moments and one for measuring axial forces. We mounted the gauges in the orientation shown in Figure 41. To achieve this, first the mating surface of the aluminum was dry sanded, wet sanded, and cleaned. Then we oriented the gauge using a specific mounting tape. By peeling back the tape with the gauge attached, we could apply glue to the mating surface and reapply the tape to hold the gauge in place while the glue dried. In this way, we took special care to ensure that each gauge was completely secured to the notched aluminum section and oriented to measure the correct strain.

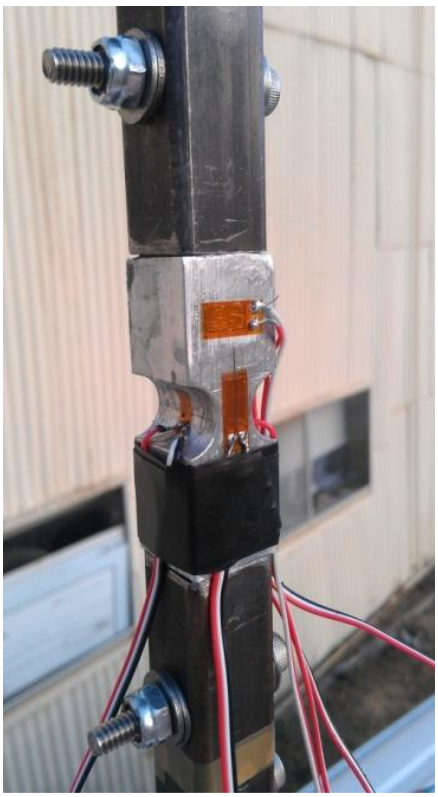

Figure 41. Gauged support shown with gauges in place.

Roll Tube

The only preparation that the roll tube required was cutting a notch in one end using a cut-off wheel to accept the pitching collar. With this notch cut, we inserted the collar in the proper location and MIG welded it in place along with the roll arm. Refer to Figure 42 for a detailed view of the results of this process.

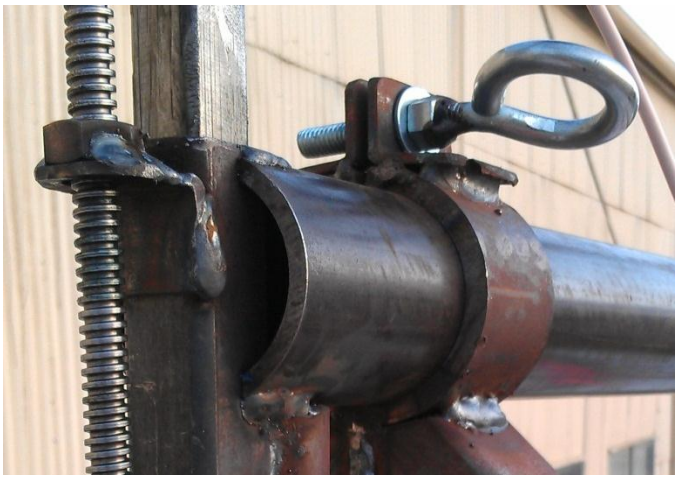

Figure 42. Detail view of roll tube, pitching collar, and winged tube

Winged Tube Clamps

We prepared each of the tube clamps by cutting each to its specified length using a chop saw. With the same saw, we cut a single gap in each to accommodate circumference tightening action of the clamp. Each L-strip was produced from leftover lengths of 1.50-inch square support tubing by cutting along the diagonal with the chop saw and grinding to the proper length. Then we MIG welded the L-strips on either side of the gaps in the tubes. With the welding completed, the tube clamps could be closed with a pair of C-clamps and fixed to the drill press to have through-holes for the eyelet bolts bored out. With the eyelet bolt and nuts inserted through the L-strips and tightened in place, the nut on the end of the eyelet could be welded to the L, and the nut on the eyelet side could be welded to the bolt, in order to accommodate tightening without the use of a wrench. Finally, we MIG welded the shorter two tube clamps to the lower support frame with the roll tube fed through each as a guide.

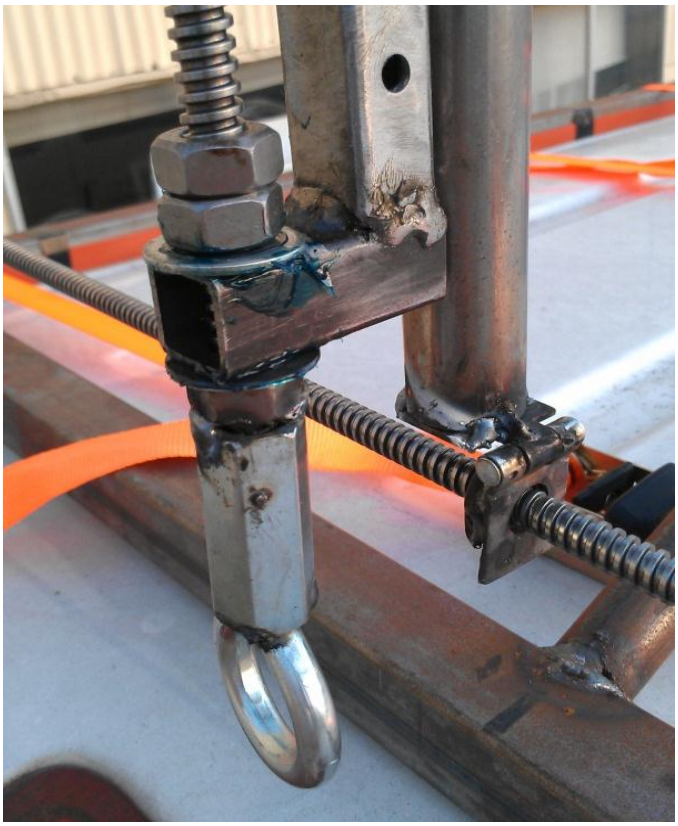

Figure 43. Detail view of bottom of pitching assembly and nut pivot at the end of roll arm.

Pitching Assembly

Construction of the pitching assembly begins with the rear support and collar. In order for the rear support to slide smoothly through the collar, its surface needed to be ground down slightly using a grinding wheel. Once the support was cleanly sliding through the collar, each could have the appropriate hole drilled on the drill press. Next, after drilling a through hole for the 3/8-inch acme screw in left over section from the L-strips described earlier, we MIG welded the nut cup to the collar. Using another leftover

section of the 3/4-inch square tube used for the supports drilled with a through hole for the acme screw, we welded on the seat for the bottom of the support (listed in the bill of materials as the "bottom plate"). By sliding the support through the collar (after it was attached to the roll tube), the acme screw could be fitted in place with one acme nut above the nut cup, two just above the bottom plate, and one just below. With all of these components in place as a sort of jig, we welded the topmost acme nut to the nut cup, and the bottommost nut to the acme screw itself. Finally, we welded the eyelet bolt to the end of the screw, making use of a bolt coupler. Refer to Figures 42 and 43 for detailed images of the pitching assembly's construction, and Figure 45 for a more holistic view of the ATP's pitching jack.

Rolling Assembly

The rolling assembly is comprised of two basic parts: the roll arm, and the ball joint rod end. We constructed the roll arm from the same material used in the stiff crossbar. After cutting it to size on the chop saw, we MIG welded the arm to the roll tube, in parallel with the rear support collar. Then, using a standard door hinge with a 3/8-inch through-hole drilled in one end, we welded the nut pivot to the end of the arm. Next we hand drilled a through-hole for the ball joint rod end in the corner of the lower support frame, and fastened it in place with the provided nuts at a slight upward facing angle. Finally, in the same fashion employed in constructing the pitching assembly, we fed the acme screw through both components, placing one acme nut above the nut pivot, two just above the ball joint rod end, and one just below. We completed the rolling assembly by welding the topmost acme nut to the nut pivot and the bottommost acme nut to the end of the acme screw along with a coupler and eyelet bolt.

Figure 44. Detail view of rolling jack eyelet and lower support frame welds.

Lower Support Frame

The construction of the lower support frame was fairly straightforward. We cut all of the 1.5-inch square tube members to length with the chop saw, adding the 45° angled cuts to the A-frame members as well. Then, by clamping all of the members in place with C-clamps, and using the roll tube as a sort of jig, the members could be tack-welded together, before we solidified everything with thick MIG welds. Figure 44 shows an example of a few of these welds, and Figure 45 shows the entire support frame with a few welds visible.

Figure 45. Full view of lower support frame, pitching assembly, and rolling assembly.

Prototype Implementation Modifications

As alluded to earlier, a few key differences exist between the final design depicted in the manufacturing packet and the final ATP prototype. Refer to the following list for a quick reference of these discrepancies.

- Acme Nut Pivot – Designed to hold an acme nut for the rolling acme screw, the outlined construction was perhaps unnecessarily complicated. Instead, we implemented a small door hinge in replacement. Using the hinge induces a negligible moment on the acme nut, and satisfactorily achieves the necessary degrees of freedom required in actuation of the rolling assembly.
- Acme Screws/Nuts – Instead of welding the screws permanently in place, we chose to lock them using two stacked acme nuts on the upside of the lower pivot. This allows for the acme screws to be easily removed for maintenance. This requires a total of 8 acme screws for the entire ATP rather than the four originally specified.
- Eyelet Cranks – We outfitted each acme screw with an eyelet rather than the hand crank indicated in the CAD model. These eyelets are compatible with the cranking apparatus that would be used to open and close the tube clamps. In this way, limitations on the pitching range associated with protruding hand cranks could be avoided while still maintaining operability while the operator stands on the ground beside the van.
- Dropout Pin Hubs – Each hub was outfitted with a bearing spacer (described in the previous section) to reduce shear stress on the bearings. The spacers are placed inside the hubs between the bearings and make contact with the inner races.

We believe these small changes have improved the ATP's operation with negligible change to the overall design.

Recommendations for Future Production

While the ATP prototype was not designed for multiple reproductions, we have determined a few recommendations for fabrication of other similar prototypes. These include welding at a slower pace as an extra precaution against warping in the materials and constructing more sophisticated jigs for holding components in place during the welding process.

Chapter 6 — Design Verification

To ensure that each of the ATP's critical specifications is met, we have developed a Design Verification Plan (DVP). The DVP is composed of a list of the different tests and how they are linked to specific engineering specifications. The next sections (following presentation of our DVP in Table 4) include brief descriptions of each test, and discuss the results. Refer to Appendix G for established testing procedures. Refer to the Specification Verification Checklist provided in Table 5 to compare engineering specifications to validated, attainable values.

DVPR Sample

The preliminary Design Verification Plan is included in Table 4. This provides an idea of how test results are catalogued and used to confirm whether or not specifications have been met. In the "Test Stage" column, test procedures are categorized by their timing; either in the concept validation (CV), design validation (DV), or product validation (PV) design step.

Table 4. DVP outlining the link between specifications and test procedures.

ATP for Cal Poly HPV Design Verification Plan					
Report Date	6/6/2012		Sponsor	Dr. Kim Shollenberger	
TEST PLAN					
Item No	Specification or Clause Reference	Test Description	Acceptance Criteria	Test Responsibility	Test Stage
1	#1 Vehicle Speed	Maiden voyage, Maximum force test	> 60 mph	All	PV
2	#2 Measure lift force	Lab tension, Maiden voyage	> 100 lbf	Lillywhite	PV
3	#3 Measure drag force	Lab tension, Maiden voyage	> 100 lbf	Lillywhite	PV
4	#4 Pitch fairing	Dry run	> 10 degrees	Davis	PV
5	#5 Roll fairing	Dry run	> 45 degrees	Davis	PV
6	#6 Wheelbase compatability range	Mounting test	36 to 56 inches	Wangerin	DV
7	#7 Frame/dropout compatability range	Mounting test	3 to 6 inches	Wangerin	DV
8	#8 Minimum weight support	Dry run	> 100 lbf	Davis	PV
9	#9 Height of system [with van]	Maiden voyage	14 feet	All	PV
10	#10 Width of system [with van]	Maiden voyage	8.5 feet	All	PV
11	#16 Total weight	Weigh station	< 200 lbf	Wangerin	PV
12	#17 Chip van paint	Paint chip test	No chips	Davis	PV
13	#19 Withstand crosswind	Dropout strength test, Maximum force test	> 30 mph	All	CV,PV
14	#25 Packing volume	Dry run	< 90 cu. feet	Davis	PV
15	#26 Time to install	Maiden voyage	< 30 minutes	All	PV

Mounting Test

The purpose of the Mounting Test is to verify that the wheelbase and frame dropout compatibility ranges are satisfied. The first portion of this test involves attaching the dropout pins to past and current HPV frame dropouts. During this stage, we confirm that the degrees of freedom associated with the pin connection are present and that all of the frames fit correctly. Next, we check to see that the largest range of past and current HPV wheelbases can be accommodated with the roll tube by attaching the HPV to the front and rear gauged supports. For both parts of the test we can accept nothing less than compatibility.

We were unable to perform the mounting test on all past HPV frames because they were either difficult to access or were not fully assembled. However, we did mount three separate frames representing a wide range of wheelbase lengths and variations in dropout separation. All frames were soundly secured and full functionality of the hubs was verified.

Paint Chip Test

This test is fairly simple, and largely self-explanatory. We will gingerly place sections of steel beams with the rubber support feet onto a section of the van's roof and check for paint chipping. If any local chipping does occur, we will need to reassess the rubber protection in this area. Without any significant testing, it is clear that gouging or scratching resulting from insufficient control of the ATP when mounting on the roof will result in damage to the van's paint job. Solutions to these cases include grinding/smoothing all sharp corners, adding handholds for easing the mounting process, and reducing overall weight.

The ATP has proven that it will not chip any paint while mounting or in operation, provided that the user take some care in lifting the platform onto the van roof. The rubber L-sheets protect the van from steel contact at all times.

Dry Run Test

The Dry Run Test is the first step towards implementing the ATP on the van roof. This test consists of fully mounting different HPV frames and fairings onto the ATP and demonstrating/measuring whether or not the specified pitch and roll angles can be achieved. This won't require any special measuring equipment beyond protractors and rulers.

We have verified that the pitching and rolling mechanisms can span and exceed their specified ranges for the three frames described in the mounting test. Refer to the Specification Verification Checklist provided in Table 4 for validated, attainable values.

Weigh Station Test

This is another fairly simple test that confirms whether or not the total weight specification was met. It will require heavy duty scales, which are available at the ME Hangar for automotive weight measurements.

We were unable to perform the Weigh Station Test due to restricted access to automotive scales. However, we can safely say that our actual weight is very close to the weight approximated by our CAD model prototype varied very little from our laid out design. Furthermore, we know the ATP can be comfortably carried by two people and can also be partially disassembled if weight is an issue.

Maximum Force Test

The Maximum Force Test verifies that all of the design loads can be supported by the ATP when it is mounted on the van roof. Essentially, we will attach a simulated HPV to a fixed surface (like a wall or robust pillar) using strapping or rigid cabling and tension to the appropriate magnitude by pressing on the attachment in a transverse direction. Utilizing a fish scale or weight-and-pulley assembly, we can verify that the cable's tension matches the design frontal and/or side drag and confirm that the ATP can withstand these loads safely.

Figure 46. Maximum Force Test shown with a simulated frontal drag of 96 lbs.

Using the simple weight and pulley system shown in Figures 46, 47, and 48, we tested the ATP subjected to the worst-case front and side drag loads. The testing apparatus consisted of a small pulley, a short length of cord, and cinder blocks with known weights. By mounting the frame to the ATP and attaching a cord to the approximate center of mass, we assured that the line of action of the force induced a realistic bending moment on the platform. We secured the pulley at a height that was level with the bike center so that horizontal forces could be applied using the weight of the cinder blocks. To simulate a side wind, the cord was threaded through a pulley which was located to the side of the of the bicycle frame. Likewise, for frontal drag, the pulley was located to the rear of the frame. In this way we tested the ATP's resistance to side forces up to 80 pounds and a frontal drag of up to 96 pounds. Due to lack of additional cinderblocks, we were unable to test up to the 150-pound worst-case frontal load. While the strength of this section does not appear to be in question under the design load, perhaps this test should be repeated with weights exceeding 150 pounds to ensure absolute safety.

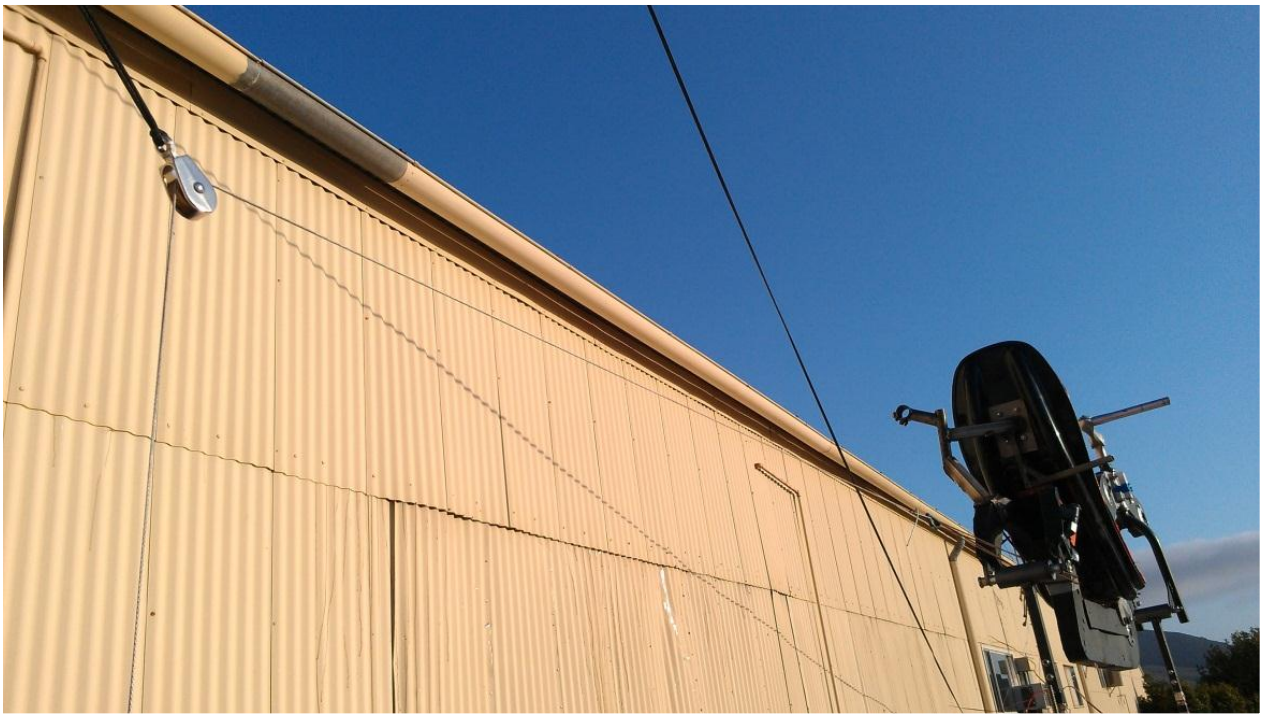

Figure 47. Detail view of pulley and rigging during Maximum Force Test.

Lab Tension Test

This test is designed to calibrate the strain gauges and ensure that they will register the proper lift and drag measurements. With the ATP fully fixed to a ground surface, we will apply known loads to a simulated HPV in a similar fashion as the Maximum Force Test using tensioned cables with calibrated weights and ball-bearing pulleys.

We were unable to fully assemble a completed DAQ, partially due to a lack of access to the proper circuit board. However, Cal Poly does have access to these boards, and they should be implemented before performing aerodynamic testing. Despite lacking the proper boards, we were able to verify that our strain gauge bridges are capable of registering readings when subjected to realistic drag forces on the ATP. As described in the test, we placed the ATP on the ground and used a small scale to apply a load to the bike frame (between 0 and 20 pounds). Using a smaller and less sophisticated, single-bridge board, we observed a significant change in bit output which could be used to correlate to forces applied to the frame.

Figure 48. Detail view of cinderblock weights used in Maximum Force Test.

Specification Verification Checklist

Table 5 in this section reveals how well the ATP meets the original design specifications. Following the table is a brief discussion of the results.

Table 5. Specification Verification Checklist depicting the comparison between specifications and the actual values attained.

	Parameter Description	Requirement or Target	Tolerance	Actual Value	Specification Met
Critical Specifications	Vehicle speed	65 mph	Min	~70 mph	yes
	Time to install	30 min	Max	~25 min	yes
	Measure lift force	100 lbf	Min	~100 lbf	yes
	Measure drag force	100 lbf	Min	~100 lbf	yes
	Pitch fairing	10°	Min	12°	yes
	Roll fairing	45°	Min	50°	yes
	Wheelbase compatibility range	36 to 60 in	Range	10 to 60 in	yes
	Frame/dropout compatibility range	3 to 6 in	Range	3.1 to 6.25 in	yes
	Minimum weight support	100 lbf	Min	~100 lbf	yes
	Height of system [with van]	14 ft	Max	13 ft 10 in	yes
	Width of system [with van]	8.5 ft	Max	~7.0 ft	yes
	Total cost	$2,000.00	Max	$926.93	yes
	Wheels touch ground	no	N/A	no	yes
	Total weight	200 lbf	Max	~180 lbf	yes
	Holes in van roof	no	N/A	no	yes
	Withstand crosswind	30 mph	Min	> 30 mph	yes
	Mounts on Ford E-350 roof rack	yes	N/A	yes	yes
	Fatigue life	1000 hrs	Min	N/A	N/A
Non-Critical Specifications	Measure side forces	100 lbf	Min	no	no
	Length of system [with van]	40 ft	Max	18 ft	yes
	Chip van paint	no	N/A	no	yes
	Flow visualizer density	1 units/sq. ft	Min	N/A	N/A
	Number of camera views	1 view	Min	N/A	N/A
	Model ground effects	yes	N/A	no	no
	Model wheel pumping effects	yes	N/A	no	no
	Measure moments	100 ft-lbf	Max	no	no
	Packing volume	90 cu. ft	Max	no	no
	Yaw fairing	30°	Min	0°	no

As is indicated above, some specifications remain unmet. The only critical specification we were unable to verify was fatigue life. We did not verify this specification because we were unable to design or perform an adequate test. Though we were unable to verify this specification, considering the vibrational analysis presented earlier in this report, it is reasonable to assume that the ATP is safe to operate for a considerable amount of time with respect to fatigue. The aluminum support sections experience the highest stresses and will fatigue the most quickly. These stresses should be monitored using the strain gauges which are already mounted on the ATP.

Additionally, many of the non-critical specifications were also remain unaddressed. These specifications were deemed to be of secondary importance by our sponsor early in the design process. Although, they are not currently met, many of these specifications could be exceeded with small modifications to the

ATP. Refer to the Recommendations section of a discussion of some possible improvements of the ATP to this effect.

Chapter 7 — Management Documentation

Each Team Anemoi member was involved in all of the major phases of this project, but each member specialized and/or took the lead on certain tasks and project subsystems, determined collectively by the group and advisor, Dr. John Ridgely. Below, each member is listed with their primary areas of specialty.

Colburn Davis

Design/Analysis

- Sizing and selection of bearings in dropout hubs
- Implementation of strapping in van/frame interface
- Refinement of screw jacks and supports for rolling and pitching actuation

Testing

- Application of rigging for Maximum Force Test
- Calibration of strain gauges

Manufacturing

- Preparation and compilation of components of rear support
- Reading screw jacks for assembly
- Sewing together strapping and gutter hooks
- Applications of strain gauges

Spencer Lillywhite

Design/Analysis

- Implementation of strain gauge measurement system
- Consideration of vibrational characteristics (hand and FEA)

Testing

- Quantification of flow field
- Collection of vibrational accelerations

Manufacturing

- Complete assembly of load cells before strain gauge attachment
- Fabrication of dropout hubs

Spencer Wangerin

Design/Analysis

- Investigation of structural concerns in lower support frame (hand and FEA)
- Verification of tube clamp feasibility

Testing

- Quantification of dropout strength
- Overseeing of Lab Tension Test

Manufacturing

- Assembly and welding of lower support frame
- Combination of other components through MIG welding
- Fabrication of tube clamps

Schedule of Design Tasks

Refer to Appendix H for a rough outline of the schedule of design tasks over the course of the project.

Chapter 8 — Conclusions and Recommendations

We believe that our ATP design has satisfactorily met the critical specifications of this project, and will therefore provide the Cal Poly HPV Club with a means of performing aerodynamic testing on past and future HPV designs without the use of a full-scale wind tunnel. That said, we have several recommendations for system improvements that we think the club could easily implement with the ATP in their possession. These include the following:

- Pitot Tube – A Pitot tube should be permanently mounted onto the ATP frame near the fairing location to attain actual wind speeds in this location. Currently speed must be visually read from the speedometer of the vehicle. Collecting data from a Pitot tube while simultaneously measuring lift and drag would produce more accurate correlations than using the speedometer.
- Shielded Wire – While testing the strain gauges we noticed considerable noise in the signal. This is partly due to the length of the wires running into the van and could be partly alleviated by using shielded wires to limit interference.
- Swoop Board – To measure lift or drag data from the ATP in real-time, all 12 strain gauges (4 strain bridges) must be simultaneously recorded. This requires the more sophisticated board alluded to earlier (known as a "swoop board") to be implemented.
- Damping on Top Supports – Due to the relatively low stiffness of the upper supports, coupled with the weight of the HPV, the ATP is relatively susceptible to vibration. While it seems that road noise may not appreciably affect the strain signals, modifying the supports to dampen out this vibration would allow for more accurate and safe data to be collection.
- Stronger Toggle Clamp – The toggle clamp used for the prototype proved to be far too weak to fulfill its intended purpose of firmly securing the rear support in the collar. It is possible the toggle clamp was even made inoperable during the welding process. A larger and more forceful toggle clamp could solve this problem and help to reduce vibration in the rear support.
- Lightweight Base Frame – When compared to the sleek upper supports, whose size was dictated by the strains required for measurement, our base frame is much more robust than what is necessary. In subsequent iterations this support frame, weight could be greatly reduced without significantly affecting the ATP's robust nature compared to worst-case loading. This would make the ATP easier to mount and cheaper to construct.
- Ground Plane – As outlined in our specification verification chart, a ground plane wasn't implemented in this prototype. However, adding a ground plane should produce more realistic drag and lift measurements to those that the HPV would see during operation on the racetrack. This could be implemented without much difficulty using the existing base frame.

- Camera – A camera with adjustable attachment mount could be added to the ATP to visualize flow during aerodynamic testing. This would increase the utility of the ATP from a qualitative standpoint for a relatively low cost.

Chapter 9 —References

American Society of Mechanical Engineers. "Rules for the 2012 Human Powered Vehicle Challenge." September 2011.

Cameron, L. A. "Measuring HPV Drag Forces Using and On-board Micro Computer." *Human Power: Technical Journal of the IHPVA.* 12.2 (1995): 7-12. International Human Powered Vehicle Association. Web. 10 Oct. 2011. <www.ihpva.org>

Christensen, Cameron, Christopher Hunt, & Josh Smith. "Human Powered Vehicle Frame." *Cal Poly Human Powered Vehicle Team*. 6 June 2011.

Cunningham, Glen B. "Method for measuring total force in opposition to a moving vehicle." Patent US 7,377,180 B2. 27 May 2008.

Curry, Marty. "Fact Sheets." Dryden Flight Research Center, 9 December 2009. Web. 27 November 2011. <http://www.nasa.gov/centers/dryden/news/FactSheets/FS-015-DFRC.html >

Duryea, George R. JR. "An improved piezo-electric balance for aerodynamic force measurements." *IEEE Transaction on Aerospace and Electronic Systems.* 4.3 (1968): 351-359.

"E Series Wagon Specifications." *Ford Motor Company*. Web. 19 October 2011. <http://www.ford.com/trucks/eseries/specifications/interior/>

Fox, Robert W., Alan T. McDonald, and Philip J. Pritchard. *Introduction to Fluid Mechanics*. 7th ed. Hoboken, NJ: Wiley, 2009. Print.

Ghasemi Nejhad, M. N. et al. "Hurricane: The 1998 University of Hawaii Human Powered Vehicle." *Society for the Advancement of Material and Process Engineering Journal*. 35.2 (1999): 52-57.

Godo, Matthew N., David Corson, & Steve M. Legensky. "An Aerodynamic Study of Bicycle Wheel Performance using CFD." *47th American Institute of Astronauts and Astronautics Aerospace Sciences Meeting*. Orlando, Florida: 2009.

Grappe, Frederic, Robin Candau, Alain Belli, & Jean Denis Rouillon. "Aerodynamic drag in field cycling with special reference to the Obree's position." *Ergonomics*. 1997. 40:12, 1299-1311.

Jayaraman, Divahar. "Panel method based 2-D potential flow simulator." Updated 9 November 2006. MATLAB Central. < http://www.mathworks.com/matlabcentral/fileexchange/12790-panel-method-based-2-d-potential-flow-simulator>

"Kirsten Wind Tunnel." University of Washington Aeronautical Laboratory, 2011. Web.27 November 2011. <http://www.uwal.org/index.html>

Kyle, C. R. & M. D. Weaver. "Aerodynamics of human-powered vehicles." *Proceedings of the Institution of Mechanical Engineers, Part A: Journal of Power and Energy*. 218 (2004).

Lundström, David & Kristian Amadori. "Raven – A subscale radio controlled business jet demonstrator." 26th *International Congress of the Aeronautical Sciences*. (2008).

Mariasiu, Florin. "Benchmark test for a Formula SAE student car prototyping. *Central European Journal of Engineering*. 1.4 (2011): 423-429.

Munro, Cameron, Petter Krus, & Edward Llewellyn. "Captive carry testing as a means for rapid evaluation of UAV handling qualities." *International Congress of the Aeronautical Sciences*. 831.1 (2002).

Munson, Bruce R., Donald F. Young, and Theodore H. Okiishi. *Fundamentals of Fluid Mechanics*. 6th ed. Hoboken, NJ: J. Wiley & Sons, 2009. Print.

Parker, B.A., M.E. Franke, & A.W. Elledge. "Bicycle aerodynamics and recent testing." *34th American Institute of Astronauts and Astronautics Aerospace Sciences Meeting and Exhibit*. Reno, Nevada: 1996.

Pszolla et al. "Simulator for aerodynamic investigations of models in a wind tunnel." Patent 4,658,635. 21 April 1987.

Rae, William H., and Alan Pope. *Low-Speed Wind Tunnel Testing*. 2nd ed. New York [etc.: John Wiley & Sons, 1984. Print.

Raine, J.K. & M.R. Amor. "The design and energy consumption of human-powered vehicle." *International Journal of Vehicle Design.* 12.5-6 (1991): 630-643.

Rose-Hulman Institute of Technology. "2008 Human Powered Vehicle Challenge." University of Central Florida. Web. 15 Oct. 2011. <www.rose-hulman.edu>

"Strain Gage Wind Tunnel Balances." *Modern Machine & Tool Co., Inc.* Modern Machine & Tool Company Inc. Web. 30 Nov. 2011. < http://mmtool.com/balances.html>

Tew, G. S. & A. T. Sayers. "Aerodynamics of yawed racing cycle wheels." *Journal of Wind Engineering and Industrial Aerodynamics*. 82 (1999): 209-222.

Weick, William R. "Human powered vehicle farming: a design and construction summary." *ANTEC Conference Proceedings*. (1986): 1460-1464.

White, Jonathan C. *High-Frame-Rate Oil Film Interferometry*. Thesis. California Polytechnic State University, San Luis Obispo, 2011. *DigitalCommons at Cal Poly*. Web. 10 Oct. 2011. <http://digitalcommons.calpoly.edu/theses/572/>

Appendix A — QFD House of Quality

This Aerodynamic Test Platform for Cal Poly HPV Club House of Quality is the result of QFD analysis based on requirements obtained from the Cal Poly HPV Club.

	Customers (Whos)	**Engineering Specifications (Hows)**																										**Benchmarks (Nows)**			
Requirements (Whats)	HPV Team/Sponsor	Vehicle speed (mph)	Measure lift force (lbf)	Measure drag force (lbf)	Pitch fairing (°)	Roll fairing (°)	Wheelbase compatibility range (in)	Frame/dropout compatibility range (in)	Minimum weight support (lbf)	Height of system [with van] (ft)	Width of system [with van] (ft)	Length of system [with van] (ft)	Total cost ($)	Flow visualizer density (units/sq. ft)	Number of camera views (units)	Wheels touch ground (yes/no)	Total weight (lbf)	Chip van paint (yes/no)	Holes in van roof (yes/no)	Allowable Crosswind (mph)	Mounts on Ford E-350 roof rack (yes/no)	Model ground effects (yes/no)	Model wheel pumping effects (yes/no)	Measure side forces (lbf)	Measure moments (ft-lbf)	Packing volume (cu. ft)	Time to install (min)	Yaw fairing (°)	Fatigue life (hrs)	Scaled wind tunnel testing	Computation fluid dynamics	Coast down tests	Existing aerodynamic test platforms
Needs																															
Approximates free stream	●	Δ	Δ	Δ						○	○	○		Δ															●	○	●	●
Operate at highway speeds	●	●								○						Δ				○		○		○				Δ			●	●
Measure lift force	●	○	●							Δ																			●	○	Δ	Δ
Measure drag force	●	○		●						Δ																		Δ	●	○	●	○
Pitch fairing	●				●					Δ										Δ				○	Δ			○	●	●	Δ	○
Roll fairing	●					●				Δ										Δ				○	Δ			○	●	●	Δ	○
Mount current and past HPVs	●						●	●	●																				●	●	●	●
Mount future designs	●				○	○	●	●	●																				●	●	●	●
Modular	●				○	○	●	●	●					Δ															●	●	●	●
Street legal	○									●	●	●				Δ	○					○									Δ	●
Must meet budget	●												●		○							○		○	○				Δ	●	●	●
Flow visualization	●	Δ			Δ	Δ								●	○													○		●	●	Δ	○
Video camera	●													Δ	●																Δ	○
Mount without damage to fairing	●						○	○	○	○	Δ	Δ								○		○							●	●	○	●
Wheels don't touch ground	●															●				●		○							●	●	●	●
No damage to van	○								○						○	Δ	●	●	○	●		○										●
Safe	●						○	○	●	●	○	○			○	○	○		●	●		○					○		●	●	●	Δ	●
Wants																																
Mount on Ford E-350 roof rack	○						○	○	○	○	○				Δ	Δ	●	Δ		○	●		○			Δ	○					●	○
Model ground effects	○	○												Δ	○	●						●	○	Δ					○	○	●	Δ
Model wheel pumping effects	○	○												Δ	○	●						○	●						○	○	●	Δ
Measure side forces	○	○			○	○				○										Δ				●				Δ		●	○	Δ	Δ
Measure moments	○	○			○	○				○										Δ					●			Δ		●	○	Δ	Δ
Fit inside van for transportation	○									●	●					○	○					Δ	Δ			●					Δ	Δ
Assembles easily	○						○	○		●	○				○		●	○	●		○	Δ	Δ			○	○			Δ	Δ	●	Δ
Assembles fast	○						○	○		●	○				○		●	○	●		○	Δ	Δ			○	●			Δ	Δ	●	Δ
Yaw fairing	Δ																											●		●	○	Δ	Δ
Last for many future tests	○						○	○	○					Δ						Δ									●	●	●	●	●
	Targets	65	100	100	10	45	36 to 60	3 to 6	100	14	8.5	40	2000	1	1	no	200	no	no	30	yes	yes	yes	100	100	90	30	30	100				
● = Strong Correlation	**Scaled wind tunnel testing**		●	●	●	●	●	●	●				Δ			○						○	○	●	●			●					
○ = Medium Correlation	**Computational fluid dynamics**		○	●	●	●	●	●	●				○			○						○	○	○	○			●					
Δ = Small Correlation	**Coast down tests**	●	Δ	●	Δ	Δ	●	●	●				●			●				○		●	●	Δ	Δ		●	Δ					
Blank = No Correlation	**Existing aerodynamic test platforms**	○	Δ	Δ	Δ	Δ	●	●	●	●	●	●	●		Δ	Δ	●	○	○	○	○	Δ	Δ	Δ	Δ	Δ	Δ	Δ	○				

Interpreting the House of Quality

The House of Quality (the results of QFD analysis) shows how needs expressed by the Cal Poly HPV Club and inferred by Team Anemoi were translated into targetable engineering specifications. Figure A1 provides a quick reference to each of the areas of the House of Quality. Needs developed from conversations with representatives from the Cal Poly HPV Club populate the "What" section. Since we are developing the ATP directly for the club, they are the only customer listed in the "Who" section. "Who vs. What" demonstrates the importance of each of the listed needs relative to the customer. We populated the "How" section by converting each Cal Poly HPV Club need into a targetable engineering specification. Similarly, the "What vs. How" shows the correlation between each specification and customer need. Directly below this section, the "How Much" area quantifies each specification with a targetable value, and relates these targets to the upper right section, the "Now." The "Now" area refers to what available benchmarks exist. Finally, the "Now vs. What" demonstrates how well each current solution satisfies the needs of the Cal Poly HPV Club.

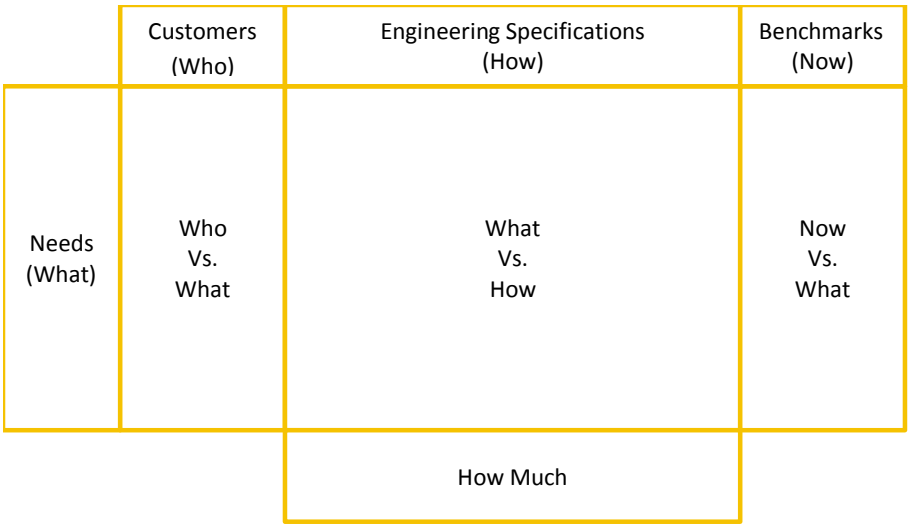

Figure A1 - Quick reference guide for interpreting the House of Quality found in Appendix A.

Appendix B — California State Highway Law

This appendix section outlines the relevant California State highway laws that guide the design process, taken from California Department of Transportation website (www.dot.ca.gov).

35100. (a) The total outside width of any vehicle or its load shall not exceed 102 inches

35111. No passenger vehicle shall be operated on any highway with any load extending beyond the line of the fenders on its left side or more than six inches beyond the line of the fenders on the right side.

35110. Door handles, hinges, cable cinchers, chain binders, and holders for placards warning of hazardous materials may extend three inches on each side of the vehicle.

35250. No vehicle or load shall exceed a height of 14 feet measured from the surface upon which the vehicle stands, except that a double-deck bus may not exceed a height of 14 feet, 3 inches. Any vehicle or load which exceeds a height of 13 feet, 6 inches, shall only be operated on those highways where deemed to be safe by the owner of the vehicle or the entity operating the bus.

35400. (a) A vehicle may not exceed a length of 40 feet. A vehicle is defined in CVC Section 670 as: "a device by which any person or property may be propelled, moved, or drawn upon a highway, excepting a device moved exclusively by human power or used exclusively upon stationary rails or tracks." According to this definition, a vehicle includes a trailer being towed.

35550. (a) The gross weight on any one axle shall not exceed 20,000 pounds, and the gross weight upon any one wheel, or wheels, supporting one end of an axle, shall not exceed 10,500 pounds.

(b) The gross weight limit for any one wheel, or wheels, shall not apply to vehicles the loads of livestock.

(c) The maximum wheel load is the lesser of the following:

(1) the load limit established by the tire manufacturer, on the tire sidewall.

(2) A load of 620 pounds per lateral inch of tire width, as determined by the manufacturer's rated tire width on the tire sidewall. The steering axle, however, must go by the load limit by the tire manufacturer.

Appendix C — Preliminary Hand Analysis

This appendix shows the details of the calculations described in the "Summary of Analysis" section.

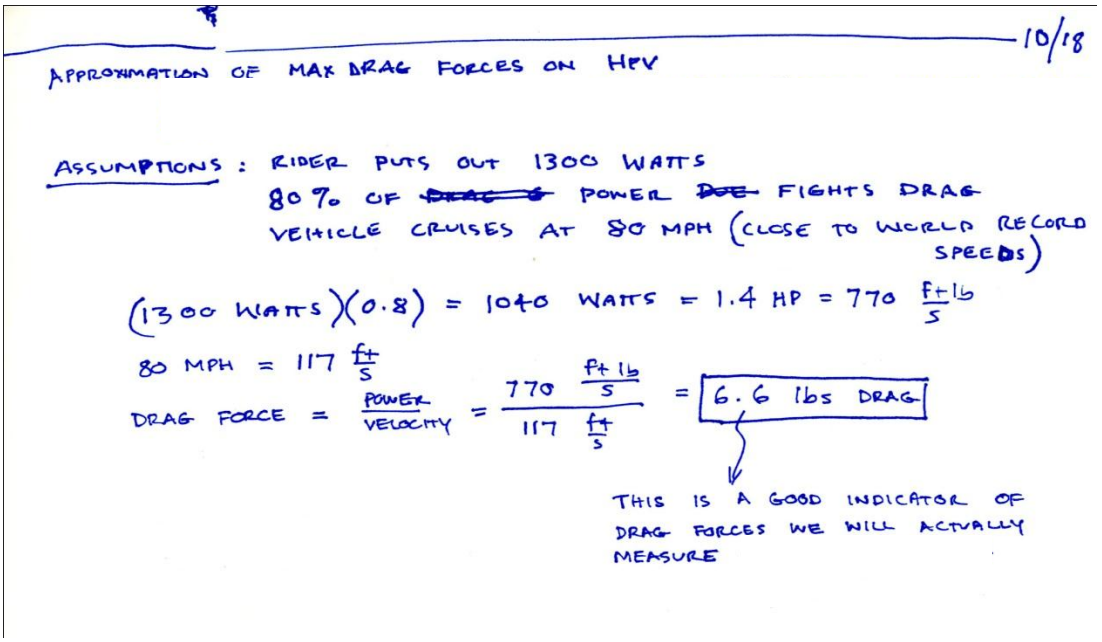

10/18

APPROXIMATION OF MAX DRAG FORCES ON HPV

ASSUMPTIONS: RIDER PUTS OUT 1300 WATTS
80% OF ~~DRAG~~ POWER ~~DOE~~ FIGHTS DRAG
VEHICLE CRUISES AT 80 MPH (CLOSE TO WORLD RECORD SPEEDS)

$(1300 \text{ WATTS})(0.8) = 1040 \text{ WATTS} = 1.4 \text{ HP} = 770 \frac{\text{ft lb}}{\text{s}}$

$80 \text{ MPH} = 117 \frac{\text{ft}}{\text{s}}$

$\text{DRAG FORCE} = \frac{\text{POWER}}{\text{VELOCITY}} = \frac{770 \frac{\text{ft lb}}{\text{s}}}{117 \frac{\text{ft}}{\text{s}}} = \boxed{6.6 \text{ lbs DRAG}}$

THIS IS A GOOD INDICATOR OF DRAG FORCES WE WILL ACTUALLY MEASURE

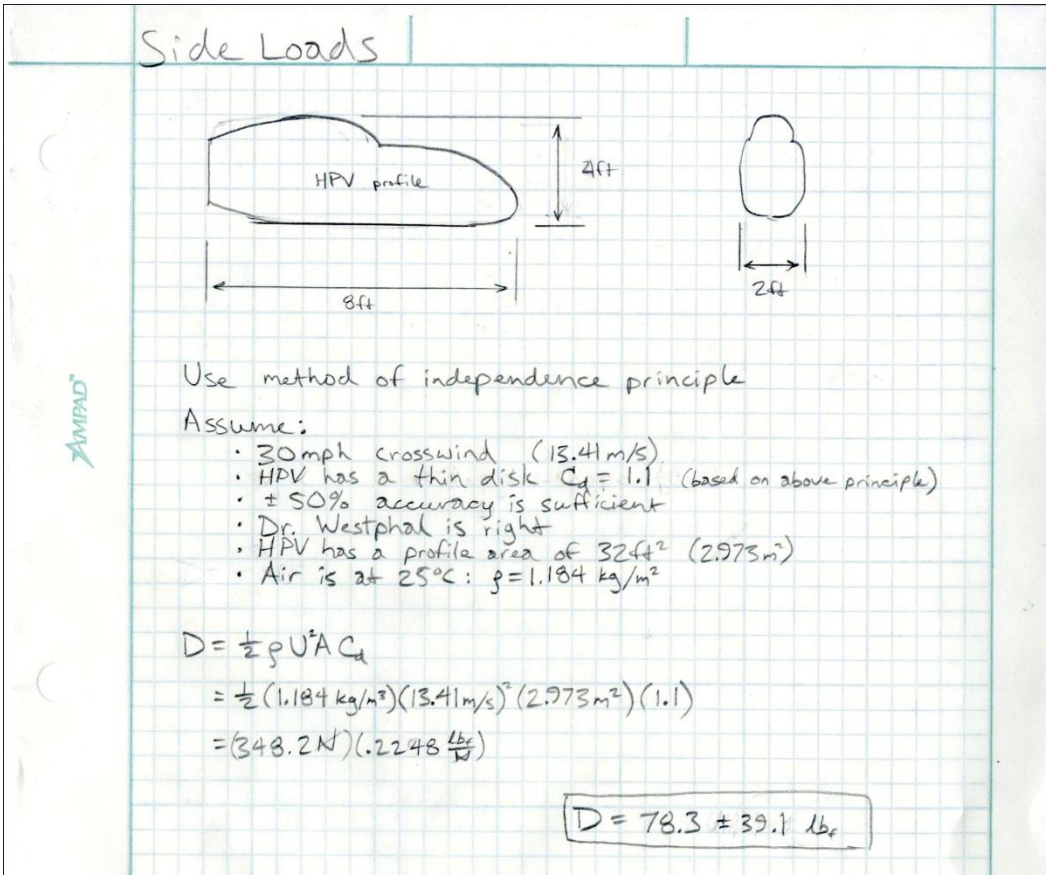

Side Loads

Use method of independence principle

Assume:
- 30mph crosswind (13.41 m/s)
- HPV has a thin disk $C_d = 1.1$ (based on above principle)
- ± 50% accuracy is sufficient
- Dr. Westphal is right
- HPV has a profile area of $32 ft^2$ ($2.973 m^2$)
- Air is at 25°C: $\rho = 1.184 \text{ kg/m}^2$

$D = \frac{1}{2} \rho U^2 A C_d$

$= \frac{1}{2}(1.184 \text{ kg/m}^3)(13.41 \text{ m/s})^2 (2.973 \text{ m}^2)(1.1)$

$= (348.2 \text{ N})(.2248 \frac{\text{lb}_f}{\text{N}})$

$D = 78.3 \pm 39.1 \text{ lb}_f$

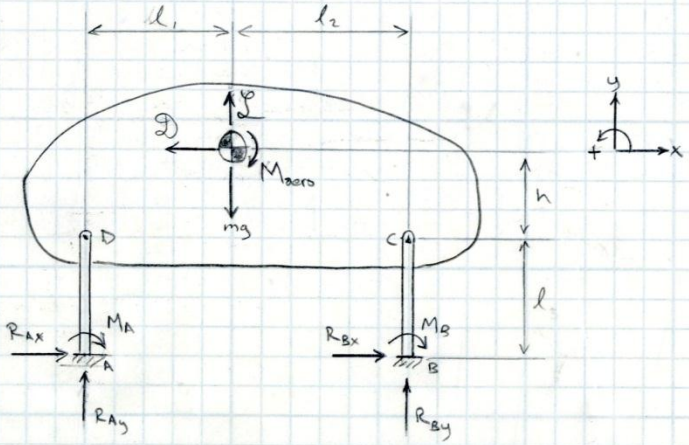

$$\sum F_y = 0 \qquad \mathcal{L} = mg - R_{Ay} - R_{By}$$

$$\sum F_x = 0 \qquad \mathcal{D} = R_{Ax} + R_{Bx}$$

$$\sum M_A = 0 \qquad M_{zero} = \mathcal{D}(l+h) + R_{By}(l_1+l_2) + l_1(mg-\mathcal{L}) - M_A - M_B$$

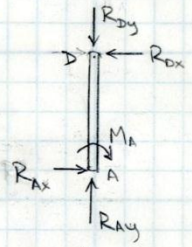

$$\sum F_y = 0 \qquad R_{Dy} = R_{Ay}$$

$$\sum F_x = 0 \qquad R_{Dx} = R_{Ax}$$

$$\sum M_A = 0 \qquad M_A = R_{Dx}\, l = R_{Ax}\, l$$

$$\sigma_{front_A} = \frac{My}{I} - \frac{R_{Ay}}{A}$$

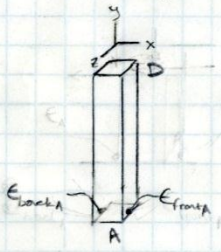

$$\epsilon_{front_A} = \frac{Mc}{EI} - \frac{R_{Ay}}{EA} = \frac{R_{Ax} l c}{EI} - \frac{R_{Ay}}{EA}$$

$$\epsilon_{back_A} = -\frac{Mc}{EI} - \frac{R_{Ay}}{EA} = -\frac{R_{Ax} l c}{EI} - \frac{R_{Ay}}{EA}$$

$$\epsilon_{front_A} - \epsilon_{back} = \frac{2 R_{Ax} l c}{EI}$$

$$* \; R_{Ax} = \frac{EI(\epsilon_{front_A} - \epsilon_{back_A})}{2lc}$$

$$* \; R_{Ay} = -\frac{EA(\epsilon_{front_A} + \epsilon_{back_A})}{2}$$

Statics | Load Cell | 2/

$$* \; R_{Bx} = \frac{EI(\epsilon_{front_B} - \epsilon_{back_B})}{2lc}$$

$$* \; R_{By} = -\frac{EA(\epsilon_{front_B} + \epsilon_{back_B})}{2}$$

} from symmetry

$$\mathcal{D} = \frac{EI}{2lc}\left[(\epsilon_{front} - \epsilon_{back})_A + (\epsilon_{front} - \epsilon_{back})_B\right]$$

$$\mathcal{L} = -\frac{EA}{2}\left[(\epsilon_{front} + \epsilon_{back})_A + (\epsilon_{front} + \epsilon_{back})_B\right] + mg$$

This calculation assumes that both the front & rear supports have identical geometry & that they are both made of the same material. The strains ϵ_{front} & ϵ_{back} will be measured with strain gauges. Length l will be known, based on the chosen design & lengths l_1, l_2, & h can be measured on the HPV. This is a statically indeterminate structure.

Appendix D — Raw RDAS Vibrational Test Data

The graph below depicts the raw vertical vibrational acceleration measured by the RDAS system during the tuft test experiment. The data ranging from around 60 to 170 seconds shows the vertical accelerations for a vehicle speed of 30 mph. The data ranging from around 200 to 270 seconds shows the vertical accelerations for a vehicle speed of 60 mph. By using a Fast-Fourier Transform method, we will be able to understand the vibrational frequencies that are most amplified during roof-top testing.

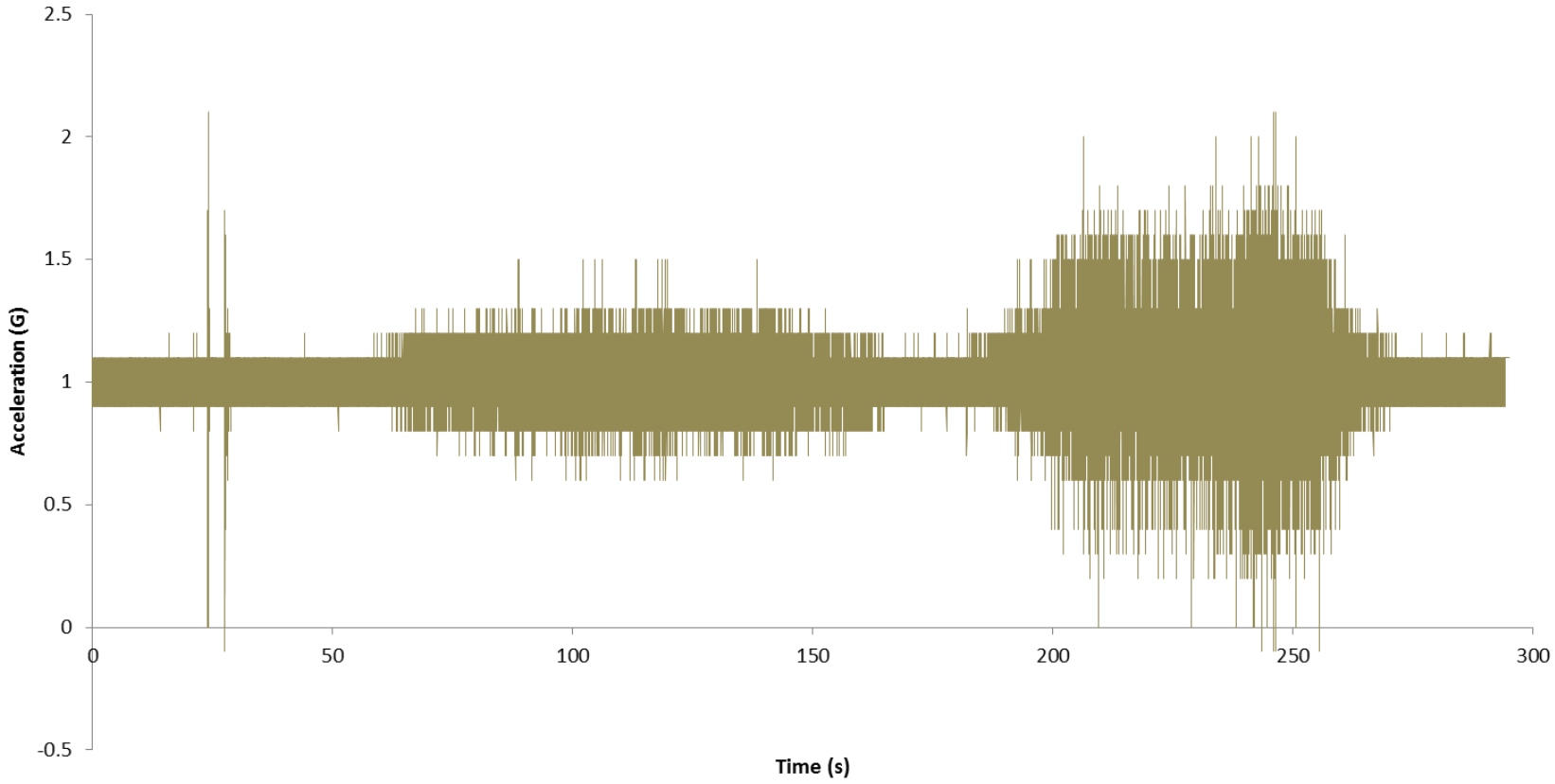

Appendix E — Analysis Results

This appendix displays all hand analysis pertaining to component sizing and strength safety checks. Refer to the titles located at the top of each picture for information about which component the calculation pertains to and/or the design goal.

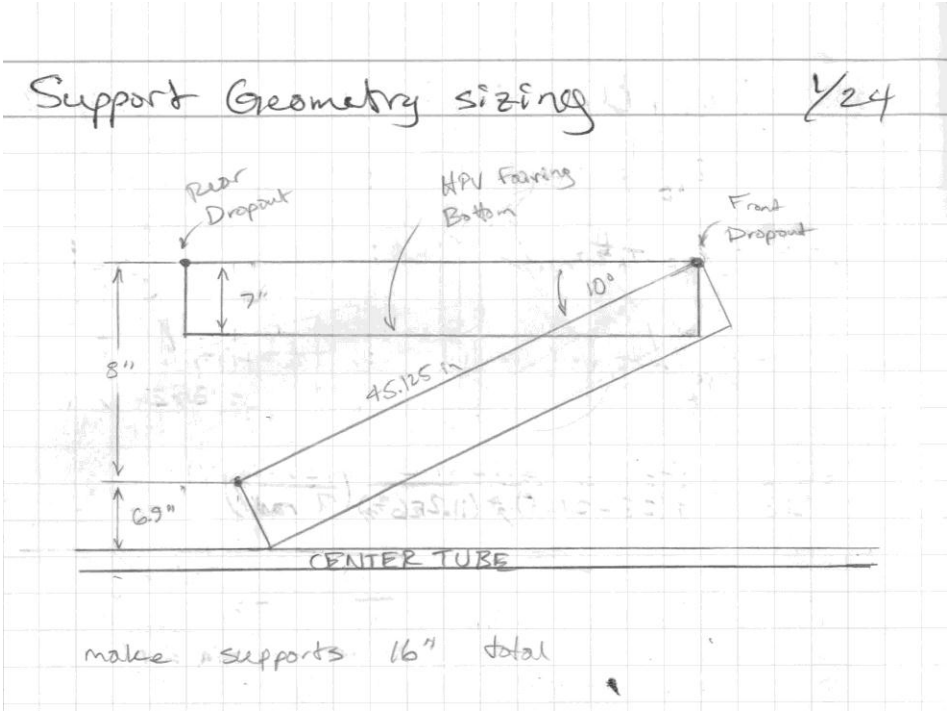

Load Cell Tube Sizing 1/22

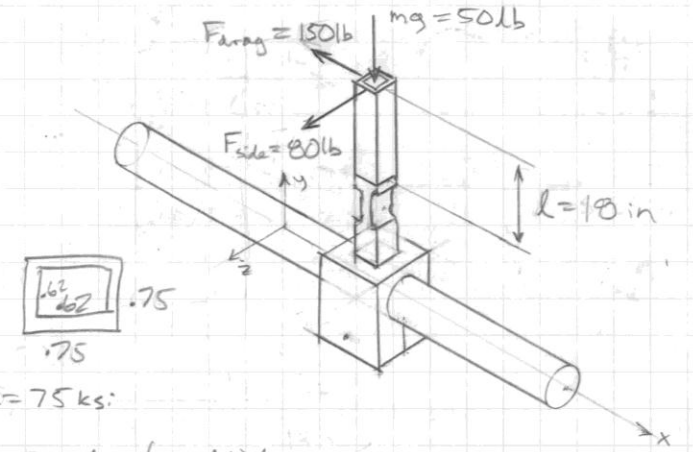

$\sigma_y = 75 ksi$

consider

$M_z = F_{drag} l = (150lb)(18in) = 2700 lb\text{-}in$

$M_y = F_{side} l = (80lb)(18in) = 1440 lb\text{-}in$

$I = \frac{(.75in)^4}{12} - \frac{(.62in)^4}{12} = .01405 in^4$

$\sigma = \frac{Mc}{I} = \frac{(2700 lb\text{-}in)(.375in)}{.01405 in^4} + \frac{50 lb}{(.75in)^2 - (.62in)^2}$

$\sigma = 72.33 ksi$ ✓

or 38.71 ksi in off axis

Assume $\tau = \frac{3V}{2A}$

$\tau = \frac{3(150(b))}{2(.1781 in^2)}$

$\tau = 1263.3 psi$ ✓

FoS = 1.03

Center Tube Calcs

1/14

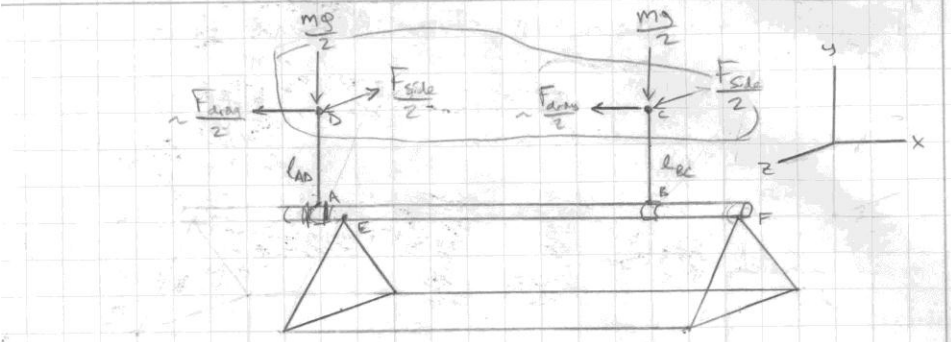

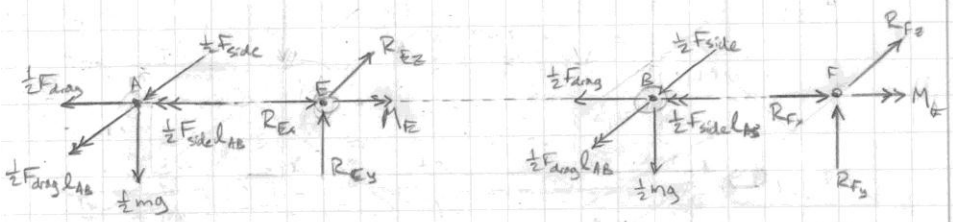

This problem is very statically indeterminate. to simplify, lump loads to the center.

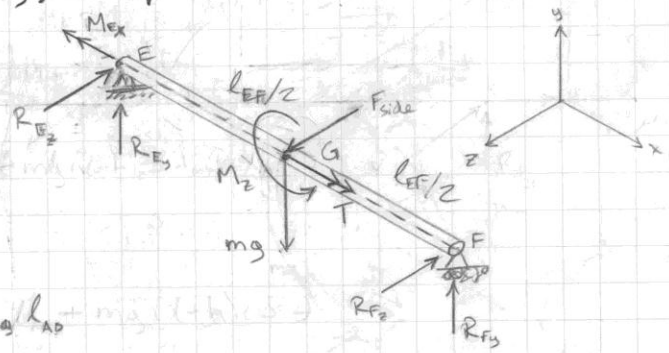

$\theta = 45$

$M_z = F_{drag} l_{AD}$

$T = F_{side} l_{AD} + mg(h + l_{AD})\cos\theta$

$\sum M_x = 0 \qquad M_{Ex} = F_{side} l_{AD} + mg(h + l_{AD})\frac{\sqrt{2}}{2}$

$\sum M_{z\,@E} = 0 \qquad R_{Fy} = \frac{1}{2}mg - F_{drag}\frac{l_{AD}}{l_{EF}}$

$\sum F_y = 0 \qquad R_{Ey} = \frac{1}{2}mg + F_{drag}\frac{l_{AD}}{l_{EF}}$

$\sum F_z = 0 \qquad R_{Ez} = R_{Fz} = \frac{1}{2}F_{side}$

More Center Tube Calcs 1/10

Find extreme normal & shear stress @ pt G

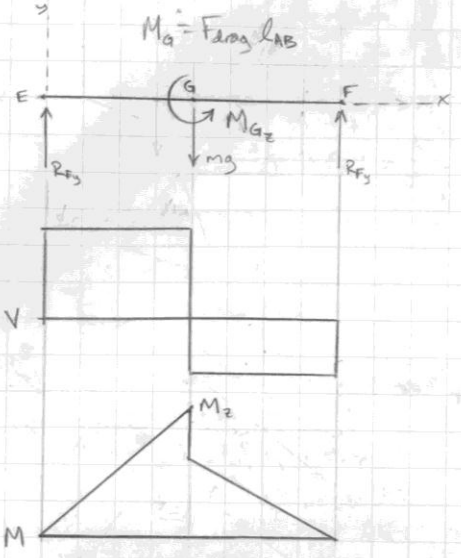

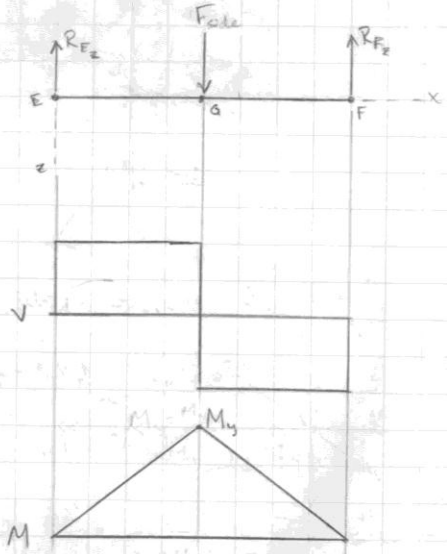

$M_z = \frac{1}{4} mg\, l_{EF} + \frac{1}{2} F_{drag}\, l_{AD}$

$M_y = \frac{1}{2} F_{side}\, l_{EF}$

$M_{max} = \sqrt{M_y^2 + M_z^2}$

$I = \frac{\pi}{64}(D^4 - d^4)$

$J = \frac{\pi}{32}(D^4 - d^4)$

$A = \frac{\pi}{4}(D^2 - d^2)$

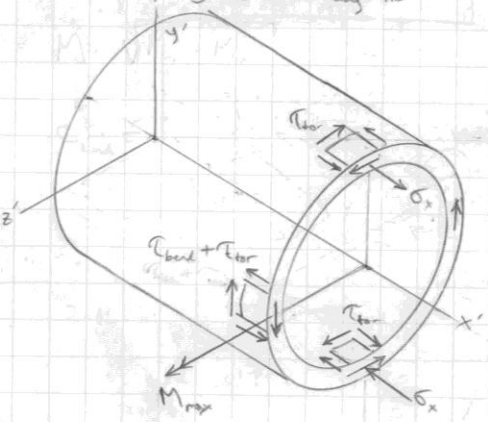

$\sigma_x = \frac{Mc}{I}$

$\sigma_x = \frac{32\sqrt{M_y^2 + M_z^2}\, D}{\pi(D^4 - d^4)}$

$\tau_{torsion} = \frac{Tr}{J}$

$\tau_{tor} = \frac{16\, T D}{\pi(D^4 - d^4)}$

$\tau_{bend_{max}} = \frac{2V}{A}$

$\tau_{bend} = \frac{4\left(mg + 2F_{drag}\frac{l_{AB}}{l_{EF}}\right)}{\pi(D^2 - d^2)}$

Neglect

More Center Tube Calcs 1/21

Return to stress

$$\sigma = \frac{32\sqrt{M_y^2 + M_z^2}\,D}{\pi(D^4 - d^4)}, \qquad \tau = \frac{16\,T\,D}{\pi(D^4 - d^4)}$$

$$M_z = \tfrac{1}{4} m g \ell_{EF} + \tfrac{1}{2} F_{drag} \ell_{AB} = \tfrac{1}{4}(50\text{lb})(72\text{in}) + \tfrac{1}{2}(150\text{lb})(10\text{in})$$

$$\rightarrow M_z = 1650\ \text{lb-in}$$

$$M_y = \tfrac{1}{2} F_{side} \ell_{EF} = \tfrac{1}{2}(80\text{lb})(72\text{in})$$

$$\rightarrow M_y = 400\ \text{lb-in}$$

$$\rightarrow T = 2002\ \text{lb-in}$$

$$\sigma = \frac{32\sqrt{1650^2 + 400^2}\,(\text{lb-in})(2.5\text{in})}{\pi(2.5^4 - 2.124^4)\,\text{in}^4}$$

$$\boxed{\sigma = 2310.7\ \text{psi}}$$

$$\tau = \frac{16\,(2002\ \text{lb-in})(2.5\text{in})}{\pi(2.5^4 - 2.124^4)\,\text{in}^4}$$

$$\boxed{\tau = 1362.4\ \text{psi}}$$

More Center Tube calcs 1/20

Find Deflection in xy & xz planes
the root-sum-square δ in x-y & δ in x-z

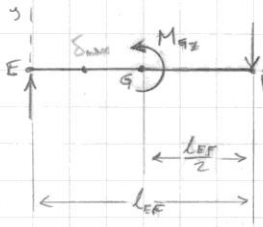

$l_{EF} = 72in$
$l_{AB} = 10in$
$F_{drag} = 150lb$
$F_{side} = 80lb$
$mg = 50lb$

$$M_{GZ} = F_{drag}\, l_{AB} = (150lb)(10in) = 1500lb\text{-}in$$

$$\delta_{EF} = \frac{32 M_{GZ} x}{3\pi E (D^4 - d^4) l_{EG}} \left(x^2 - \frac{1}{4} l_{EF}^2\right)$$

$$= \frac{32(1500lb\text{-}in)x}{3\pi (30E6 \frac{lb}{in^2})(D^4 - d^4)(72in)} \left(x^2 - \frac{1}{4}(72in)^2\right)$$

$$\delta_{EF}\left(\frac{l_{EF}}{4}\right) = 2.358E\text{-}6 \frac{(18in)\, in^2}{(D^4 - d^4) in^4} \left[(18in)^2 - 1296in^2\right]$$

$$\boxed{\delta_{\frac{l_{EF}}{4}} = -\frac{.04253}{D^4 - d^4}\, in}$$

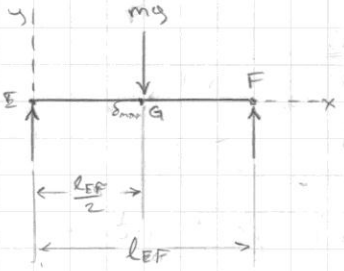

$$\delta_{EG} = \frac{4mgx}{3\pi E (D^4 - d^4)} \left(4x^2 - 3 l_{EF}^2\right)$$

add

$$\delta_{EG}\left(\frac{l_{EF}}{4}\right) = \frac{4(50lb)(18in)}{3\pi (30EG \frac{lb}{in^2})(D^4 - d^4)} \left[4(18in)^2 - 3(72in)^2\right]$$

$$\boxed{\delta_{\frac{l_{EG}}{4}} = -\frac{.18151}{D^4 - d^4}\, in}$$

$$\delta_{EG}\left(\frac{l_{EF}}{2}\right) = \frac{-4(50lb)(72in)^3}{3\pi (30EG \frac{lb}{in^2})(D^4 - d^4)}$$

$$\times \quad \boxed{\delta_{\frac{l_{EG}}{2}} = -\frac{.26402}{D^4 - d^4}\, in}$$

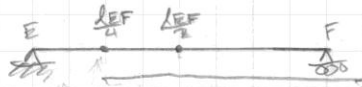

$$\boxed{\delta\left(\frac{l_{EF}}{4}\right) = -\frac{.22277}{D^4 - d^4}\, in} \quad \times \quad \boxed{\delta\left(\frac{l_{EF}}{2}\right) = -\frac{.26402}{D^4 - d^4}\, in} \quad \text{ok}$$

Even More Center Tube 1/20

More deflection

x-z plane

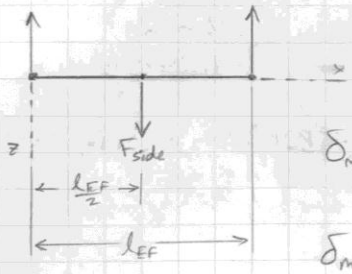

$$\delta_{max} = \frac{4 F_{side} l_{EFF}^3}{3\pi E (D^4 - d^4)}$$

$$\delta_{max} = \frac{4(80lb)(72in)^3}{3\pi (30E6 \frac{lb}{in^2})(D^4 - d^4)}$$

$$\boxed{\delta\left(\frac{l_{EFF}}{2}\right) = \frac{.42243}{D^4 - d^4} in}$$ x-z plane

$$\delta_{max} = \sqrt{\delta_{max_{xz}}^2 + \delta_{max_{yz}}^2}$$

$$= \frac{\sqrt{.4224^2 + .2640^2}}{D^4 - d^4} = \frac{.4981}{D^4 - d^4} in$$

Assume $D = 2in$ $d = 1.75in$

$$\delta_{max} = \frac{.4981}{2^4 - 1.75^4} in$$

$\delta_{max} = .07523 in$

A little high, reiterate

Assume $D = 2.5in$, $d = 2.124in$

$\delta_{max} = .02662 in$

Better

Even More Center Tube Calcs 1/20

Tube deflection in Torsion:

$\theta = \frac{Tl}{GJ}$ Assume: $h = 24$ in, $G = 11.2\text{E}6$ psi

$T = F_{side} l_{AD} + mg(l_{AD}+h)\frac{\sqrt{2}}{2} = (80\text{lb})(10\text{in}) + (50\text{lb})(34\text{in})\frac{\sqrt{2}}{2}$

$\rightarrow T = 2002.\ \text{lb-in}$

$\theta = \frac{16\,T\,l_{EF}}{\pi G(D^4-d^4)} = \frac{16(2002\text{lb-in})(72\text{in})}{\pi(11.2\text{E}6\ \frac{\text{lb}}{\text{in}^2})(D^4-d^4)\text{in}^4}\left(\frac{180\ \text{deg}}{\pi\ \text{rad}}\right)$

$\rightarrow \theta = \frac{3.756}{D^4-d^4}\ \text{deg}$

Assume: $D = 2$in $d = 1.75$in $\theta = .567$ deg ok

Assume: $D = 2.5$in $d = 2.124$in $\theta = .201$ deg ok

More Center Tube Calcs.

Change $l_{AD} = 18"$ from 10"

$M_z = \frac{1}{4}mgl_{EF} + \frac{1}{2}F_{drag}l_{AB} = \frac{1}{4}(50\text{lb})(72\text{in}) + \frac{1}{2}(150\text{lb})(18\text{in})$

$\rightarrow M_z = 2250\ \text{lb-in}$

$M_y = T = F_{side}l_{AD} + mg(l_{AD}+h)\frac{\sqrt{2}}{2} = (80)(18)+(50)(42)\frac{\sqrt{2}}{2}$ in-lb

$\rightarrow M_y = 2924.9$ in-lb

$\theta = \frac{TL}{JG} = \frac{(2924.9\text{in-lb})(72\text{in})16}{\pi(2.5^4-2.124^4)\text{in}^4(11.2\text{E}6\frac{\text{lb}}{\text{in}^2})}\left(\frac{180\ \text{deg}}{\pi\ \text{rad}}\right)$

$\theta = .293°$ ✓

not a big deal

2.5" OD x .188" Tube still works!

Load Cell Sizing 1/5/12

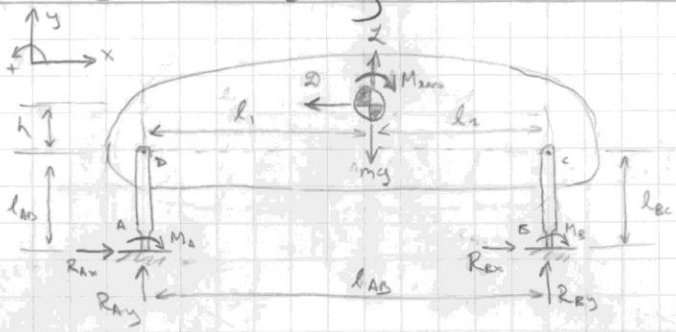

Want: moment of inertia I; length l_{BC}, l_{AD}

Know: modulus E; weight mg; wheelbase l_{AB}; strains ϵ_{front_A}, ϵ_{back_A}, ϵ_{front_B}, ϵ_{back_B}

Unknown: center of gravity location h, l_1, l_2; reaction forces R_{Ax}, R_{Ay}, R_{Bx}, R_{By}; drag D; lift L; pitching moment M_{zero}

Assumed Values: drag D; lift L; pitching moment M_{zero}, K stress concentration

Design Decision: length l_{AD} l_{BC}

$$L = mg - R_{Ay} - R_{By}$$

$$L = mg - \tfrac{1}{2} E A (\epsilon_{front_A} + \epsilon_{front_B} + \epsilon_{back_A} + \epsilon_{back_B})$$

$$\boxed{A = \frac{2(mg - L)}{E(\epsilon_{fA} + \epsilon_{fB} + \epsilon_{bA} + \epsilon_{bB})}}$$

Load cell cross-sectional area based on lift forces

More Load Cell Sizing 1/12

$$D = R_{Ax} + R_{Bx}$$

$$D = \frac{EI}{2lyK_t}\left[(\epsilon_A+\epsilon_B)_{front} - (\epsilon_A+\epsilon_B)_{back}\right]$$

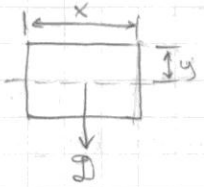

$$I = \frac{bh^3}{12} = \frac{x(2y)^3}{12} = \frac{2xy^3}{3}$$

$$D = \frac{Exy^2}{3lK_t}\left[(\epsilon_A+\epsilon_B)_{front} - (\epsilon_A+\epsilon_B)_{back}\right]$$

$$\boxed{xy^2 = \frac{3lK_tD}{E\left[(\epsilon_A+\epsilon_B)_{front} - (\epsilon_A+\epsilon_B)_{back}\right]}}$$

Return to Load Cell Sizing 1/28/12

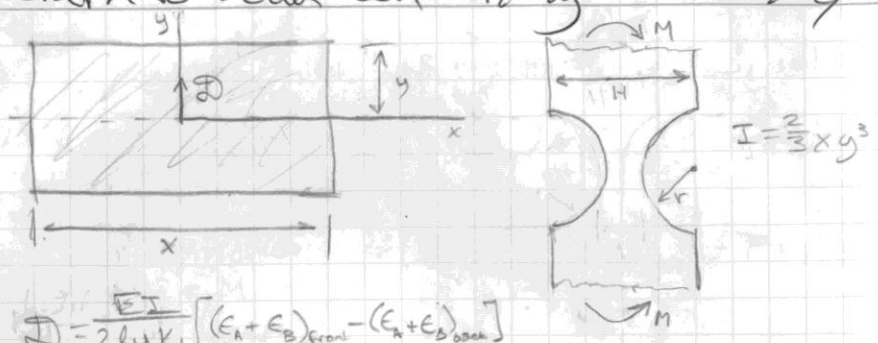

$I = \frac{2}{3} x y^3$

$$D = \frac{EI}{2lyK_t}\left[\underbrace{(\epsilon_A+\epsilon_B)_{front}-(\epsilon_A+\epsilon_B)_{back}}_{4\epsilon_{avg}\text{ - assumption}}\right]$$

$$\frac{3K_t D l}{4Exy^2} = \epsilon_{avg}$$

$$\epsilon = \frac{3K_t D l}{Ex(H-2r)^2} \qquad \sigma_{max} = \frac{K_t 3lD_{max}}{(H-2r)^2 x}$$

$H = x = .75in$ $\quad 2y = H-2r \quad y = \frac{1}{2}(H-2r)$

$3in < l < 15in$ $\quad r = \frac{1}{2}(H-y)$

$E = 10.4E6\ psi$

$S_y = 56\ ksi$

$\epsilon = 500\ \mu\epsilon$

$D = 10lb$

$D_{max} = 150lb$

$$K_{tn} = 3.065 - 6.633\left(\frac{2r}{H}\right) + 8.229\left(\frac{2r}{H}\right)^2 - 3.663\left(\frac{2r}{H}\right)^3$$

Choose: $r = .225in$ $\sim 7/32"$

Aluminum 7075 Alloy

More Load Cell Calcs 1/1/12

$I = \frac{(.30in)(.75in)^3}{12} = .01055\ in^4$

Side Load strength of Notch

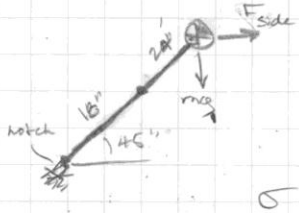

from torsion calc,

$M \sim \frac{I}{2} = \frac{2000 lb\text{-}in}{2} = 1000 lb\text{-}in$

$\sigma = \frac{Mc}{I} = \frac{(1000lb)(.375in)}{.01055in^4}$

$\sigma = 35556 psi$

$SY = 57 ksi$

$FOS = 1.575$

PRELIMINARY WORST CASE FORCE ESTIMATION 1/10/12

KNOWN: A_S, SIDE AREA A_F, FRONT AREA
ρ, AIR DENSITY U, FREE STREAM VELOCITY

FIND: D_S AND D_F

ASSUME: CONTRIBUTION OF α NEGLIGIBLE IN FRAME
SIDE AND FRONT HAVE $C_D = 1.0$

ANALYSIS:

$$D = \frac{1}{2}\rho U^2 A C_D = \frac{1}{2}\rho U^2 A$$

WORST CASE U: $U_S = 30$ MPH, $U_F = 70$ MPH

PRELIMINARY (cont'd) 1/11/12

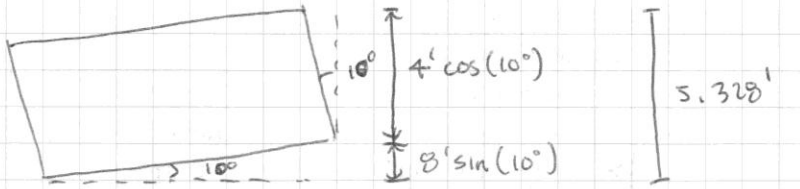

THUS $A_f = (5.328')\cdot(2') = 10.657 ft^2 = 1534.58 in^2$
(HEIGHT, WIDTH)

$A_s = (8')(4') = 32 ft^2 = 4608 in^2$
(LENGTH, HEIGHT)

NOTE: THESE ARE VERY CONSERVATIVE ESTIMATES OF AREA (FLAT PLATE VS. ACTUAL HPV)

$\rho = 2.571E\text{-}3$ slugs/ft^3 [MUNSON, p. 717]

$U_s = [30 \text{ MPH}]\left[\frac{hr}{3600s}\right]\left[\frac{5280 ft}{mi}\right] = 44 ft/s$

$U_f = [70 \text{ MPH}]\left[\frac{hr}{3600s}\right]\left[\frac{5280 ft}{mi}\right] = 102.67 ft/s$

$D_s = \frac{1}{2}\rho U_s^2 A_s C_D = \frac{1}{2}(2.571E\text{-}3 \frac{slug}{ft^3})(44 ft/s)^2(32 ft^2)(1.0)$

$\boxed{D_s = 79.64 \text{ lbf}}$

$D_f = \frac{1}{2}\rho U_f^2 A_f C_D = \frac{1}{2}(2.571E\text{-}3 \frac{slug}{ft^3})(102.67 ft/s)^2(10.657 ft^2)(1.0)$

$\boxed{D_f = 144.40 \text{ lbf}}$

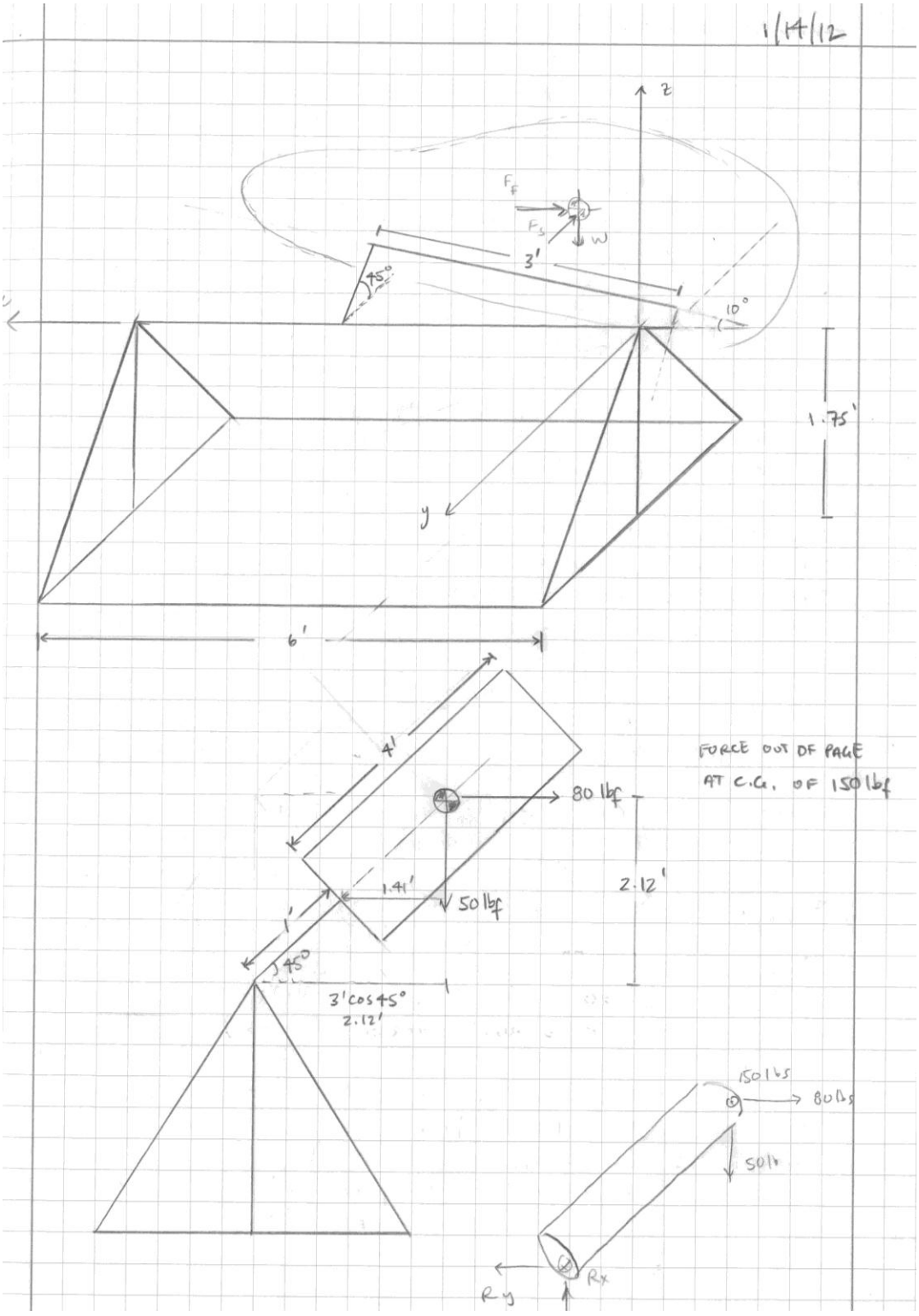
1/14/12
z
F_F
F_s
W
3'
45°
10°
1.75'
y
6'
4'
80 lbf
1.41'
50 lbf
2.12'
1'
45°
3'cos45°
2.12'
FORCE OUT OF PAGE
AT C.G. OF 150 lbf
150 lbs
80 lbs
50 lbs
Rx
Ry

SUPERPOSITION ON LOWER FRAME (1) 1/18/12

START WITH AXIAL FORCES FIRST

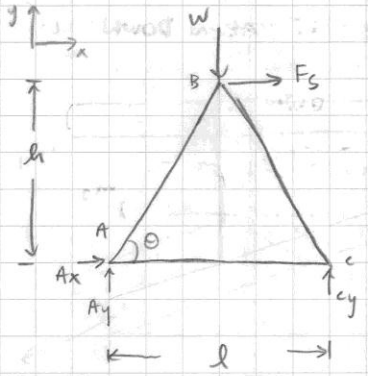

$\Sigma F_y = 0 = A_y + C_y - W$

$\Sigma F_x = 0 = A_x + F_S$

$\boxed{A_x = -F_S}$

$\Sigma M_A = 0 = -W\frac{l}{2} - F_S h + C_y l$

$\boxed{C_y = \frac{W}{2} + F_S\frac{h}{l}}$

$\boxed{A_y = \frac{W}{2} - F_S\frac{h}{l}}$

$\theta = \tan^{-1}\left(\frac{2h}{l}\right)$

JOINT A

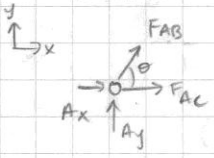

$\Sigma F_y = 0 = A_y + F_{AB}\sin\theta$

$F_{AB} = \left(-\frac{W}{2} + F_S\frac{h}{l}\right)\frac{1}{\sin\theta}$

$\Sigma F_x = 0 = A_x + F_{AC} + F_{AB}\cos\theta$

$F_{AC} = -F_{AB}\cos\theta - A_x$

$F_{AC} = F_S - \left(-\frac{W}{2} + F_S\frac{h}{l}\right)\frac{\cos\theta}{\sin\theta}$

$= \frac{W}{2\tan\theta} + F_S - F_S\frac{h}{l\tan\theta}$

$= \frac{W}{2}\cdot\frac{l}{2h} + F_S - F_S\frac{h}{l}\cdot\frac{l}{2h}$

$= \frac{Wl}{4h} + \frac{F_S}{2}$

JOINT C

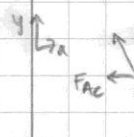

$\Sigma F_y = 0 = C_y + F_{BC}\sin\theta$

$F_{BC} = -\left(\frac{W}{2} + F_S\frac{h}{l}\right)\frac{1}{\sin\theta}$

$\Sigma F_x = 0 = -F_{AC} - F_{BC}\cos\theta$

$F_{AC} = \left(\frac{W}{2} + F_S\frac{h}{l}\right)\frac{\cos\theta}{\sin\theta}$

$= \frac{W}{2\tan\theta} + F_S\frac{h}{l\tan\theta}$

$= \frac{W}{2}\frac{l}{2h} + F_S\frac{h}{l}\frac{l}{2h}$

$= \frac{Wl}{4h} + \frac{F_S}{2}$

SUPERPOSITION ON LOWER FRAME (2) 1/18/12

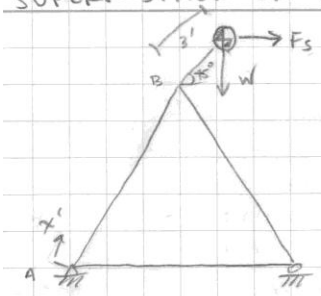

JUST ANALYZE BENDING MOMENT NOW

ASSUME ALL MOMENT TAKEN DOWN LEFT LEG (HUB PINS/CLAMPS NOT ALL SECURE IN ABOVE ASSEMBLY).

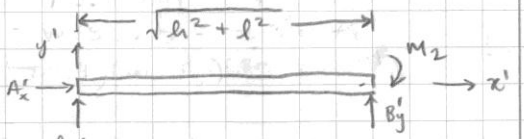

$$M_2 = W(3'\cos 45^\circ) + F_S(3'\sin 45^\circ)$$
$$= (2.121)(W + F_S)$$

$$\Sigma M_A = -M_2 + B_y'\left(\sqrt{h^2+l^2}\right) = 0$$

$$B_y = \frac{M_2}{\sqrt{h^2+l^2}}$$

$$\Sigma F_x = 0 = A_x'$$

$$\Sigma F_y = 0 = A_y' + B_y'$$

$$A_y = -\frac{M_2}{\sqrt{h^2+l^2}}$$

$$\sigma_{AX} = \frac{P}{A} \qquad \sigma_b = \frac{Mc}{I} \qquad \tau = \frac{V}{A}$$

$$\sigma_{TOT} = \sigma_{AX} + \sigma_b$$

LET $l = 56"$, $h = 28"$

$F_{AB} = 21.21$ lbf (T)
$F_{AC} = 65.0$ lbf (T)
$F_{BC} = 91.92$ lbf (C)

$M = 3309.26$ in-lbf

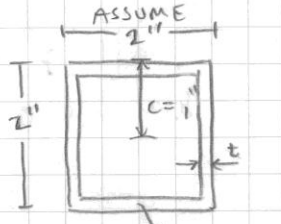

$A = 4 \cdot 1\text{in}^2 - (2" - 2t)^2$
$E = 30E6$ psi
$I = \frac{1}{12}(2")^4 - \frac{1}{12}(2" - 2t)^4$

ASSUME SHEAR NEGLIGIBLE COMPARED WITH BENDING

BY MMS FAILURE CRITERION WITH $\sigma_z = \tau_{xy} = 0$

$$\frac{S_y}{FS} \geq \sigma_{TOT}$$

LOWER FRAME SIZING (cont'd) 1/19/12

FOR WORST CASE AXIAL FORCE (MEMBER Bc):

$$\frac{\sigma_{ys}}{FS} \geq \frac{91.92\ lbf}{4\ in^2 - (2" - 2t)^2} + \frac{3309.26\ in\text{-}lbf}{\frac{1}{12}(2")^4 - \frac{1}{12}(2" - 2t)^4}$$

FOR FS = 2.5 AND σ_{ys} = 24E3 psi AISI 1006 HR

SOLVING FOR t [ON CALC.]

$t \geq 0.0734"$

NOW ASSUME

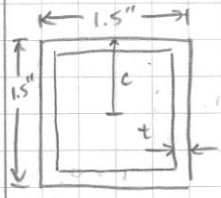

$c = 0.75"$

$A = 1.5^2 - (1.5 - 2t)^2$

$I = \frac{1}{12}(1.5)^4 - \frac{1}{12}(1.5 - 2t)^4$

FOR FS = 2.5 AND σ_{ys} = 24E3 psi AISI 1006 HR

$t \geq 0.2636"$

$$\frac{23E4\ psi}{FS} \geq \frac{91.92\ lbf}{4" - (2" - 2(.120"))^2} + \frac{3309.26\ in\text{-}lbf}{\frac{1}{12}(2")^4 - \frac{1}{12}(2" - 2(.120"))^4}$$

FS = 3.81

CLAMPING SUPPORT DESIGN 1/20/12

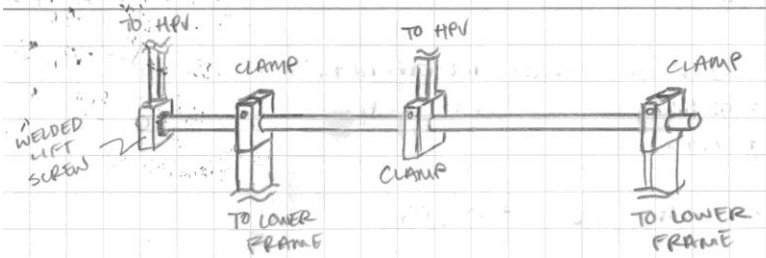

DUE TO WELD ON LEFT HPV SUPPORT, ASSUME FRAME CLAMPS SUPPORT MORE TORQUE (I.E. ARE MORE CRITICAL)

ASSUME WORST CASE, ONE CLAMP NOT FULLY TIGHTENED AND SINGLE CLAMP MUST SUPPORT ALL OF TORQUE

ALSO, ASSUME REQUIRED CLAMPING FORCE TO RESIST AXIAL SLIPPAGE IS NEGLIGIBLE (FOR NOW)

TORQUE IN ROLL BAR

$T = 36'' \sin 45° (F_s + W)$

$= 3309.26$ in-lbf

$F_s = 80$ lbf

$W = 50$ lbf

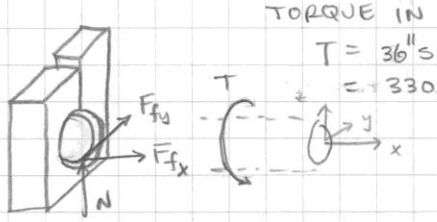

$F_{fy} \geq \frac{T}{r} \cdot FS \Rightarrow \mu_s N \geq \frac{T}{r} \cdot F_s$

ASSUME $\mu_s = 0.6$ [hypertextbook.com/facts/2005/steel.shtml] COMPARES MULTIPLE SOURCES

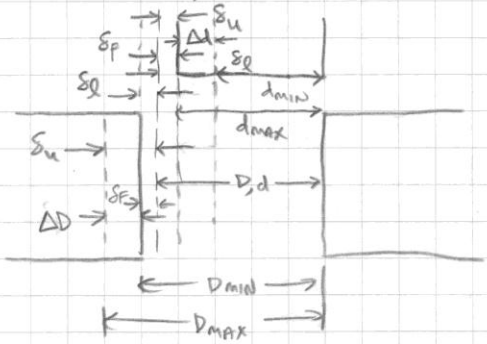

HOLE

$D_{MAX} = D + \Delta D$

$D_{MIN} = D$

SHAFT

$d_{max} = d + \delta_F$

$d_{min} = d + \delta_F + \Delta d$

FOR INTERFERENCE

$\delta = d_{SHAFT} - d_{HUB}$

$\delta_{MIN} = d_{MIN} - D_{MAX}$

$\delta_{MAX} = d_{MAX} - D_{MIN}$

D = NOM. HOLE SIZE

ΔD = TOL. GRADE HOLE

d = NOM. SHAFT SIZE

δ_F = FUND. DEV.

Δd = TOL GRADE SHAFT

$$p = \frac{E\delta}{2d^3}\left[\frac{(d_o^2 - d^2)(d^2 - d_i^2)}{d_o^2 - d_i^2}\right]$$

P.397 SHIGLEY'S

CLAMPING SUPPORT DESIGN (cont'd)

MCMASTER PT# 8995K7 2.500" ± 0.020" OD
0.188" WALL THICKNESS ± .0282"

$d_{SHAFT,MAX} = 2.52"$
$d_{SHAFT,MIN} = 2.48"$

FOR THIS SHAFT SIZE, $\delta_F = +0.0034"$

LET $d = 2.500"$, $E = 30E6$ psi ASSUME $\delta = .0007$
$d_i = 2.124"$ $\delta = d_{SHAFT} - d_{HUB}$ $d_o =$

$$P = \frac{(30E6\ psi)(.0007)}{2(2.500")^3}\left[\frac{(d_o^2 - 2.5"^2)(2.5"^2 - 2.124"^2)}{d_o^2 - 2.124"^2}\right]$$

$N = P \cdot A = P\left(2\pi \frac{d}{2} l\right)$ WHERE LET $l = 2"$, FS = 4.0

$$(0.6)P\left(2\pi(2")\frac{2.5}{2}\right) \geq \frac{2(3309.26\ lbf)}{\uparrow}(4.0)$$

FROM CALC: $d_o \geq 7.064$ in
(SEE ATTACH EES CODE, VALIDATED BY ABOVE CASE)

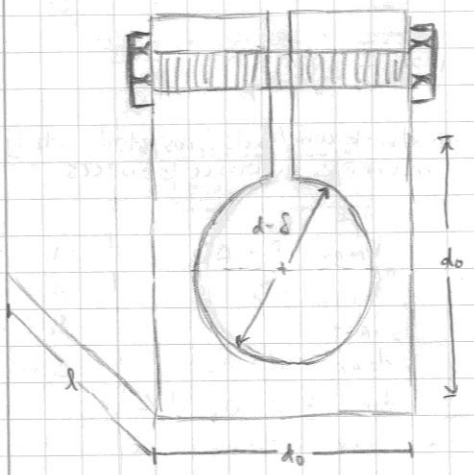

FOR $\delta = 0.001"$
$\delta_o = 3.5"$
$d = 2.5"$
$l = 2.0"$
$\mu_s = 0.6$

$\Rightarrow$ FS = 4.607

"Interference Fit Calculation"
"This program calculates the interference required between the clamping blocks and the roll tube to achieve the necessary
pressure to prevent slippage with the HPV fully loaded and rolled."

"Assumptions"
"Single clamp must support all of the torque on the roll tube."

"Known Information"

F_s = 80	[lbf]
W = 50	[lbf]
T= 36*sin(45)*(F_s+W)	
d = 2.500	[in]
E = 30e6	[psi]
thick = 0.188	[in]
d_i = d-2*thick	
delta = 0.007958	[in]
d_o = 3.0	[in]
L =2.0	[in]
mu_s = 0.6	
"FS = 4.0"	

"Analysis"

p = (E*delta)/(2*d^3)*(((d_o^2-d^2)*(d^2-d_i^2))/(d_o^2-d_i^2))
N = p*A
A = pi*d*L
mu_s*N = 2*T/d*FS

"Results"

A=15.71	E=3.000E+07 [psi]	N=127826
d=2.5 [in]	FS=28.97	p=8138
delta=0.007958 [in]	F_s=80 [lbf]	T=3309 [in]
d_i=2.124	L=2 [in]	thick=0.188 [in]
d_o=3 [in]	mu_s=0.6	W=50 [lbf]

CLAMPING SUPPORT REDESIGN 1/23/12

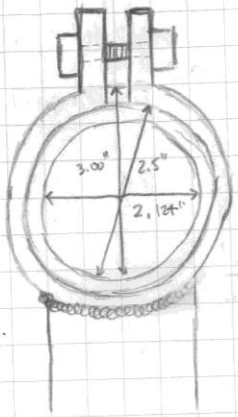

$d_o = 3.00"$
$d_i = 2.124"$
$d = 2.5"$

$C_{NOM} = \pi d$

AFTER CUTTING OUTER TUBE (BANDSAW BLADE THICKNESS)

$C_{HUB} = \pi d - 0.025" = \pi(2.5") - 0.025" = 7.82898"$

$d_{HUB} = \frac{C_{HUB}}{\pi} = 2.49204"$

$\delta = d_{SHAFT} - d_{HUB} = 0.007958"$ IF FULLY CLOSED

LET $E = 30E6$ psi

$$P = \frac{(30E6\ psi)(0.007958")}{2(2.500")^3}\left[\frac{(3.0"^2 - 2.5"^2)(2.5"^2 - 2.124"^2)}{(3.0"^2 - 2.124"^2)}\right]$$

$= 8137.42$ psi

LET $L = 3"$

$N = pA = p(\pi dL) = (8137.42\ psi)(\pi)(2.5")(3") = 191733\ lb_f$

$\mu_s N \geq \frac{2T}{d} FS$

$(0.6)(191733\ lb_f) = \frac{2(3309.26\ in\text{-}lb_f)}{(2.5")} FS$

$FS = 43.45$

ROLLING JACK ASSEMBLY 1/28/12

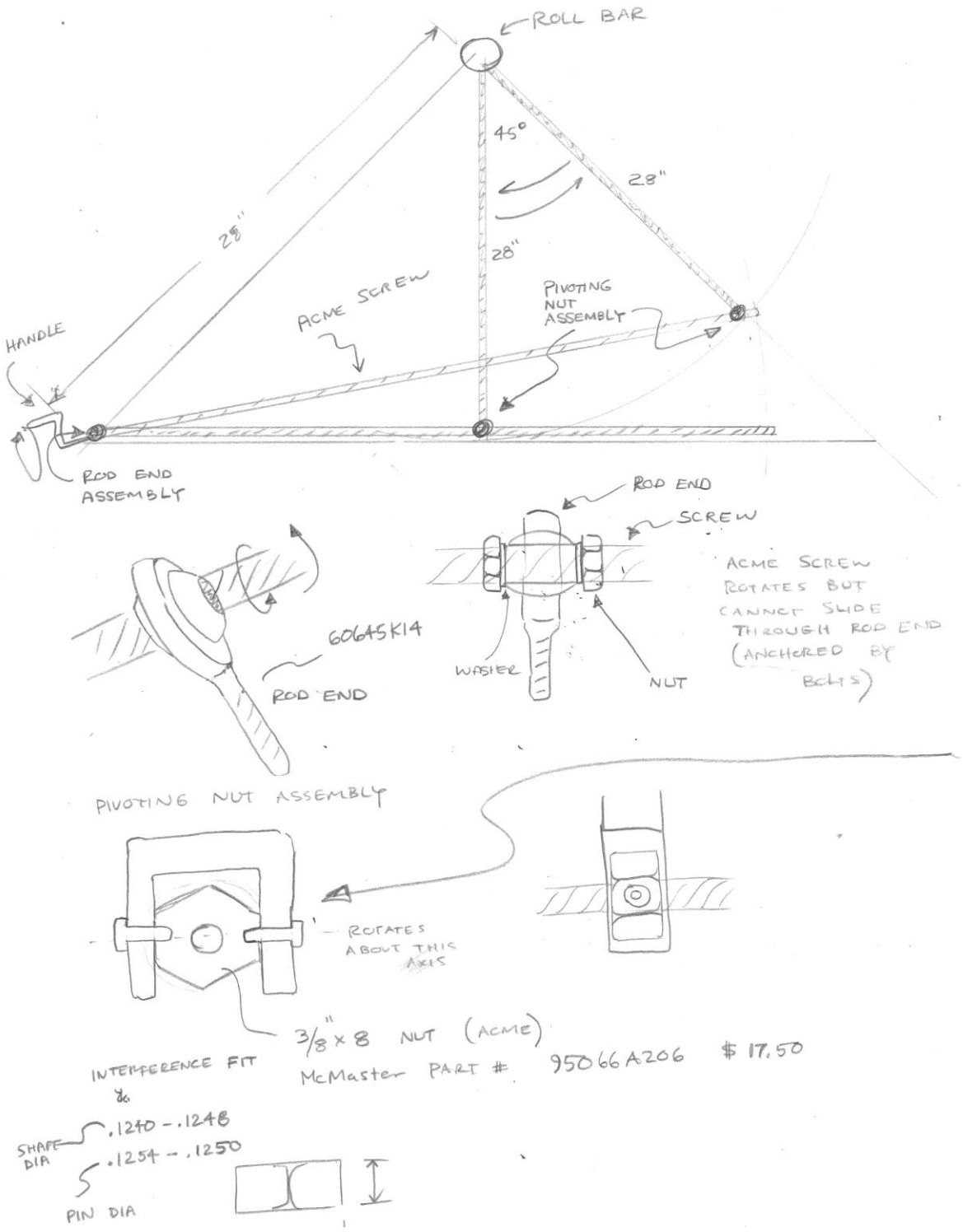

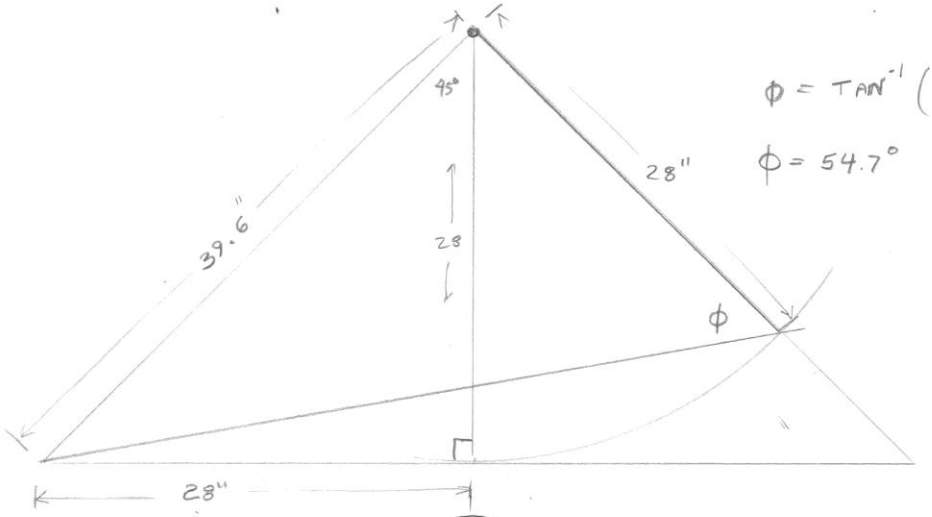

$\phi = \tan^{-1}\left(\frac{39.6}{28}\right)$

$\phi = 54.7°$

SCREW TENSION = T_S

3300 lb-in

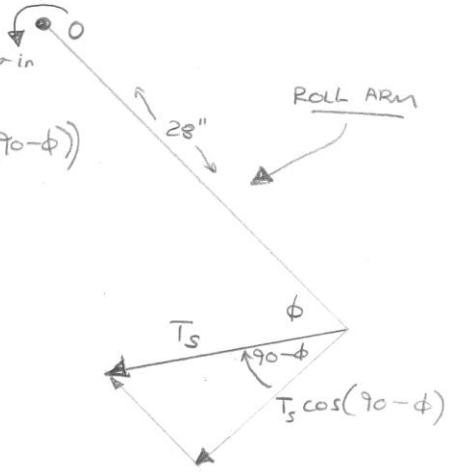

$\sum M_O = 0$

$3300 \text{ lb-in} = 28" \left(T_S \cos(90-\phi)\right)$

WHERE $\phi = 54.7$

$\frac{3300}{28(\cos(90-54.7))} = T_S$

$T_S = 144 \text{ lb}$

T_S DISTRIBUTED BETWEEN 2 PINS

$\frac{F}{\text{PIN}} = \frac{144}{2} = 122 \text{ lbs}$

FOR HIGH ALLOY STEEL YIELD STRENGTH = 300 MPa ≈ 40,000 PSI

$\tau_{PIN} = \frac{F}{A} = \frac{72 \text{ lbs}}{\pi r^2} = 26,700 \text{ PSI}$ FOR A SAFETY FACTOR OF 1.5

SOLVE FOR R

RADIUS = .029

MIN RADIUS FOR PINS IN PIVOT ASSEMBLY

2/1/12 PIN

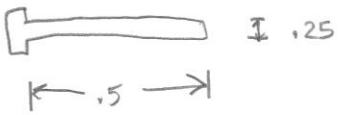

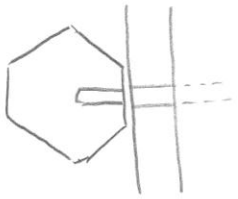

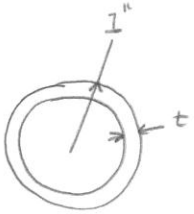

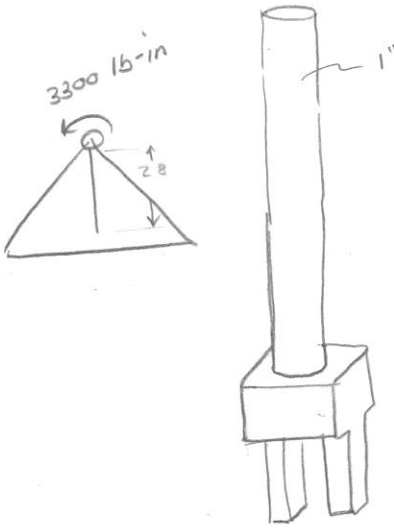

CALCULATE STRESS FOR .120" WALL THICKNESS

$$\sigma = \frac{Mc}{I} = \frac{3300\ (0.5)}{\frac{\pi}{4}\left(0.5^4 - (.5-.120)^4\right)}$$

σ = 50,000 PSI

$$S.F. = \frac{72,000}{50,000} = 1.4 \text{ ON YIELDING}$$

McMaster PART # 7767T37
1" TUBE .120" WALL THICKNESS
6' LONG @ 20.26
ASTM A513

2/1/12

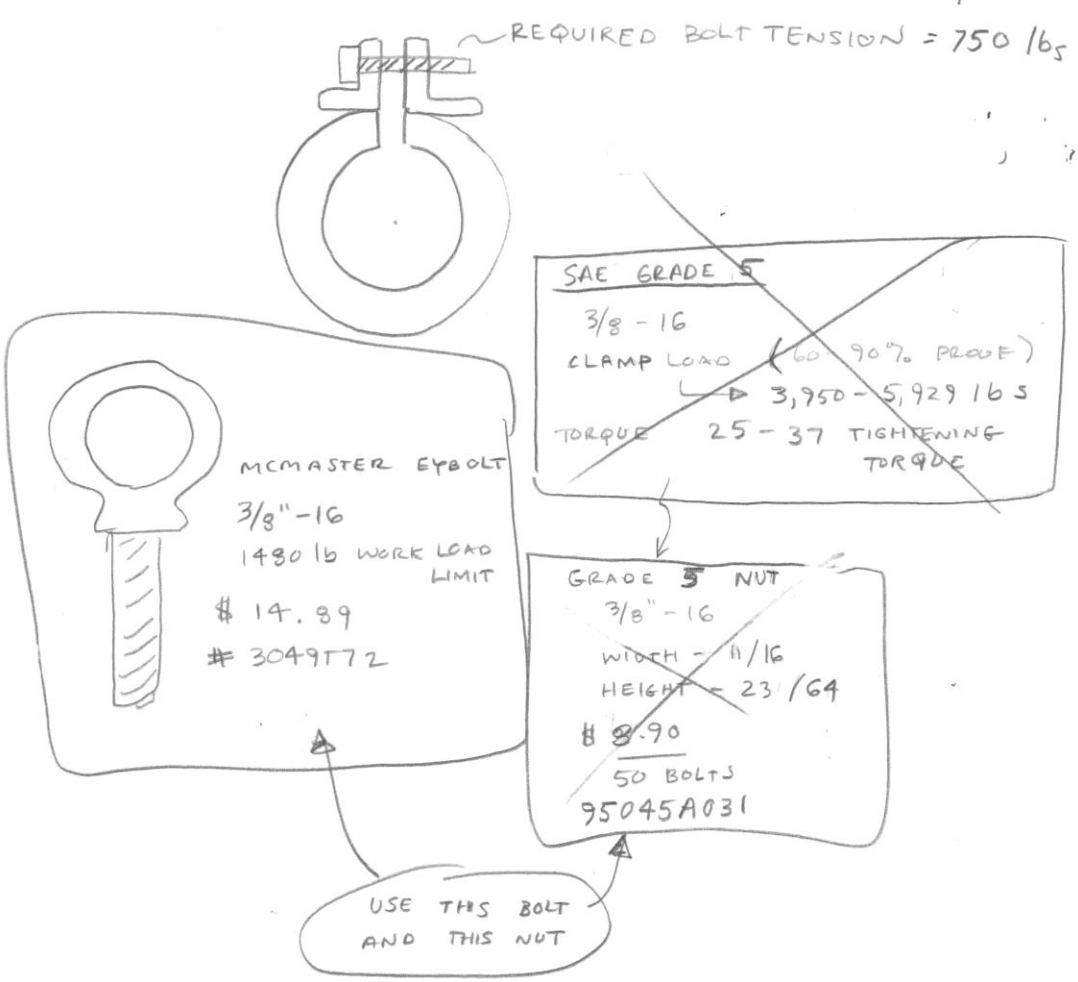
REQUIRED BOLT TENSION = 750 lbs
SAE GRADE 5
3/8 - 16
CLAMP LOAD (60 90% PROOF)
3,950 - 5,929 lbs
TORQUE 25 - 37 TIGHTENING TORQUE
MCMASTER EYBOLT
3/8"-16
1480 lb WORK LOAD LIMIT
14.89
3049T72
GRADE 5 NUT
3/8" - 16
WIDTH - 11/16
HEIGHT - 23/64
8.90
50 BOLTS
95045A031
USE THIS BOLT AND THIS NUT

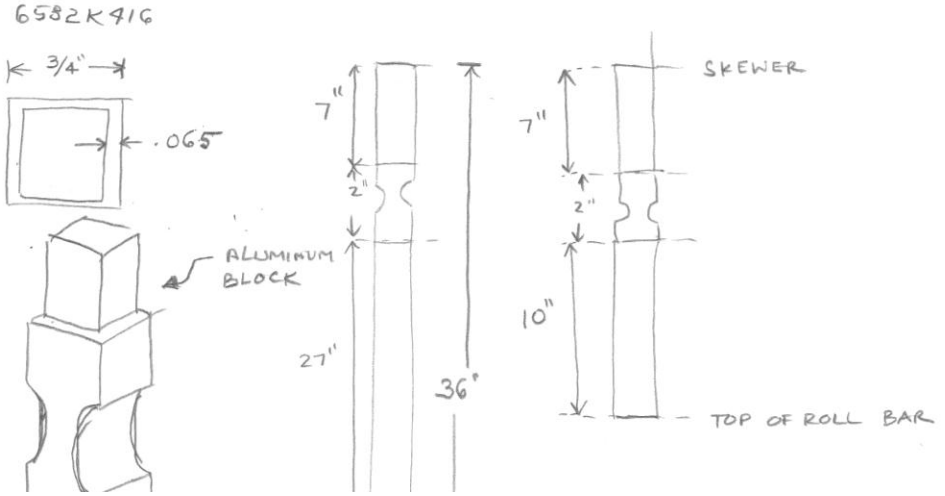
6582K416
3/4"
.065
ALUMINUM BLOCK
7"
2"
27"
36"
SKEWER
7"
2"
10"
TOP OF ROLL BAR

1/20/12 (1)

CHECK DIAGONAL SUPPORT FOR BUCKLING

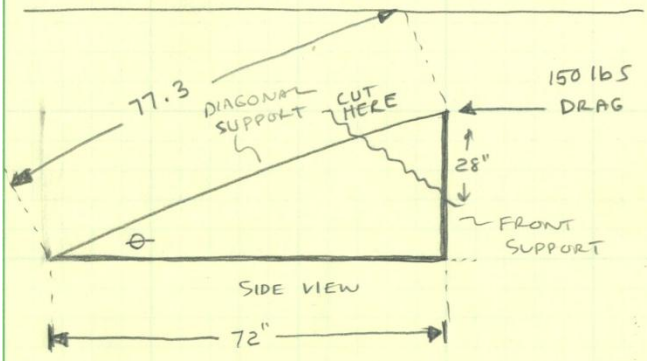

$\theta = \tan^{-1} \frac{28}{72}$

$\theta = 21.25$

TREAT AS SIMPLE TRUSS

F_D = DIAGONAL FORCE

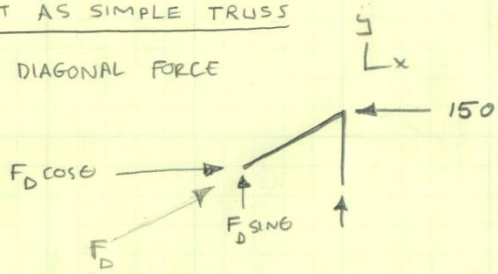

$\Sigma F_x = 0$

$150 \text{ lbs} = F_D \cos\theta$

$F_D = \frac{150}{\cos 21.25}$

$F_D = 161 \text{ lbs}$

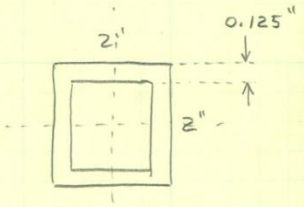

FOR PIN → PIN BUCKLING $F_{CRITICAL} = \frac{\pi^2 EI}{L^2}$

$E \approx 36 \times 10^6$ PSI

I FOR A 2" × 2" $\frac{1}{8}$" STEEL TUBE

$I = \frac{2^4}{12} - \frac{(2 - 2(0.125))^4}{12} = 0.55 \text{ IN}^4$

$F_{CRITICAL} = \frac{\pi^2 (36 \times 10^6) \frac{\text{lbs}}{\text{IN}^2} (0.55 \text{ IN}^4)}{(72 \text{ IN})^2} = 37760 \text{ lbs}$

NOW SOLVE FOR THICKNESS OF SOLID BAR STOCK WITH $F_{CRITICAL} = 150$ lbs $I = \frac{T^4}{12}$ WHERE T = THICKNESS

$F_c = 150 = \frac{\pi^2 (36 \times 10^6) \left(\frac{T^4}{12}\right)}{(72 \text{ IN})} \Rightarrow T = .138"$

MIN THICKNESS FOR SOLID STEEL STOCK

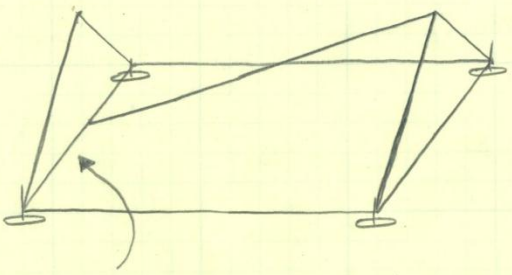

CHECK STRESS IN THIS MEMBER DUE TO FORCE FROM DIAGONAL MEMBER. TREAT AS SIMPLY SUPPORTED BEAM

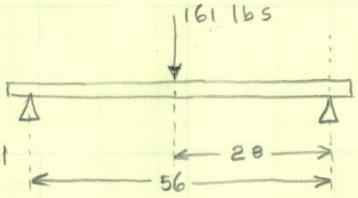

$M = 28" (161\ lbs)$

$M = 4508\ in\ lbs$

$\sigma = \frac{Mc}{I}$ WHERE $I = 0.55\ IN^4$ FOR 2"x2" SQUARE STOCK 1/8" THICKNESS

$\sigma = \frac{(4508\ in\ lbs)(1")}{0.55\ IN^4} = 8196\ PSI$ ← THIS IS MUCH LESS THAN THE 36 E6 PSI FOR STEEL

1/22/12

CALCULATE CLAMPING FORCE AS A FUNCTION OF BOLT TENSION

MODEL PILLOW BLOCK AS TO SURFACES

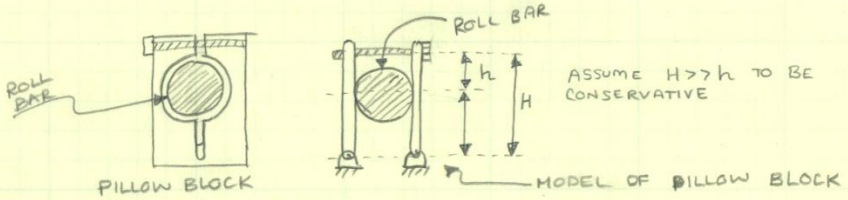

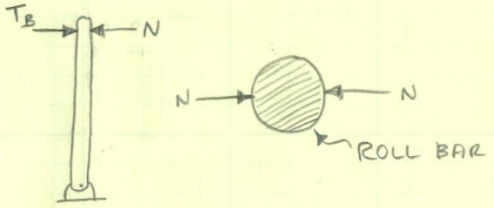

$N = T_B$

FBD OF ROLL BAR

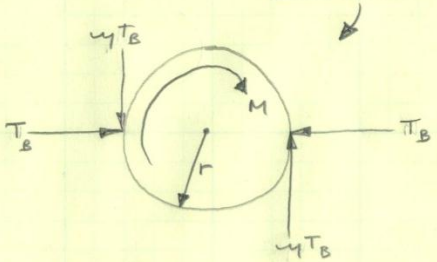

$M = 2\mu T_B r$

WITH A F.S. OF 4

$M = \frac{1}{2}\mu T_B r \Rightarrow T_B = \frac{2M}{\mu r}$

WHERE $M = 3300$ IN-lb
$r = 1.25$"
$\mu = 0.6$

$T_B = \frac{2(3300)}{0.6(1.25)}$

$T_B = 8800$ lbs (TOO BIG)

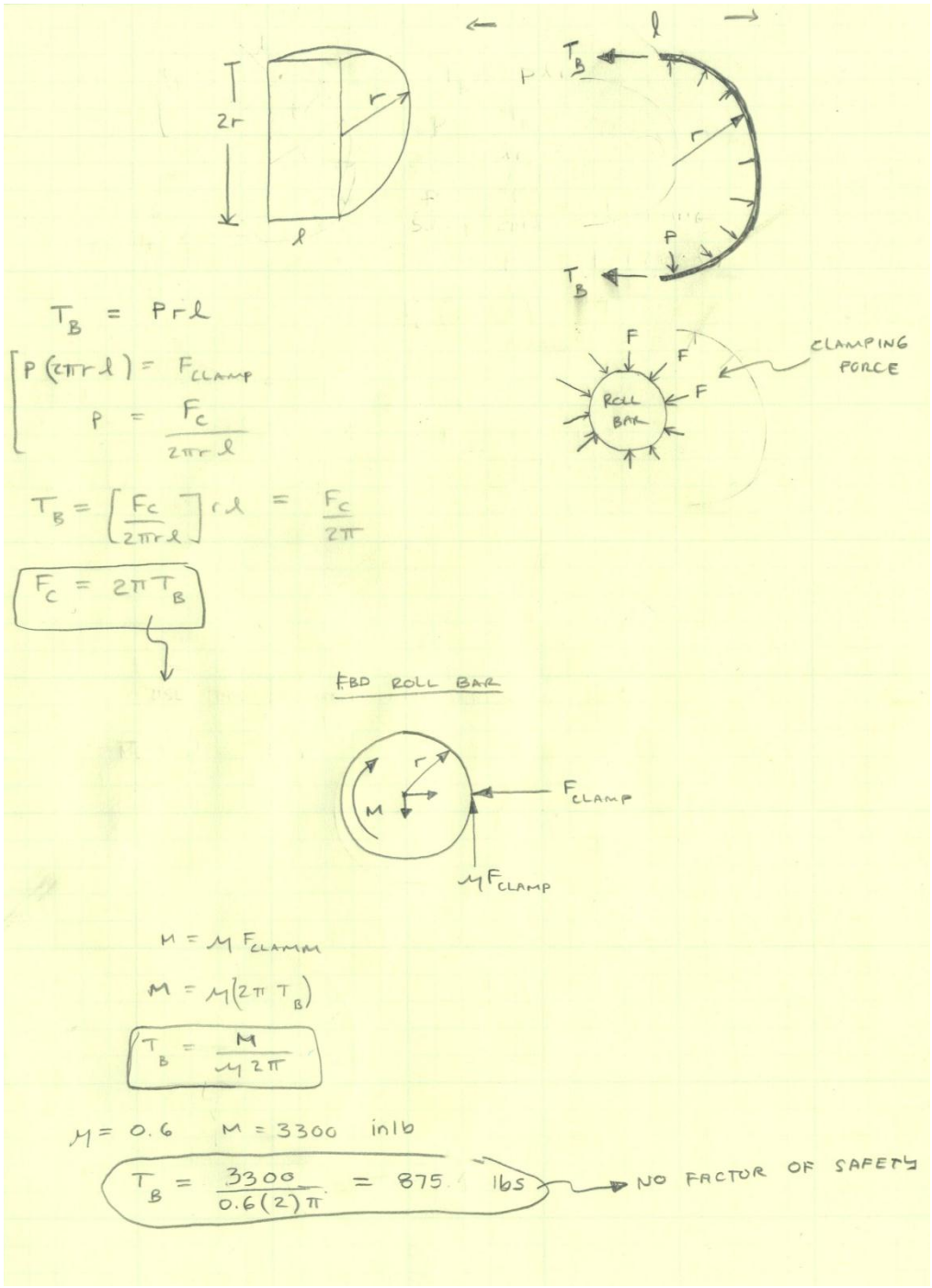

$$T_B = Prl$$

$$P(2\pi rl) = F_{CLAMP}$$

$$P = \frac{F_c}{2\pi rl}$$

$$T_B = \left[\frac{F_c}{2\pi rl}\right] rl = \frac{F_c}{2\pi}$$

$$F_c = 2\pi T_B$$

FBD ROLL BAR

$$M = \mu F_{CLAMP}$$

$$M = \mu(2\pi T_B)$$

$$T_B = \frac{M}{\mu 2\pi}$$

$\mu = 0.6 \quad M = 3300$ in lb

$$T_B = \frac{3300}{0.6(2)\pi} = 875 \text{ lbs}$$

→ NO FACTOR OF SAFETY

PIN CONNECTIONS TO DROPOUTS

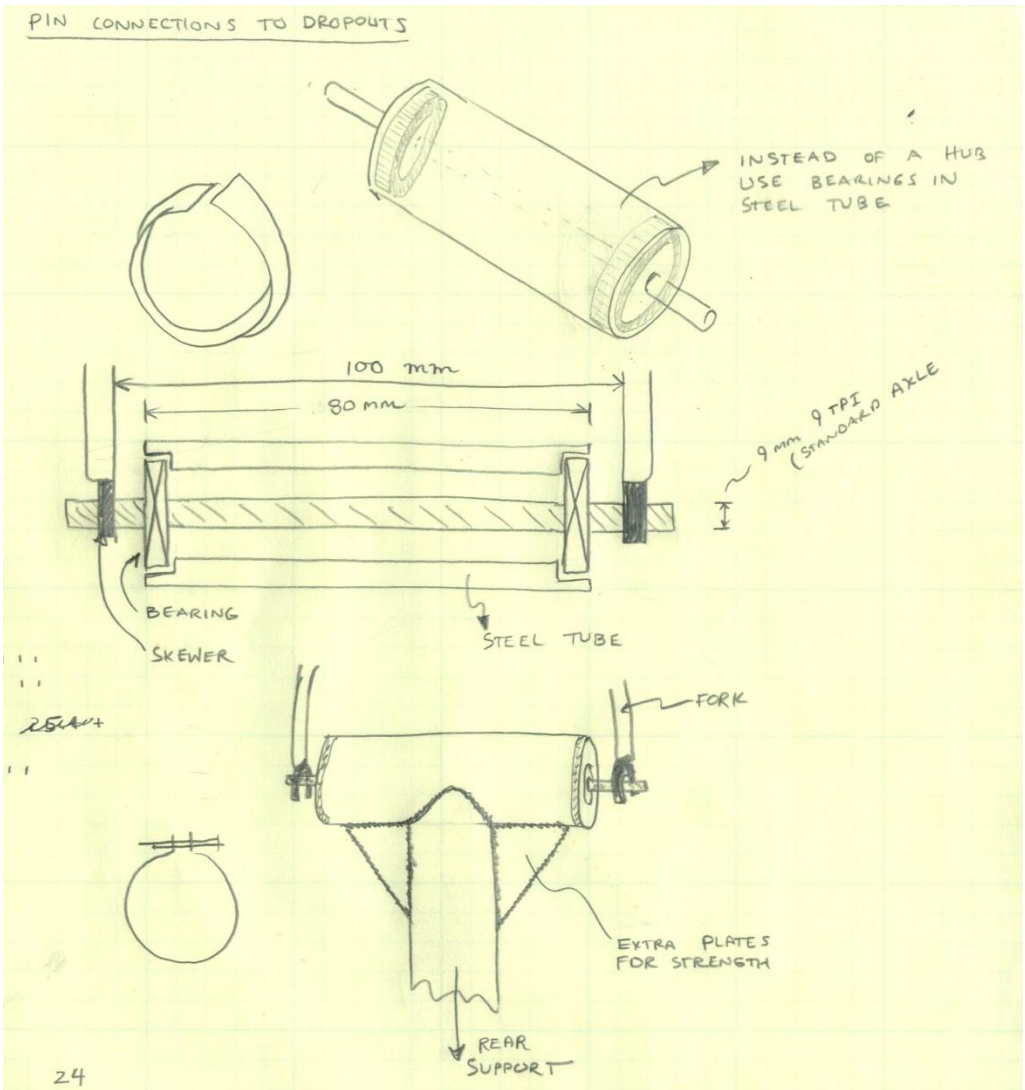

24

600 PSI $(2\pi(1.25)t)/in^2 = 15{,}000$ lb

$\mu N = 0.6(15{,}000) = 9{,}000$

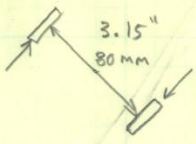

3300 lb-in $= 2\left(\frac{3.15}{2}\right)F$

$F = 1047.62$ lbs

PIN CONNECTIONS TO DROPOUTS

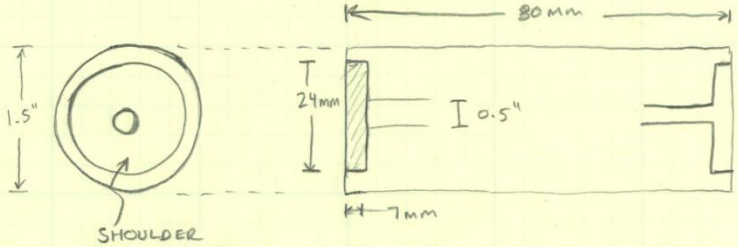

SHOULDER FOR BEARING MCMASTER ITEM # 6153K112

FRONT AXLE 9 mm
REAR AXLE 12 mm
} FROM HARRIS CYCLERY

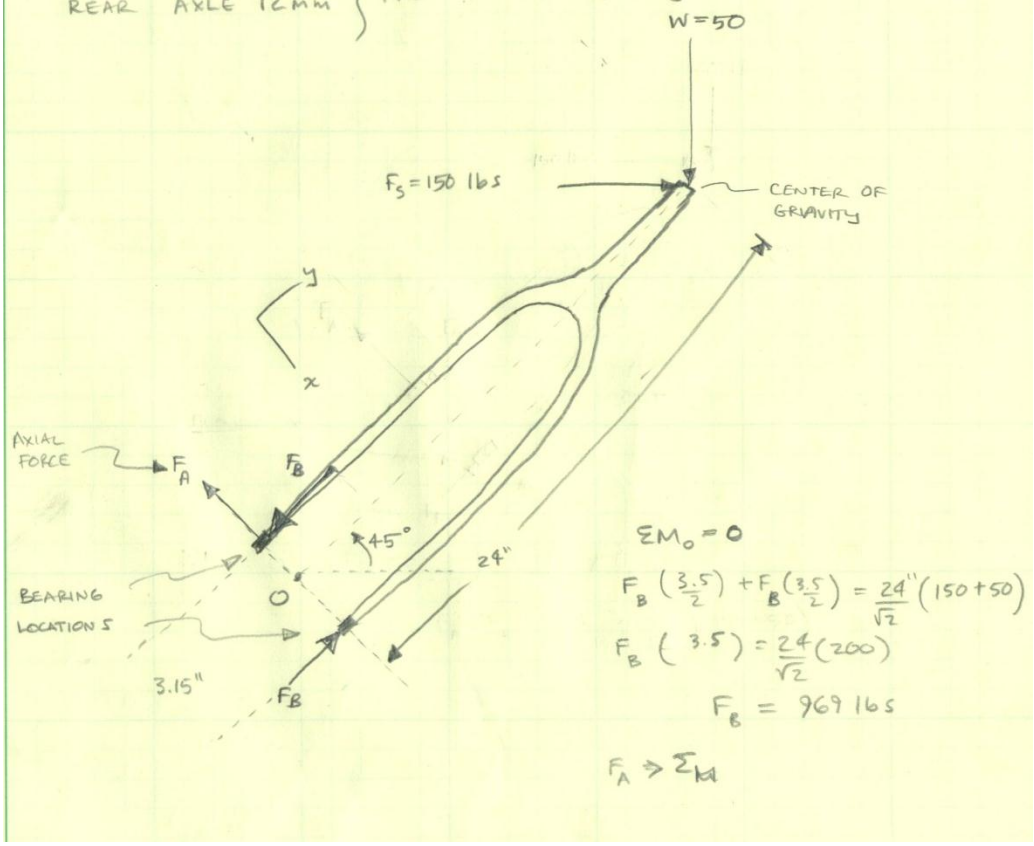

$\Sigma M_o = 0$

$F_B\left(\frac{3.5}{2}\right) + F_B\left(\frac{3.5}{2}\right) = \frac{24"}{\sqrt{2}}(150+50)$

$F_B\left(3.5\right) = \frac{24}{\sqrt{2}}(200)$

$F_B = 969$ lbs

$F_A \Rightarrow \Sigma_M$

WANGERIN, SPENCER	ATP FINITE ELEMENT PROJECT PROPOSAL HAND CALCULATIONS	2/24/11

FIND STRESS IN LOWER SUPPORT FRAME

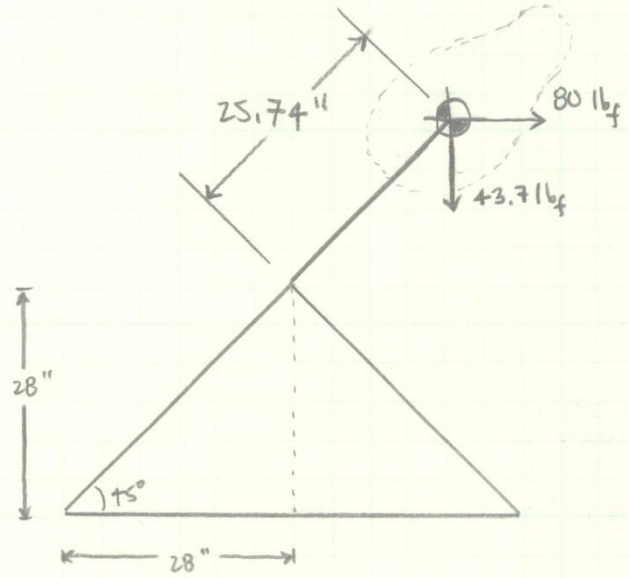

ASSUME NEGLIGIBLE CONTRIBUTION FROM FRONTAL DRAG (OUT OF PLANE IN FIGURE AT RIGHT)

ANALYZE LOWER SUPPORT FRAME USING SUPERPOSITION: FIRST AXIAL FORCES FROM TRUSS ANALYSIS, THEN CONTRIBUTION OF BENDING MOMENT

AXIAL FORCE TRUSS FBD

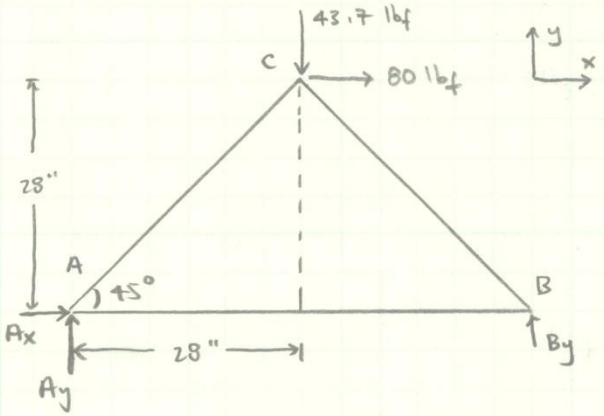

$\Sigma F_y = 0 = A_y + B_y - 43.7\,lb_f$

$\Rightarrow \underline{A_y = -18.15\,lb_f}$

CROSS-SECTIONAL GEOMETRY

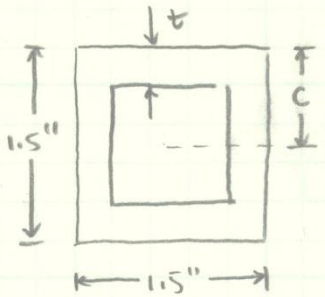

$t = 0.120"$

$c = 0.75"$

$A = (1.5")^2 - (1.5" - 2(.120"))^2$

$= 0.6624\ in^2$

$I = \frac{1}{12}((1.5")^4 - (1.5" - 2(.120"))^4)$

$= 0.211836\ in^4$

$\Sigma M_A = 0 = B_y(56") - (80\,lb_f)(28") - (43.7\,lb_f)(28")$

$\Rightarrow \underline{B_y = 61.85\,lb_f}$

$\Sigma F_x = 0 = A_x + 80\,lb_f$

$\Rightarrow \underline{A_x = -80\,lb_f}$

FBD JOINT A

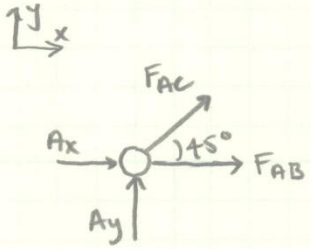

$\Sigma F_y = 0 = A_y + F_{AC}\sin(45°)$

$F_{AC} = -(-18.15\,lb_f)/\sin(45°)$

$\underline{F_{AC} = 25.668\,lb_f\ (T)}$

$\Sigma F_x = 0 = A_x + F_{AB} + F_{AC}\cos(45°)$

$F_{AB} = -(-80\,lb_f + (25.668\,lb_f)\cos(45°))$

$\underline{F_{AB} = 61.85\,lb_f\ (T)}$

FBD JOINT C

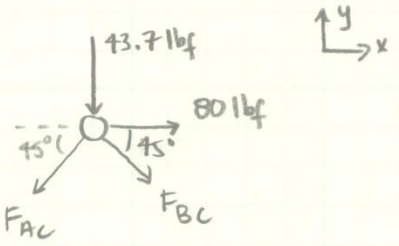

$$\Sigma F_y = 0 = (-43.71 lb_f) - F_{AC}\sin(45°) - F_{BC}\sin(45°)$$

$$F_{BC} = \frac{(-43.71 lb_f) - (25.668 lb_f)\sin(45°)}{\sin(45°)}$$

$$\underline{F_{BC} = 92.56\ lb_f\ (C)}$$

MEMBER BC IS CRITICAL BEAM!

BENDING MOMENT IN MEMBER BC

ASSUME BENDING MOMENT FROM WEIGHT AND SIDE DRAG ON HPV IS DISTRIBUTED EVENLY BETWEEN ALL 4 A-FRAME LOWER SUPPORT MEMBERS.

$$M_{TOT} = (80 lb_f)(25.74")\sin 45° + (47.3 lb_f)(25.74")\cos 45° = 2316.98\ in\text{-}lb_f$$

$$M_b = \frac{M_{TOT}}{4} = \frac{(2316.98\ in\text{-}lb_f)}{4}$$

$$\underline{M_b = 579.245\ in\text{-}lb_f}$$

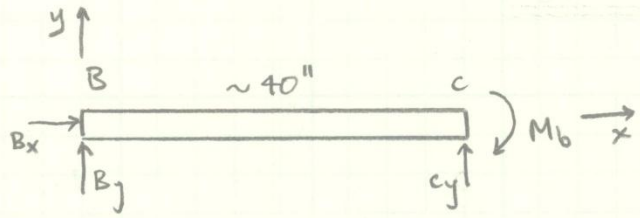

$$\Sigma M_B = 0 = C_y(40") - M_b$$

$$\Rightarrow \underline{C_y = 14.48\ lb_f}$$

$$\Sigma F_y = 0 = B_y + C_y$$

$$\Rightarrow \underline{B_y = -14.48\ lb_f}$$

$$\Sigma F_x = 0 = B_x$$

$$\Rightarrow \underline{B_x = 0}$$

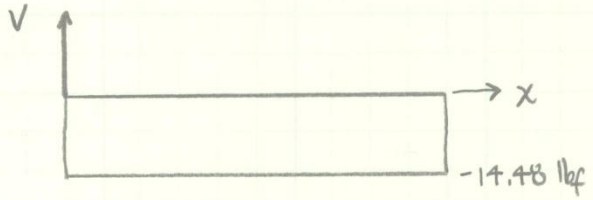

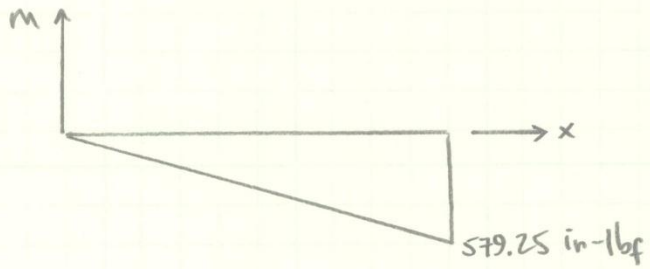

SUPERPOSITION OF LOADS

ASSUME SHEAR STRESS NEGLIGIBLE COMPARED WITH AXIAL AND BENDING STRESS.

AT OUTER FIBER OF MEMBER BC WHERE STRESSES ADD:

$$\sigma_{TOT} = \sigma_{AXIAL} + \sigma_b$$

WHERE

$$\sigma_{Ax} = \frac{F_{BC}}{A} \quad \text{AND} \quad \sigma_b = \frac{M_b c}{I}$$

$$= \frac{(92.561bf)}{(0.6624\,in^2)} \qquad = \frac{(579.245\,in\text{-}lbf)(0.75")}{(0.211836\,in^4)}$$

$$= 139.734\ psi \qquad = 2050.8\ psi$$

THUS, THE MAXIMUM NORMAL STRESS IN THE ATP LOWER SUPPORT FRAME:

$$\boxed{\sigma_{TOT} = 2190.54\ psi}$$

Appendix F — Manufacturing Drawings

Here, we have included a complete design packet of manufacturing drawings of the components of the ATP. These include exploded drawings depicting the general assembly process, detailed drawings of individual parts, and qualitative manufacturing drawings expressing special construction notes.

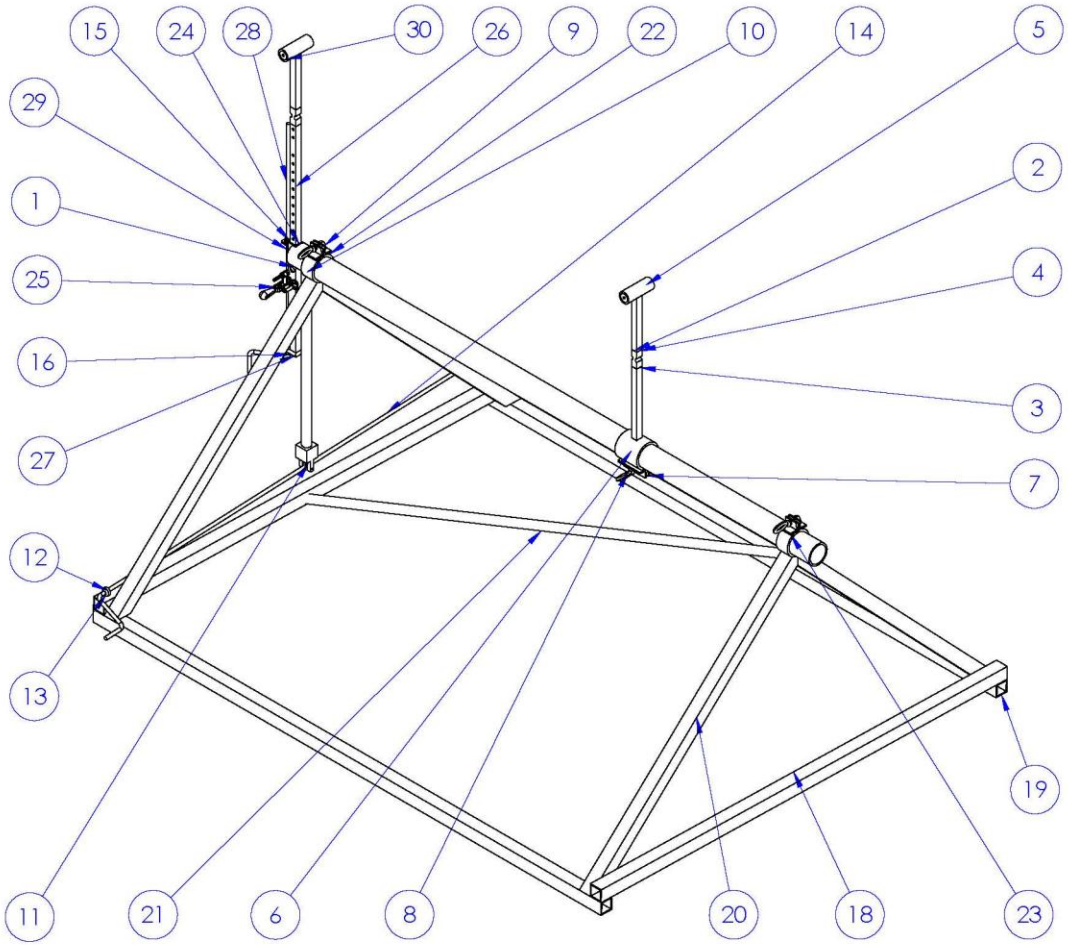

Figure G1 – Full ATP assembly. Balloon callouts indicate component numbers shown in the bill of materials.

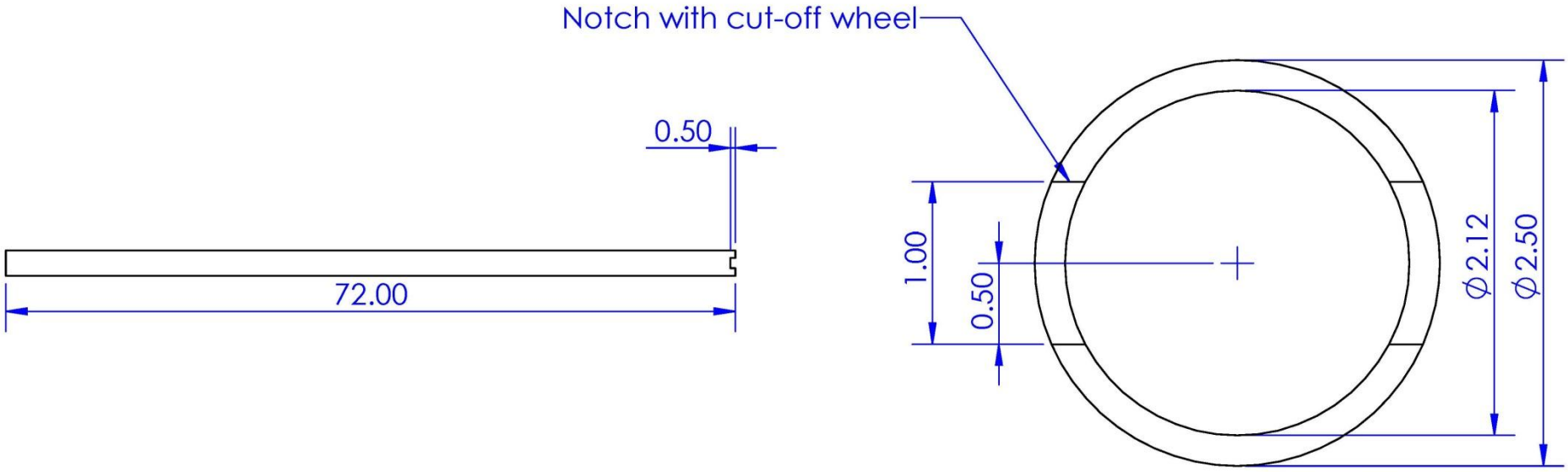

Mechanical Engineering CAL POLY	COMP NAME: ROLL TUBE		COMP #: 1
	SCALE: 1:16	UNITS: INCHES	MATERIAL: STEEL
	DATE: 3/6/12	DRAWN BY: C. DAVIS	GROUP: TEAM ANEMOI
	OTHER: CROSS SECTION 1:1 SCALE		

5 4 3 2 1

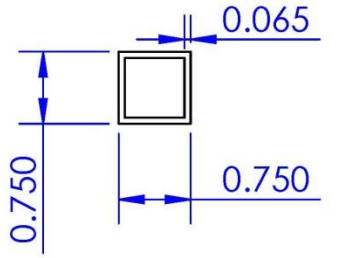

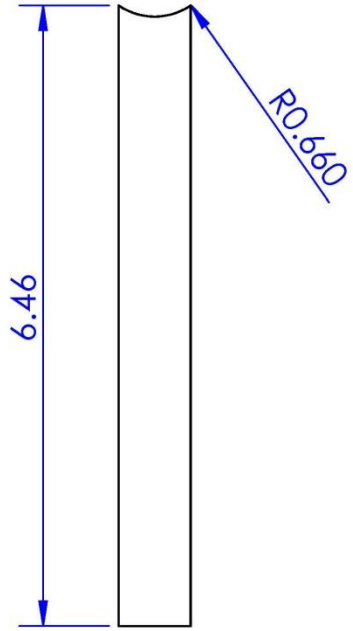

Notch with ∅1.25 hole-saw on Tube Shark

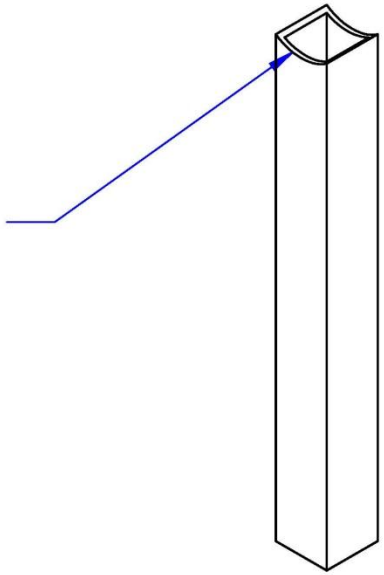

Mechanical Engineering CAL POLY	COMP NAME: GAUGED TOP SUPPORT SECTION		COMP #: 2
	SCALE: 1:2	UNITS: INCHES	MATERIAL: STEEL
	DATE: 3/6/12	DRAWN BY: C. DAVIS	GROUP: TEAM ANEMOI
	OTHER:		

5 4 3 2 1

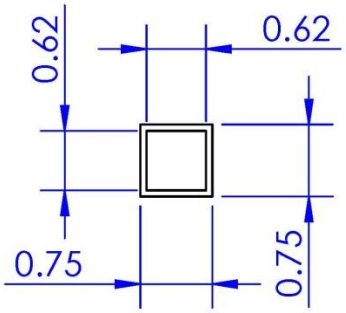

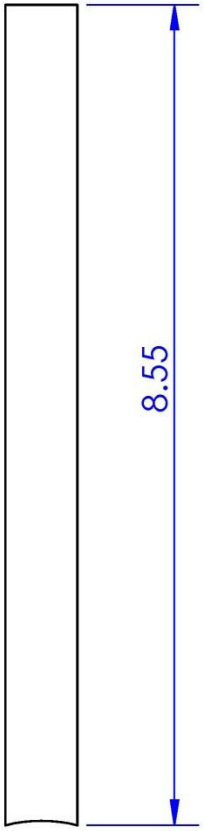

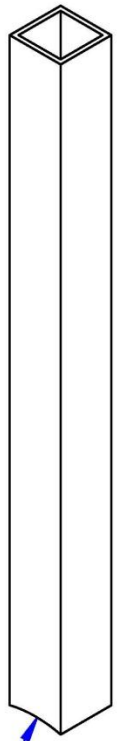

Notch with ∅1.25 hole-saw on Tube Shark with center at R 1.50

Mechanical Engineering CAL POLY

COMP NAME: FRONT GAUGED SUPPORT BOTTOM		COMP #: 3
SCALE: 1:2	UNITS: INCHES	MATERIAL: STEEL
DATE: 3/6/12	DRAWN BY: C. DAVIS	GROUP: TEAM ANEMOI
OTHER: CROSS-SECTION 2:1 SCALE		

5 4 3 2 1

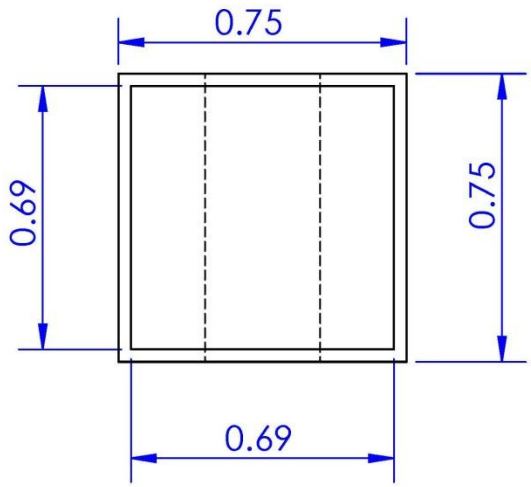

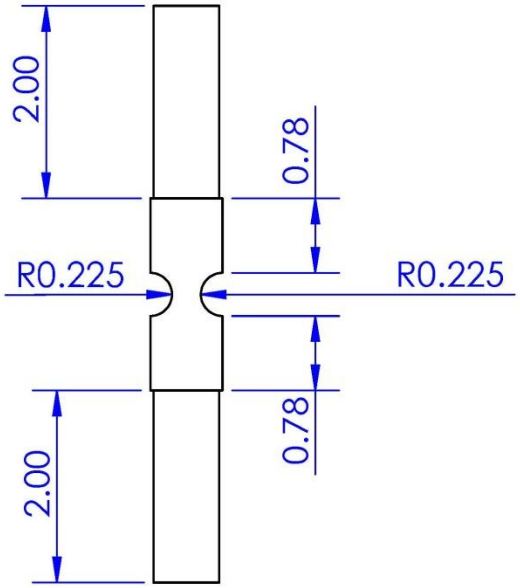

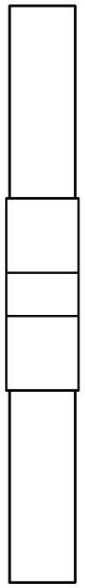

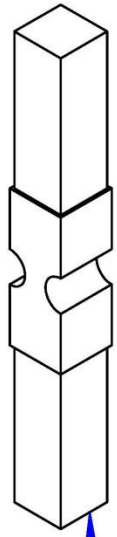

Mechanical Engineering
CAL POLY

COMP NAME: ALUMINUM SUPPORT SECTION		COMP #: 4
SCALE: 1:2	UNITS: INCHES	MATERIAL: ALUMINUM
DATE: 3/6/12	DRAWN BY: C. DAVIS	GROUP: TEAM ANEMOI
OTHER: CROSS-SECTION 2:1 SCALE		

5 4 3 2 1

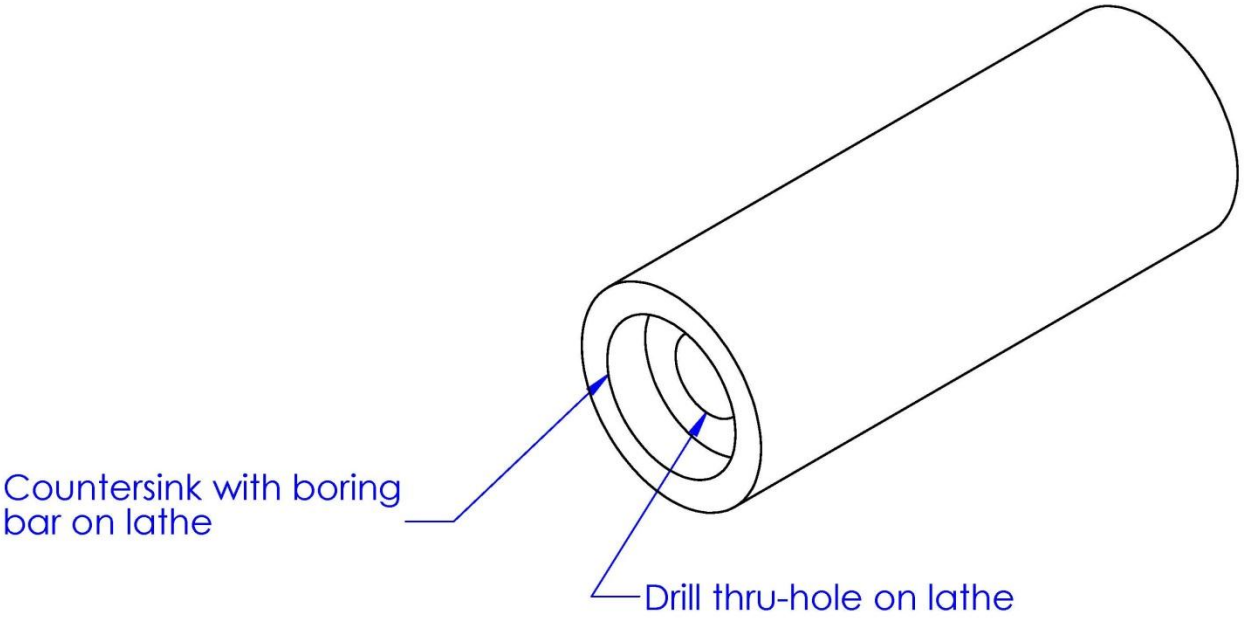

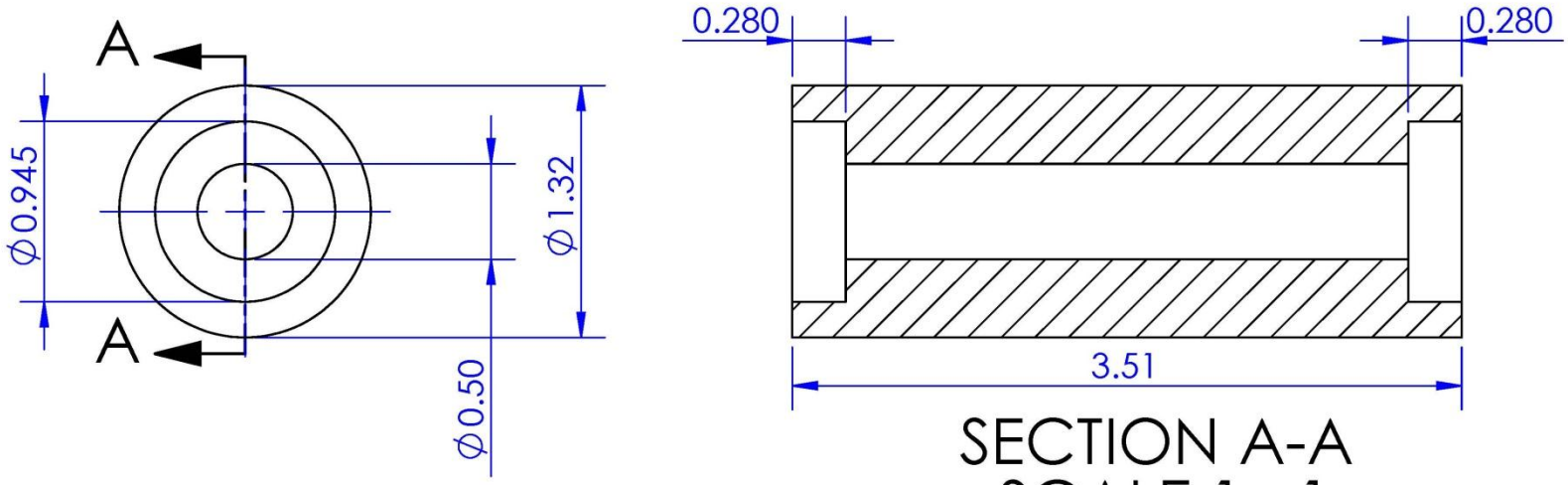

SECTION A-A
SCALE 1 : 1

Mechanical Engineering
CAL POLY

COMP NAME: HUB		COMP #: 5
SCALE: 1:1	UNITS: INCHES	MATERIAL: STEEL
DATE: 3/6/12	DRAWN BY: C. DAVIS	GROUP: TEAM ANEMOI
OTHER:		

5 4 3 2 1

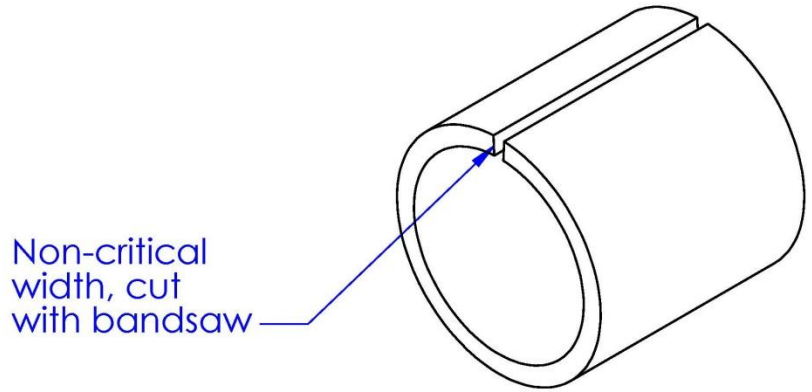

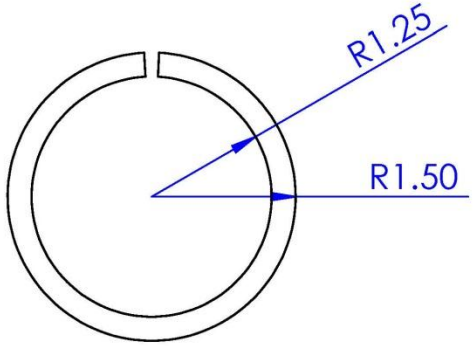

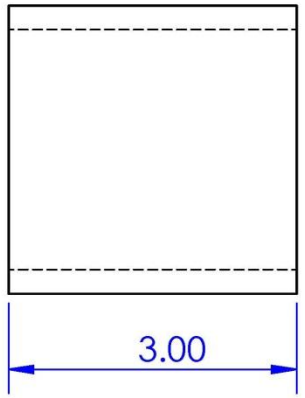

Mechanical Engineering
CAL POLY

COMP NAME: CLAMP TUBE (LONG)		COMP #: 7
SCALE: 1:2	UNITS: INCHES	MATERIAL: STEEL
DATE: 3/6/12	DRAWN BY: C. DAVIS	GROUP: TEAM ANEMOI
OTHER: NOTCH CUT WITH BANDSAW - WIDTH NOT CRITICAL		

5 4 3 2 1

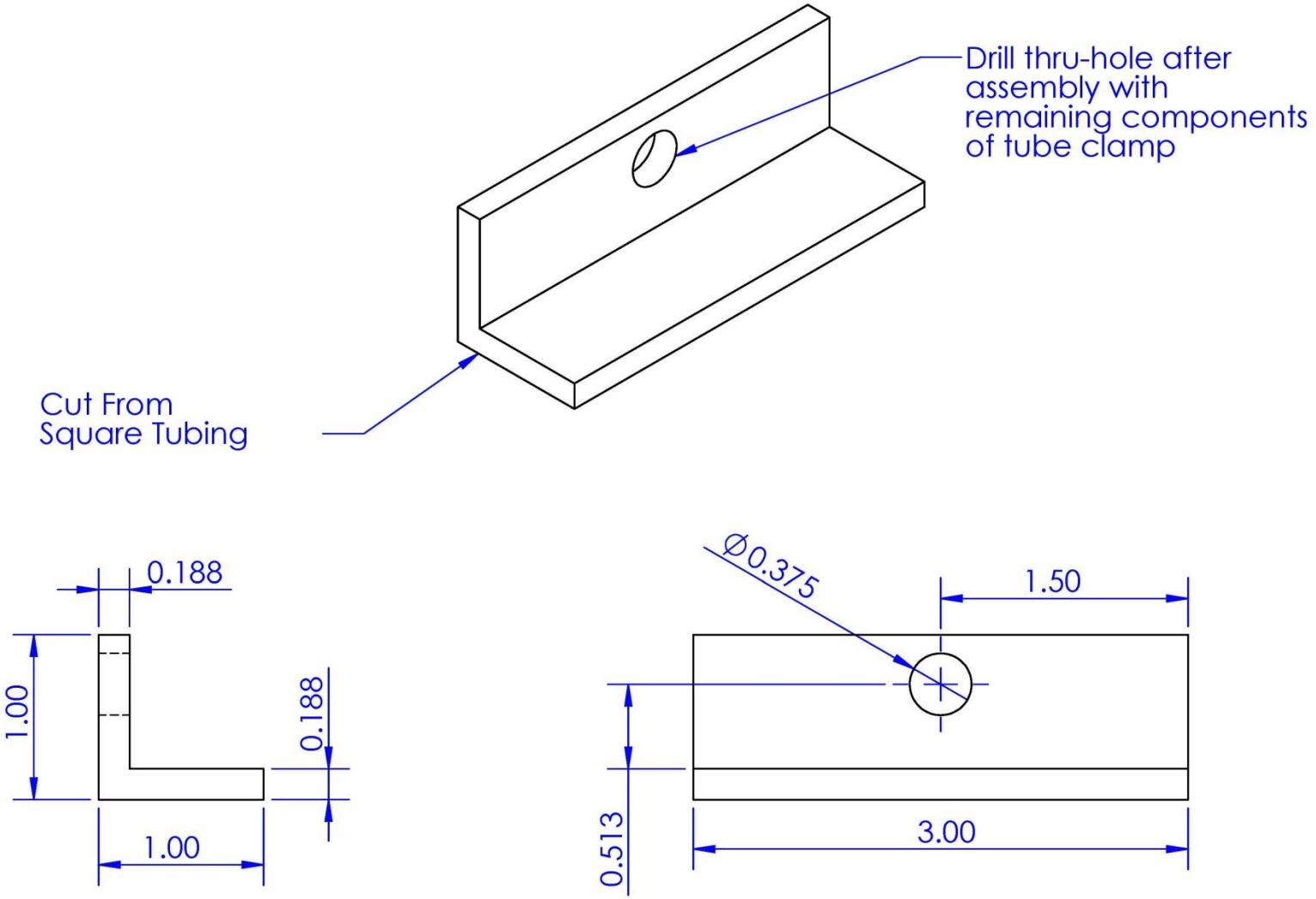

Mechanical Engineering CAL POLY	COMP NAME: CLAMP TAB LONG		COMP #: 8
	SCALE: 1:1	UNITS: INCHES	MATERIAL: STEEL
	DATE: 3/6/12	DRAWN BY: C. DAVIS	GROUP: TEAM ANEMOI
	OTHER:		

5 4 3 2 1

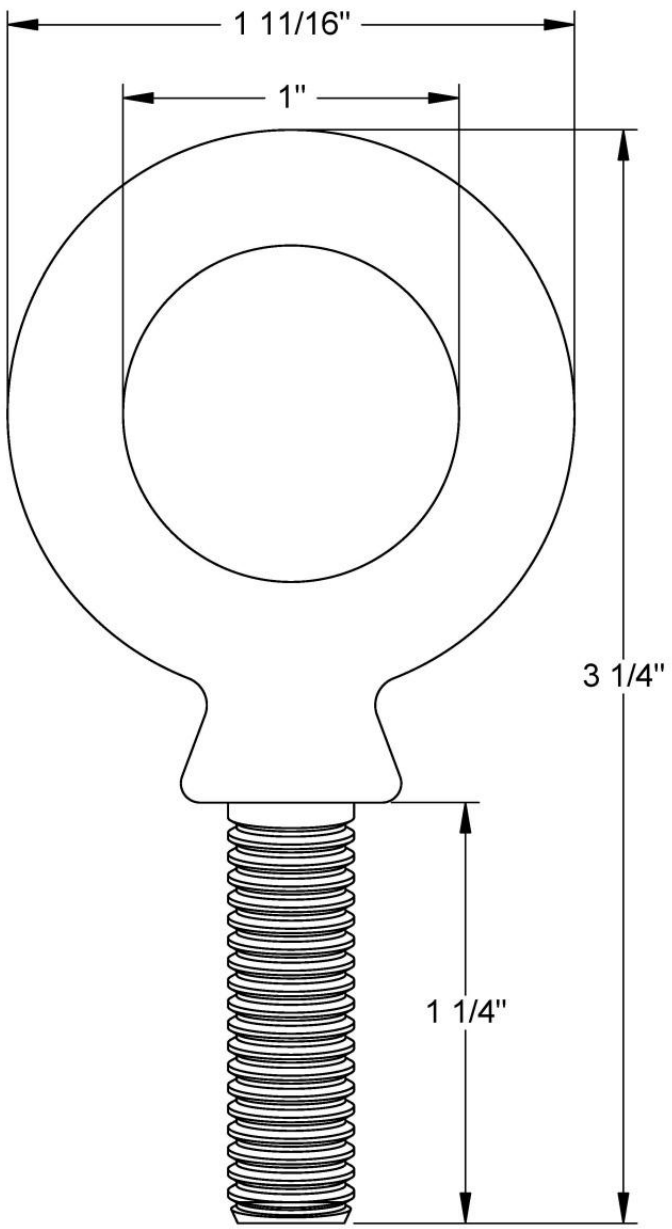

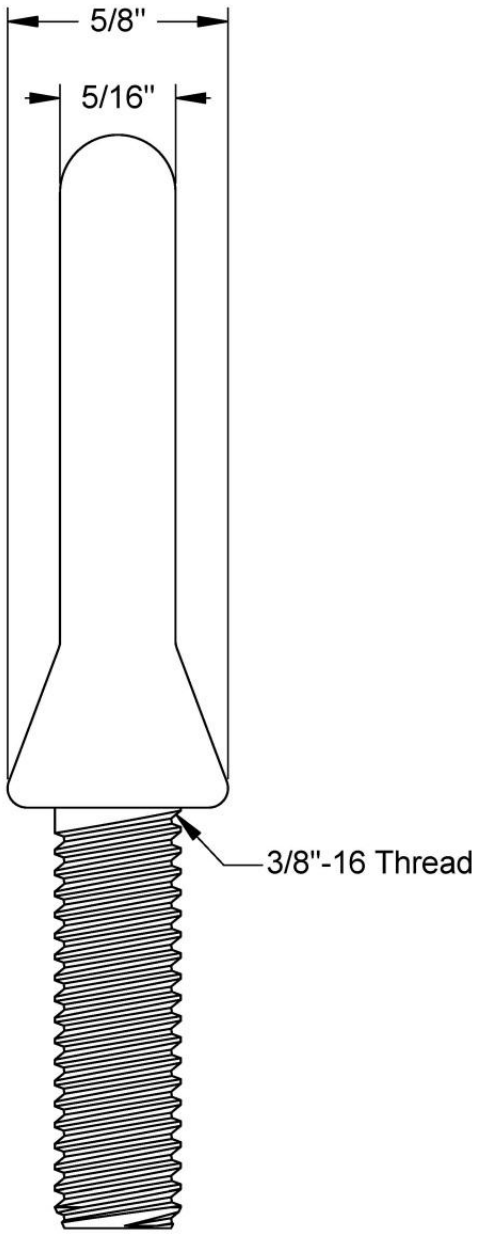

McMASTER-CARR CAD

PART NUMBER **3049T72**

http://www.mcmaster.com

8620 Alloy Steel
Lifting Eyebolt with Shoulder

Unless otherwise specified, dimensions are in inches. Information in this drawing is provided for reference only.

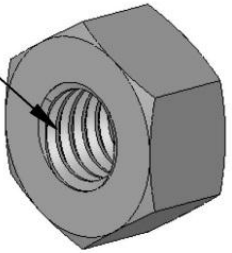

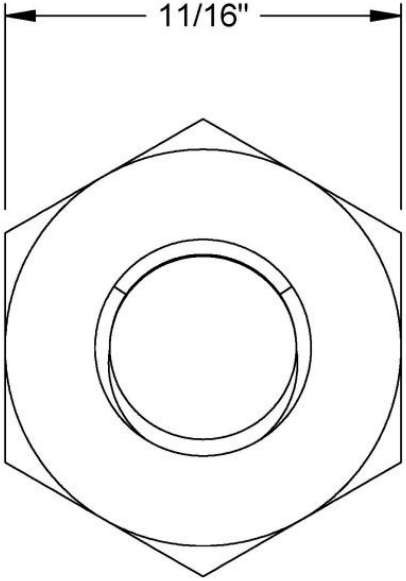

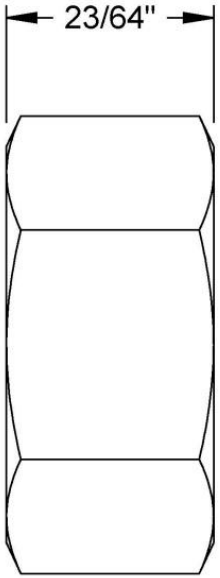

McMASTER-CARR® CAD

http://www.mcmaster.com

PART NUMBER **95045A031**

Grade 5 Steel
Hex Nut

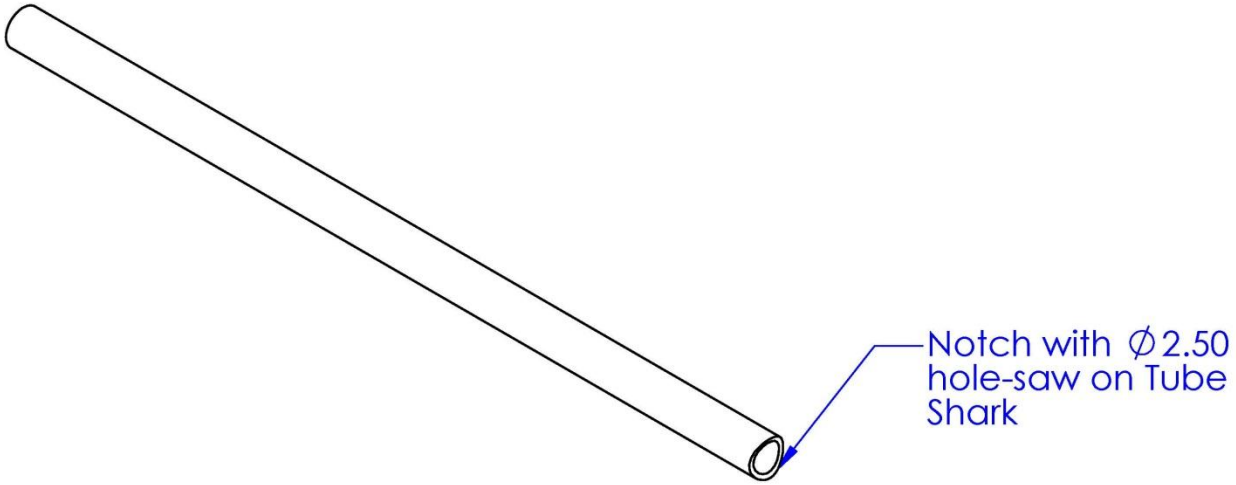

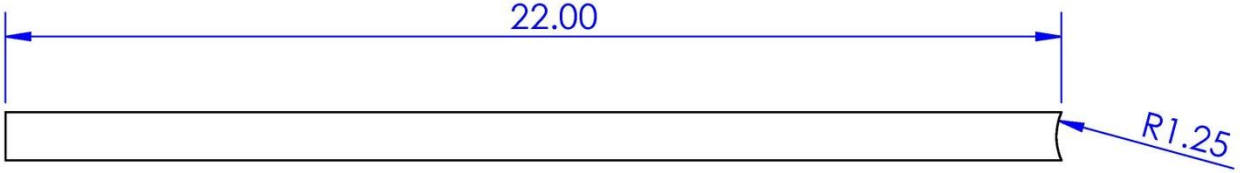

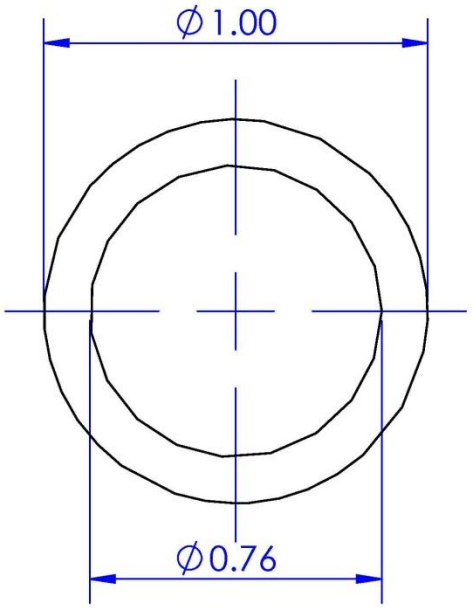

Mechanical Engineering
CAL POLY

COMP NAME: ROLL ARM		COMP #: 11
SCALE: 1:4	UNITS: INCHES	MATERIAL: STEEL
DATE: 3/6/12	DRAWN BY: C. DAVIS	GROUP: TEAM ANEMOI
OTHER: CROSS-SECTION 2:1 SCALE		

5 4 3 2 1

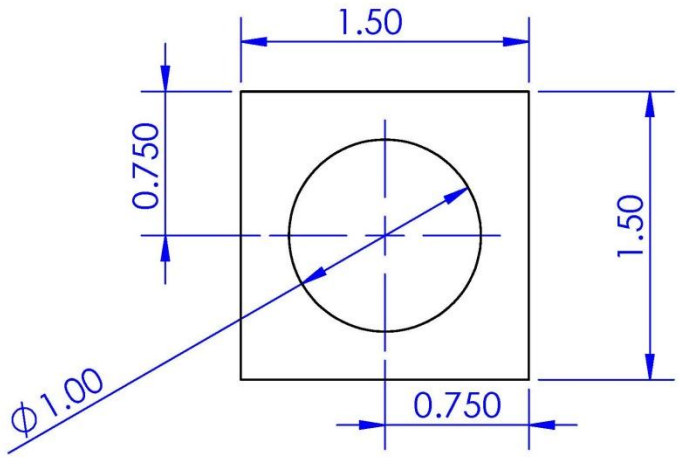

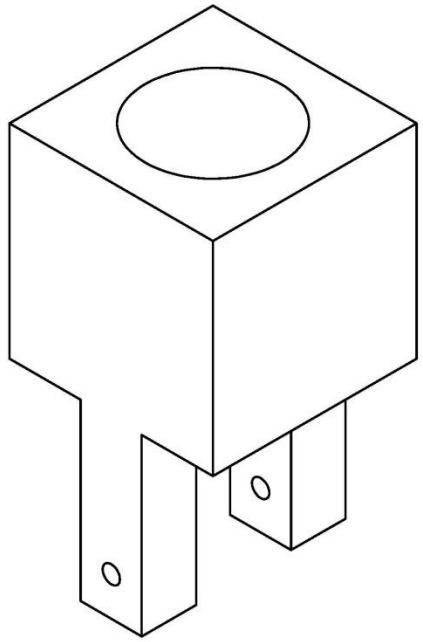

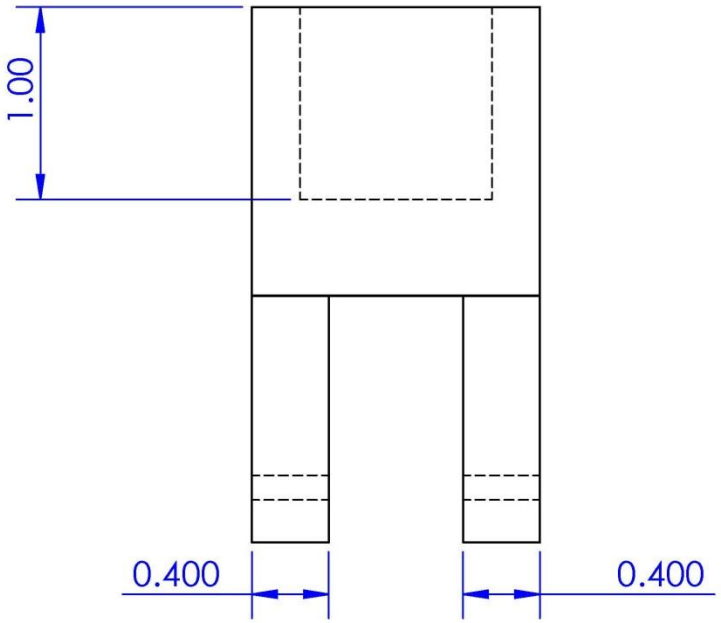

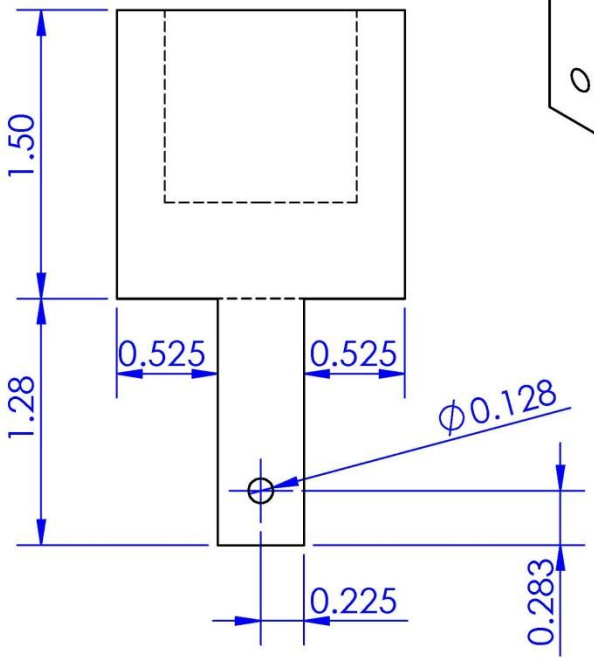

COMP NAME: ACME NUT PIVOT		COMP #: 12
SCALE: 1: 1	UNITS: INCHES	MATERIAL: ALUMINUM
DATE: 3/6/12	DRAWN BY: C. DAVIS	GROUP: TEAM ANEMOI
OTHER:		

Mechanical Engineering
CAL POLY

5 4 3 2 1

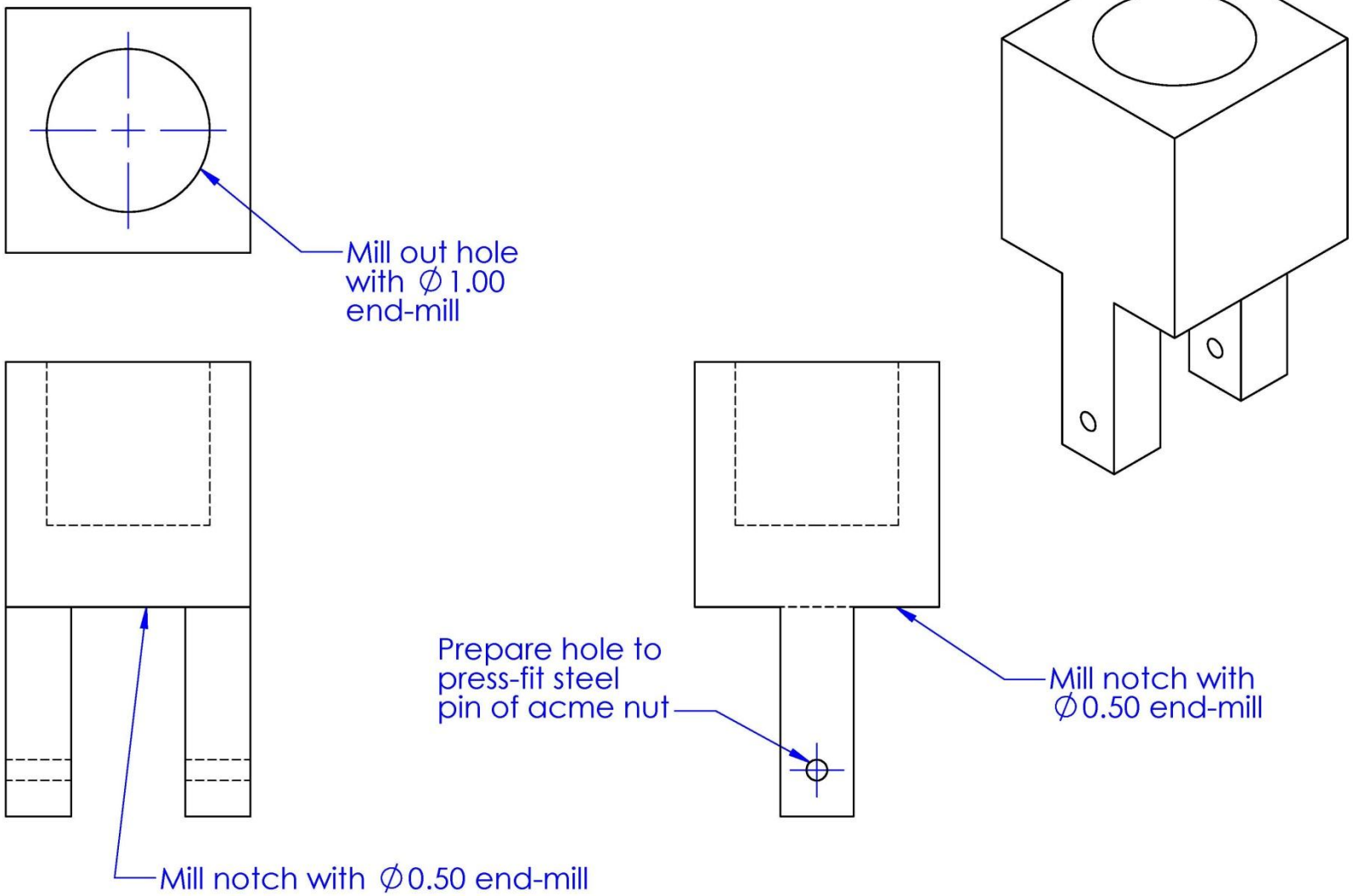

Mechanical Engineering CAL POLY	COMP NAME: ACME NUT PIVOT		COMP #: 12
	SCALE: 1: 1	UNITS: INCHES	MATERIAL: ALUMINUM
	DATE: 3/6/12	DRAWN BY: C. DAVIS	GROUP: TEAM ANEMOI
	OTHER:		

5 4 3 2 1

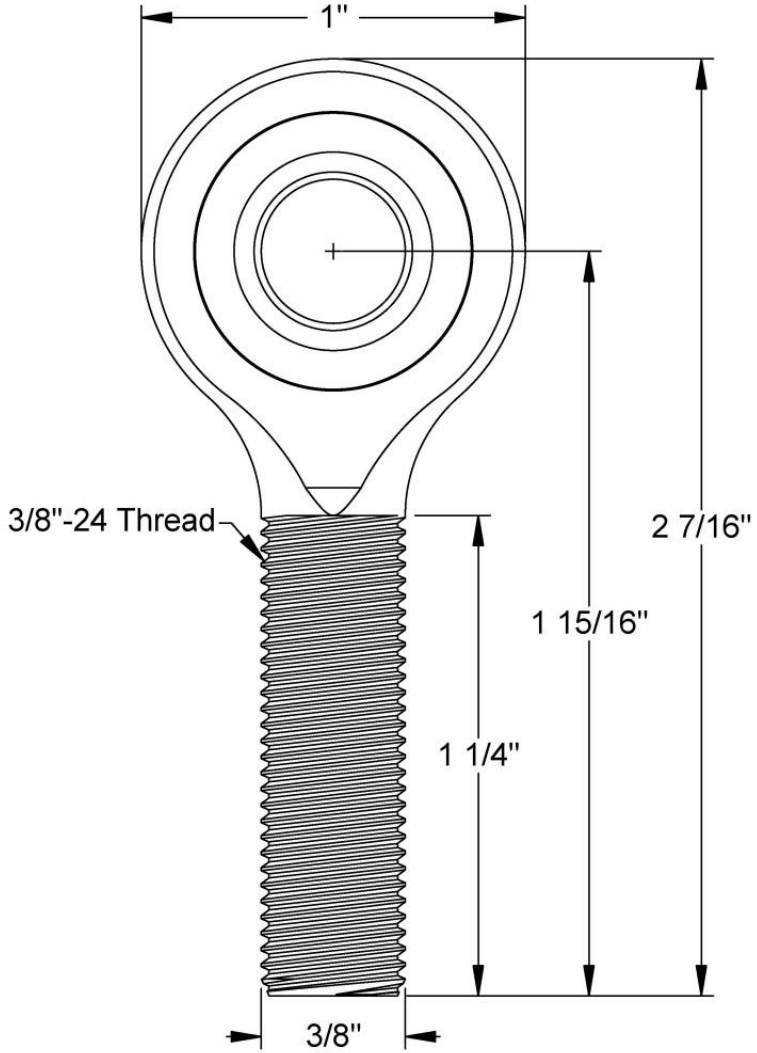

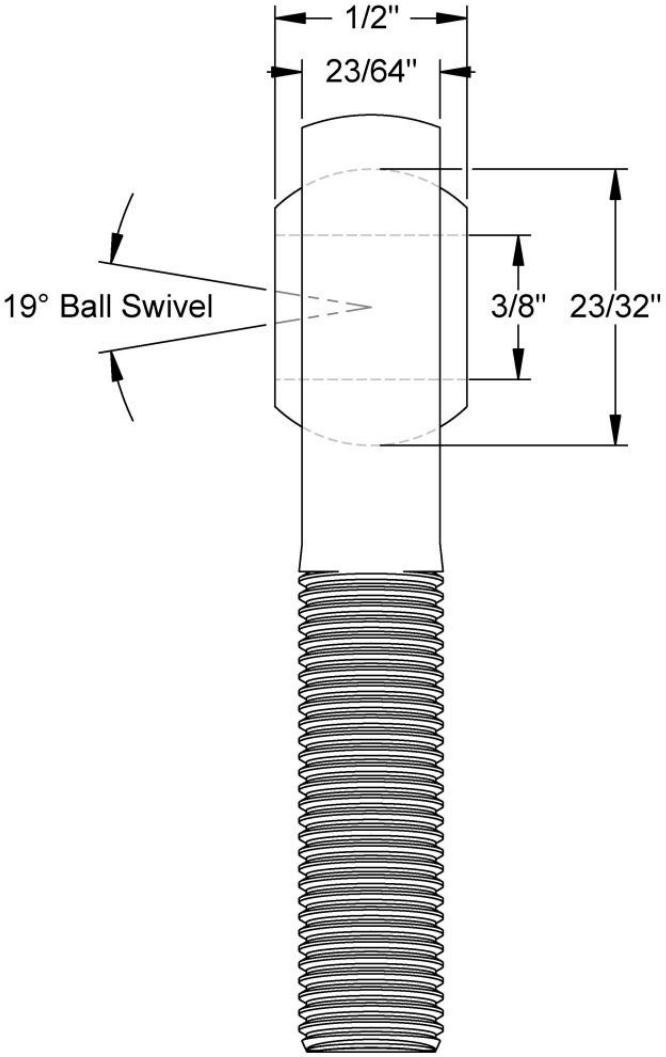

Notes:
Zinc-Plated Steel Housing
Chrome-Plated Steel Ball

McMASTER-CARR CAD

PART NUMBER **60645K141**

http://www.mcmaster.com

Right-Hand Thread
Ball Joint Rod End

Unless otherwise specified, dimensions are in inches. Information in this drawing is provided for reference only.

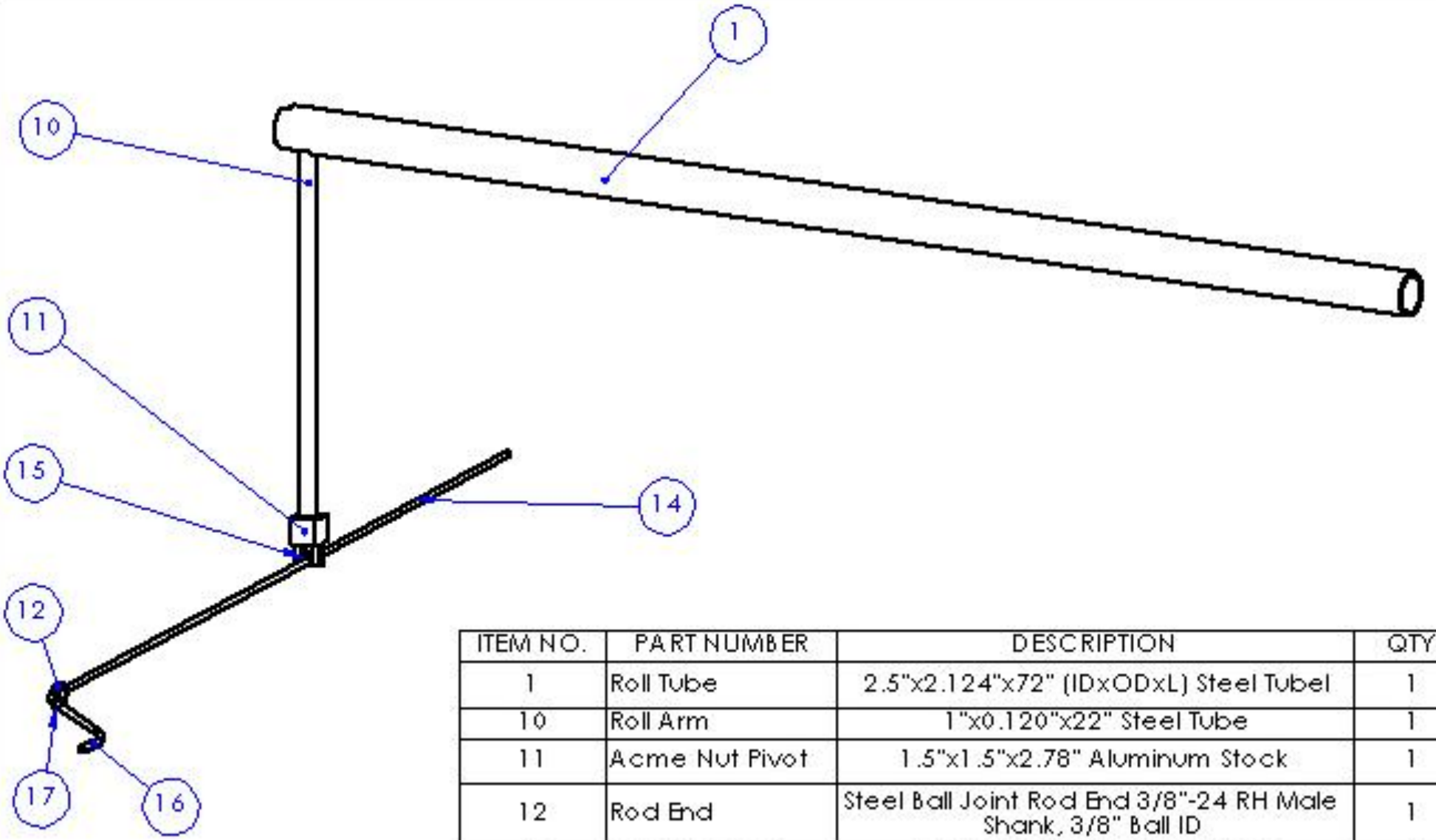

ITEM NO.	PART NUMBER	DESCRIPTION	QTY.
1	Roll Tube	2.5"x2.124"x72" (IDxODxL) Steel Tubel	1
10	Roll Arm	1"x0.120"x22" Steel Tube	1
11	Acme Nut Pivot	1.5"x1.5"x2.78" Aluminum Stock	1
12	Rod End	Steel Ball Joint Rod End 3/8"-24 RH Male Shank, 3/8" Ball ID	1
14	Rolling Screw	3/8"- 8 tpi x 57"Acme Screw	1
15	Acme Nut	3/8"- 8 Acme Nut	1
17	Rod End Nut	3/8"-24 Nut	1

Mechanical Engineering CAL POLY

ASSEMBLY NAME: ROLLTUBE AND ROLLING ASSEMBLY		
SCALE: 1:8	UNITS: INCHES	MATERIAL: STEEL AND ALUMINUM
DATE: 3/6/12	DRAWN BY: C. DAVIS	GROUP: TEAM ANEMOI
OTHER:		

5 4 3 2 1

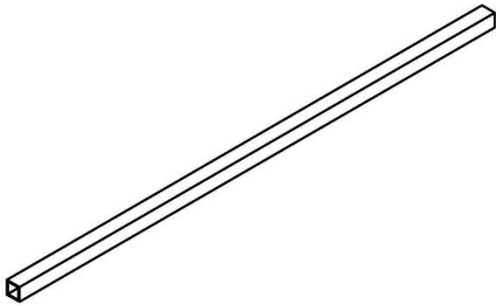

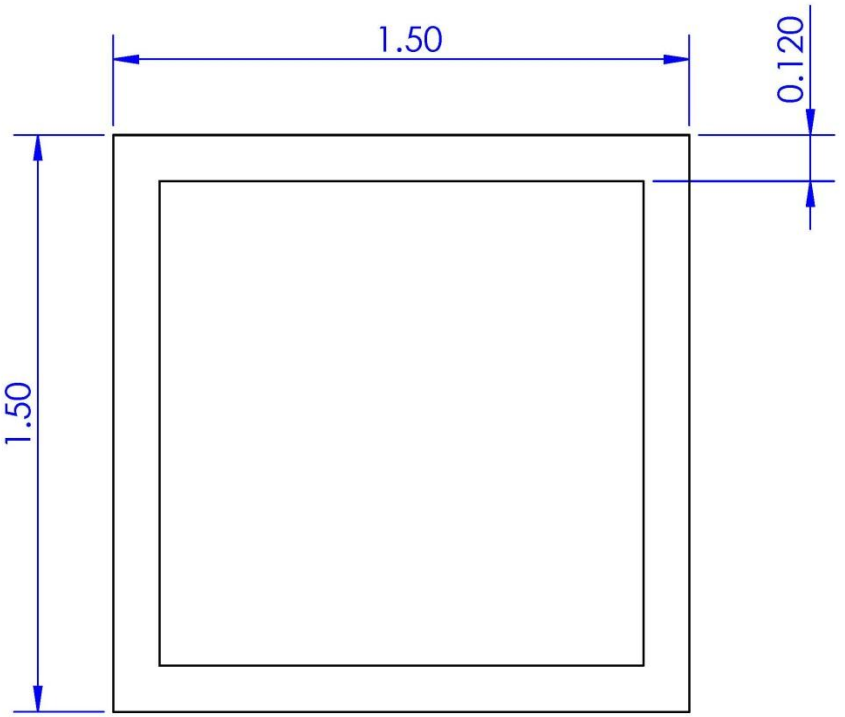

Mechanical Engineering
CAL POLY

COMP NAME: WIDTH-WISE BASE MEMBER		COMP #: 18
SCALE: 1:16	UNITS: INCHES	MATERIAL : STEEL
DATE: 3/6/12	DRAWN BY: C. DAVIS	GROUP: TEAM ANEMOI
OTHER: SCALE OF CROSS-SECTION IS 2:1		

5 4 3 2 1

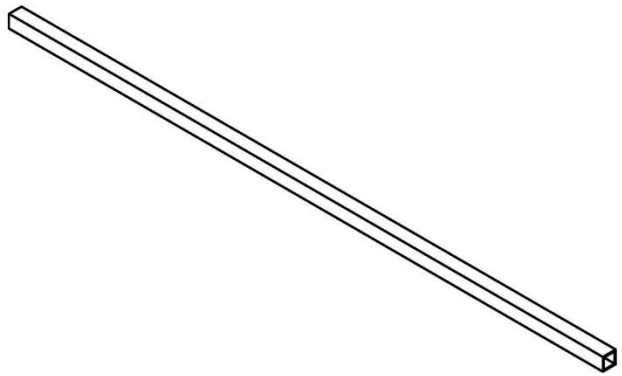

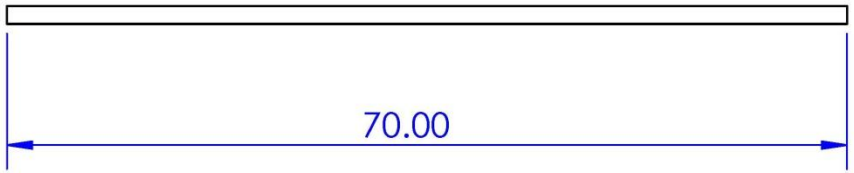

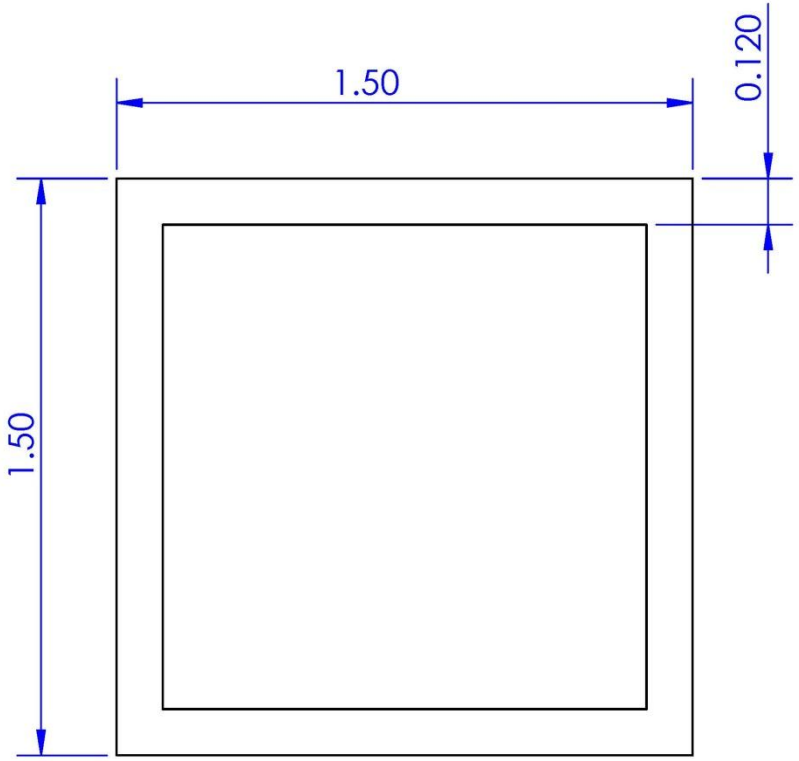

Mechanical Engineering CAL POLY	COMP NAME: LATERAL BASE MEMBER		COMP #: 19
	SCALE: 1:16	UNITS: INCHES	MATERIAL: STEEL
	DATE: 3/6/12	DRAWN BY: C. DAVIS	GROUP: TEAM ANEMOI
	OTHER: SCALE OF CROSS-SECTION IS 2:1		

5 4 3 2 1

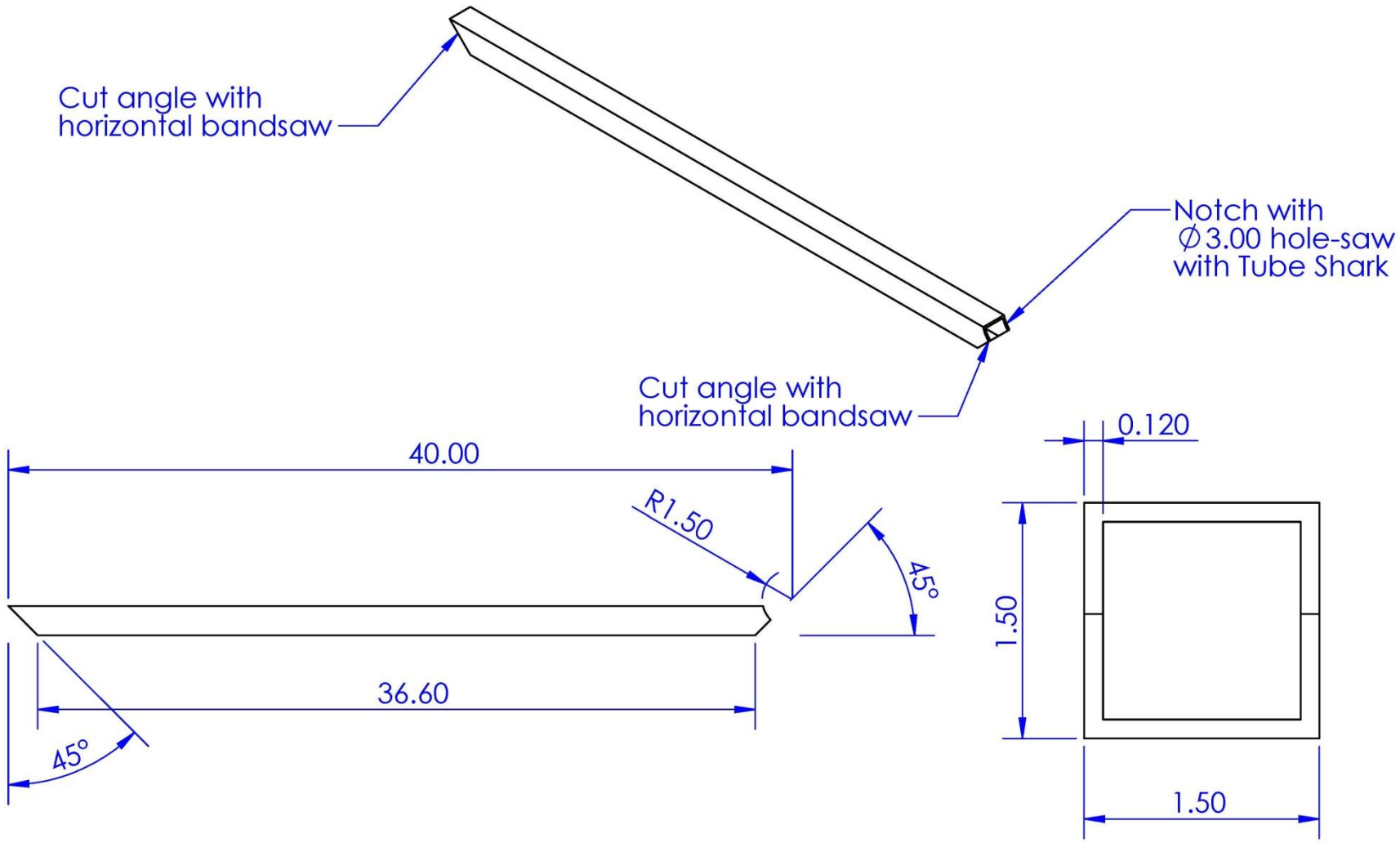

Mechanical Engineering CAL POLY	COMP NAME: A-FRAME SUPPORT		COMP #: 20
	SCALE: 1:16	UNITS: INCHES	MATERIAL: STEEL
	DATE: 3/6/12	DRAWN BY: C. DAVIS	GROUP: TEAM ANEMOI
	OTHER: CROSS-SECTION IS 1:1 SCALE		

5 4 3 2 1

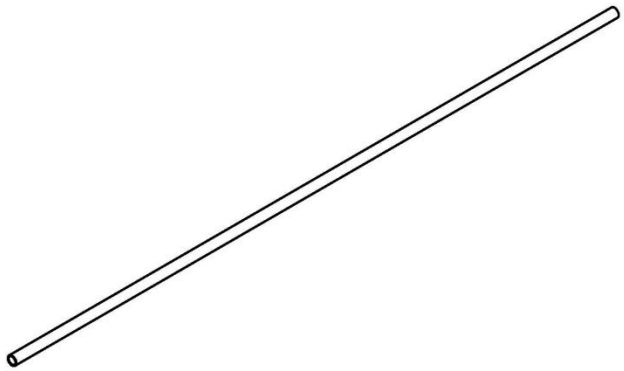

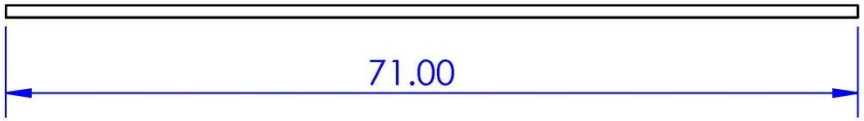

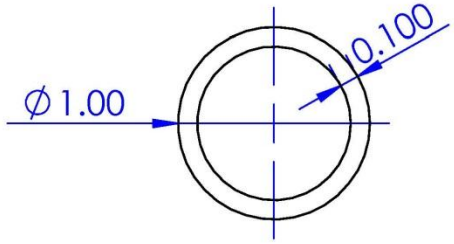

Mechanical Engineering
CAL POLY

COMP NAME: DIAGONAL BASE SUPPORT		COMP #: 21
SCALE: 1:16	UNITS: INCHES	MATERIAL: STEEL
DATE: 3/6/12	DRAWN BY: C. DAVIS	GROUP: TEAM ANEMOI
OTHER: CROSS SECTION 1:1 SCALE		

5 4 3 2 1

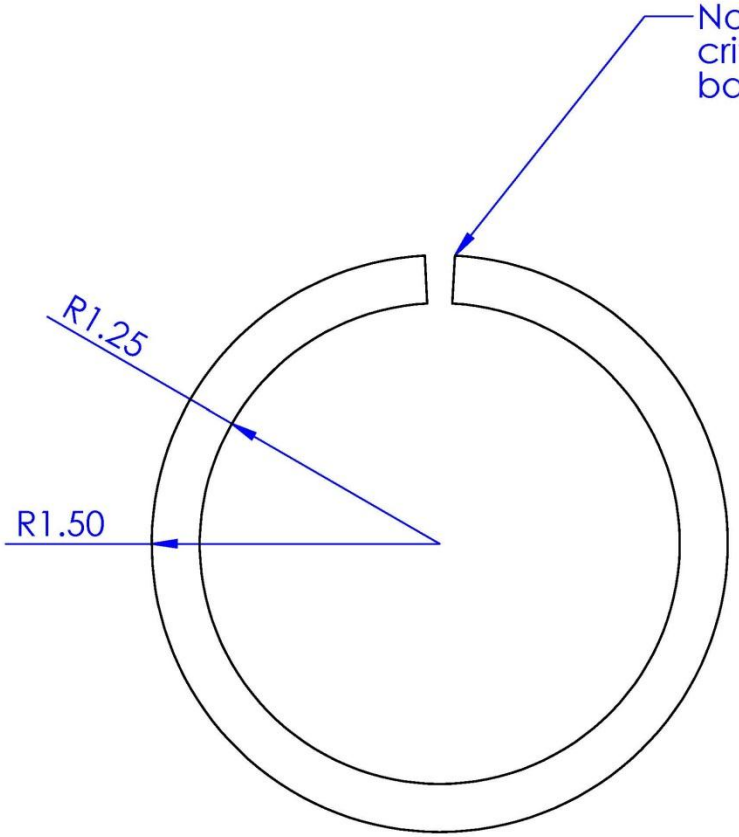

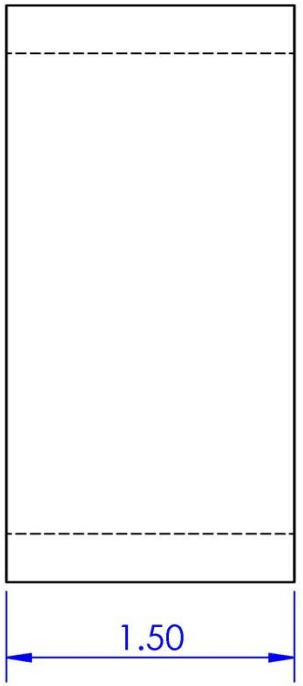

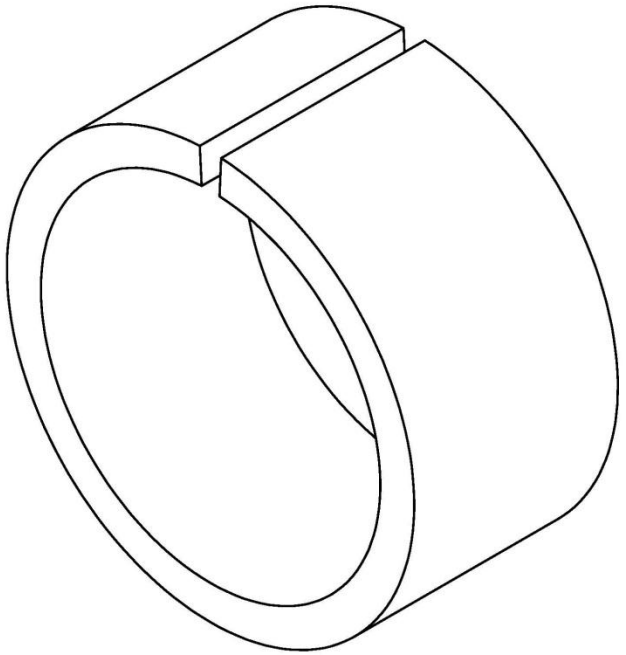

Mechanical Engineering CAL POLY	COMP NAME: TUBE CLAMP (SHORT)		COMP #: 23
	SCALE: 1:1	UNITS: INCHES	MATERIAL: STEEL
	DATE: 3/6/12	DRAWN BY: C. DAVIS	GROUP: TEAM ANEMOI
	OTHER:		

5 4 3 2 1

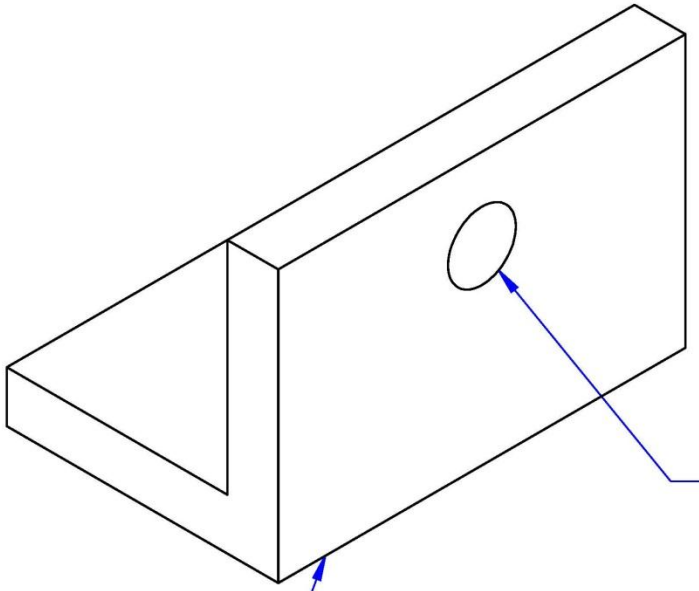

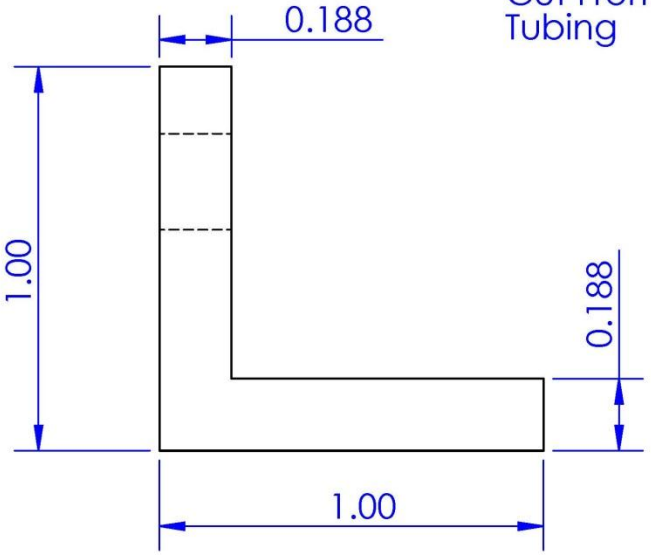

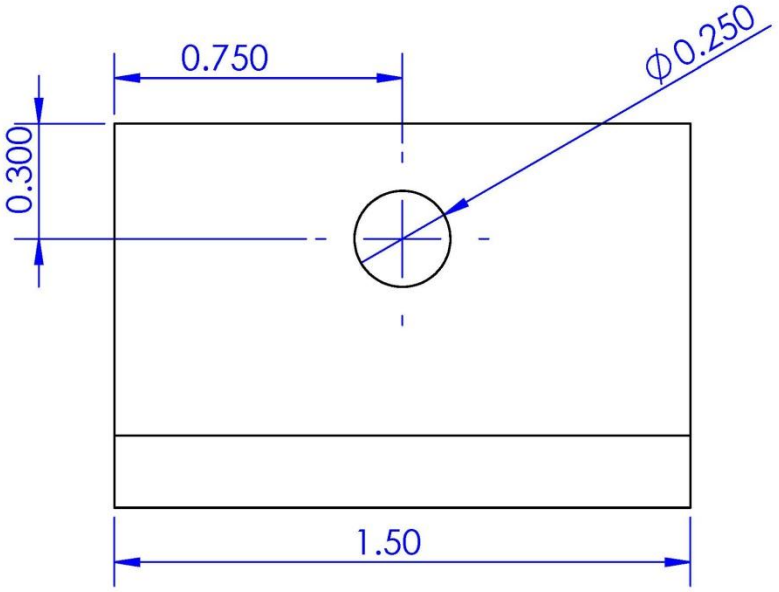

Mechanical Engineering
CAL POLY

COMP NAME: CLAMP TAB (SHORT)		COMP #: 23
SCALE: 2:1	UNITS: INCHES	MATERIAL: STEEL
DATE: 3/6/12	DRAWN BY: C. DAVIS	GROUP: TEAM ANEMOI
OTHER:		

5 4 3 2 1

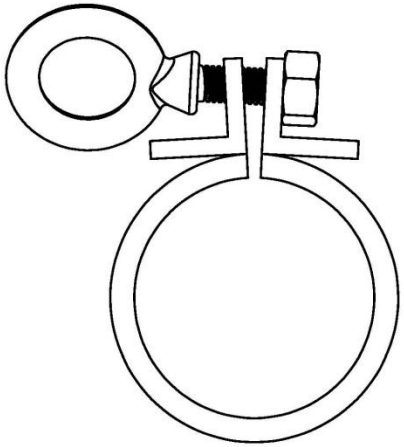

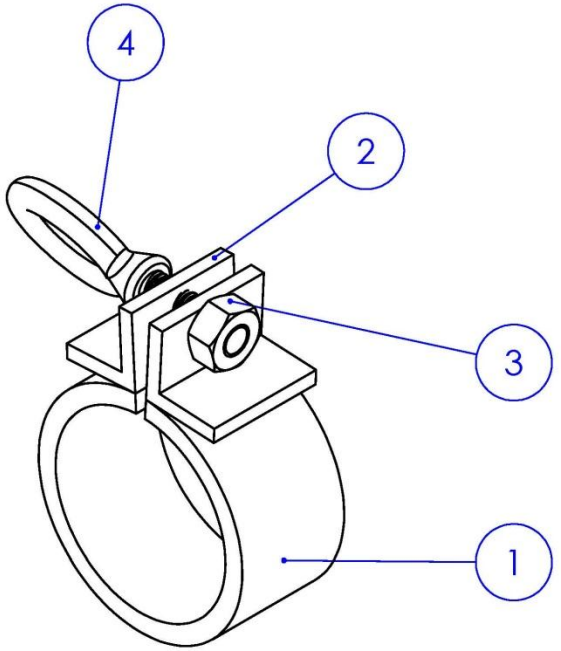

ITEM NO.	PART NUMBER	DESCRIPTION	QTY.
1	Clamp Tube Section (Short)	3"x0.25"x1.5" Steel Tube	1
2	Clamp Tab (Short)	1"x.1875"x1.5" 90 Degree Angle - Steel	2
3	95045A031		1
4	3049T72		1

Mechanical Engineering
CAL POLY

ASSEMBLY NAME: TUBE CLAMP		
SCALE: 1:2	UNITS: INCHES	MATERIAL: STEEL
DATE: 3/6/12	DRAWN BY: C. DAVIS	GROUP: TEAM ANEMOI
OTHER:		

5 4 3 2 1

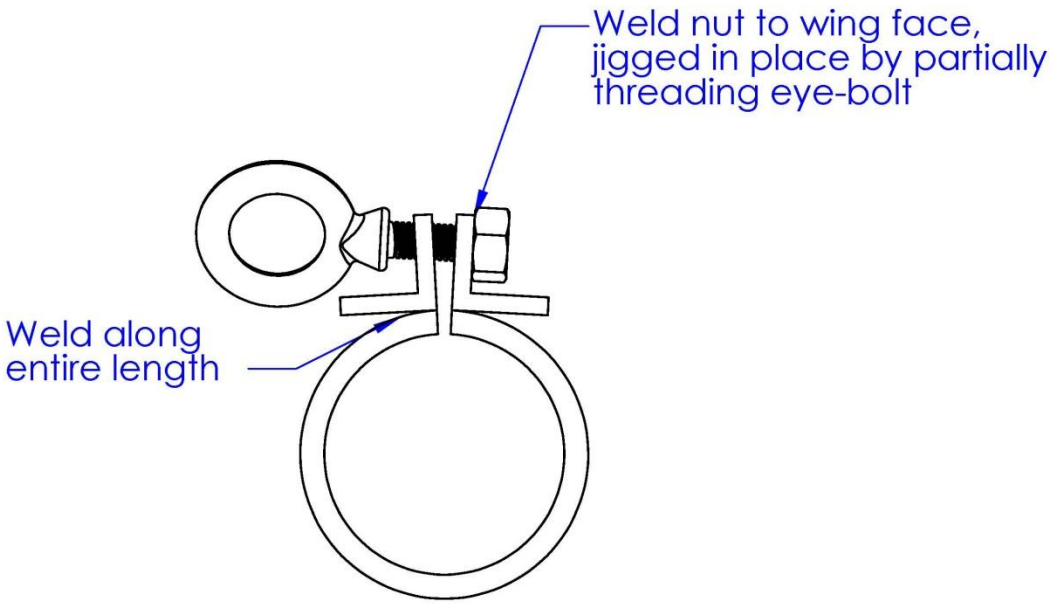

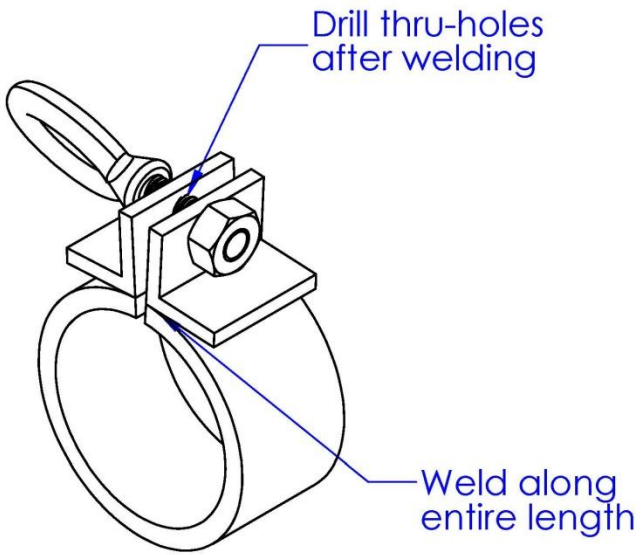

Mechanical Engineering CAL POLY

ASSEMBLY NAME: TUBE CLAMP		
SCALE: 1:2	UNITS: INCHES	MATERIAL: STEEL
DATE: 3/6/12	DRAWN BY: C. DAVIS	GROUP: TEAM ANEMOI
OTHER:		

5 4 3 2 1

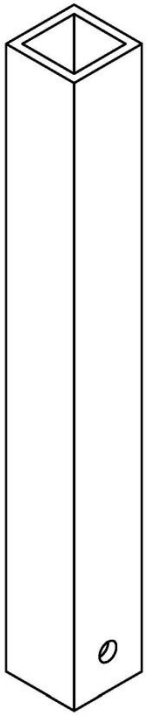

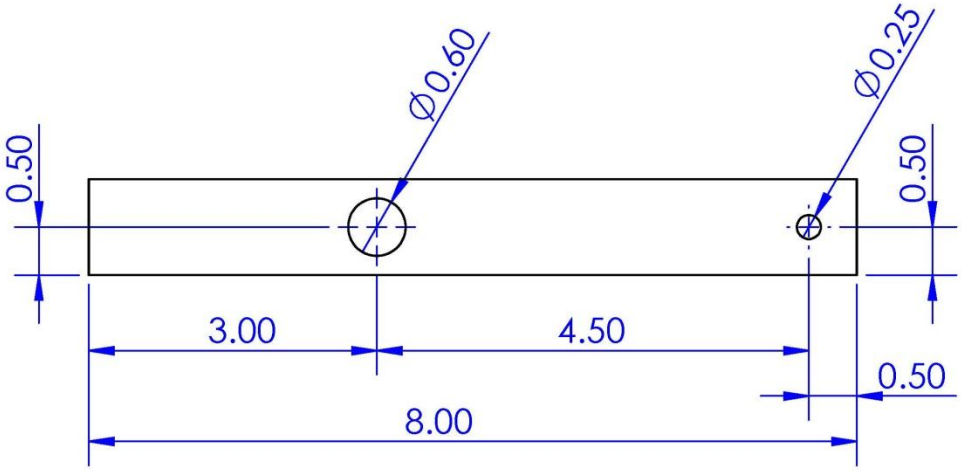

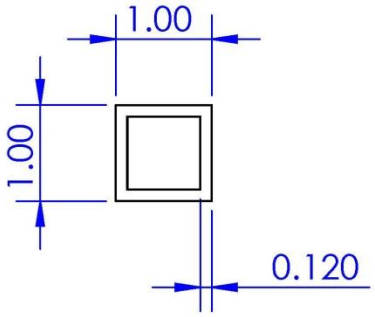

Mechanical Engineering CAL POLY

COMP NAME: REAR CLAMP TUBE		COMP #: 24
SCALE: 1:2	UNITS: INCHES	MATERIAL: STEEL
DATE: 3/6/12	DRAWN BY: C. DAVIS	GROUP: TEAM ANEMOI
OTHER:		

5 4 3 2 1

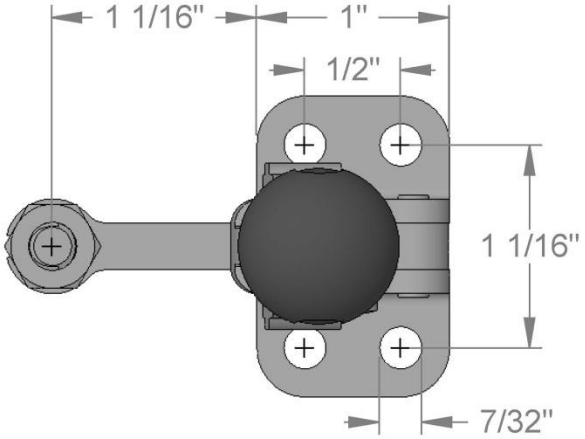

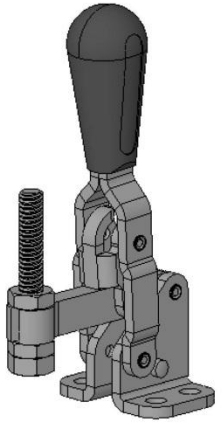

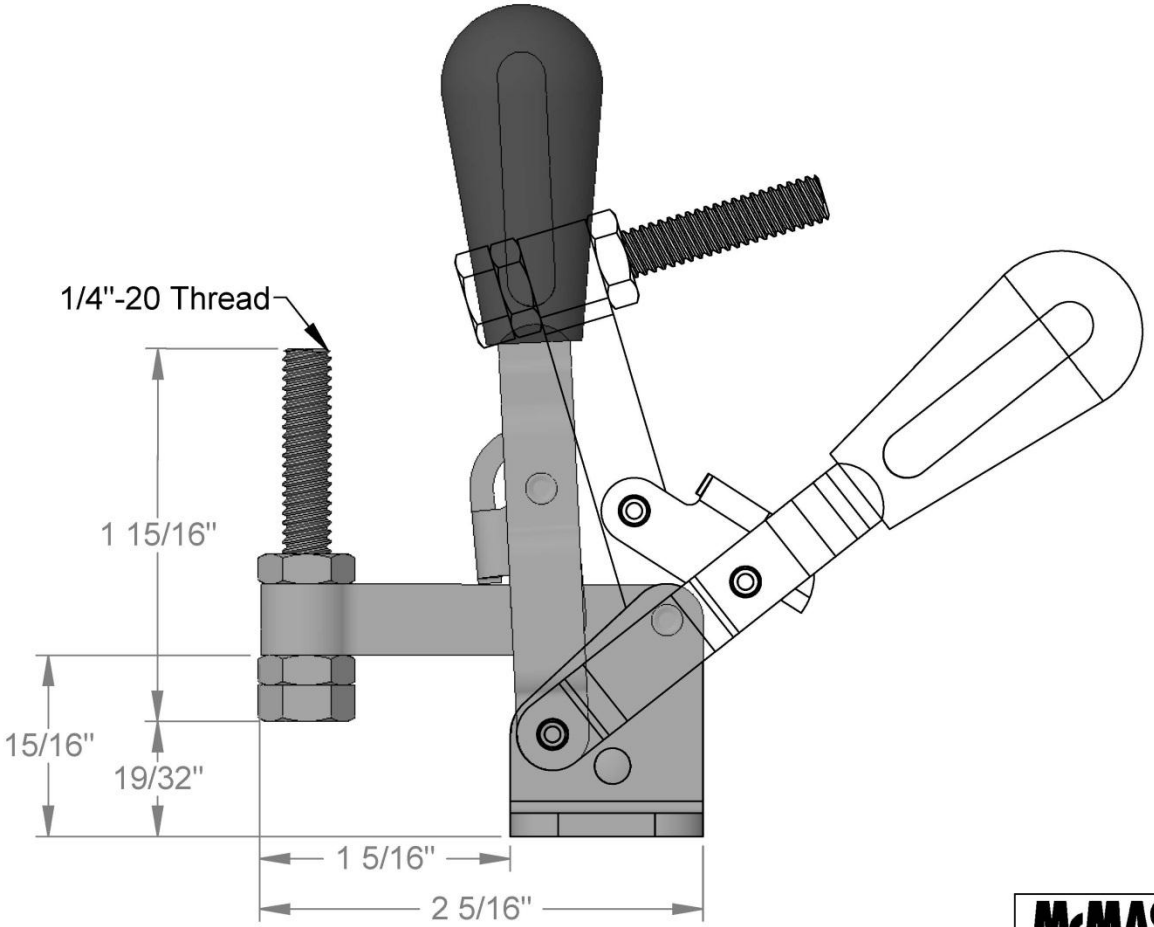

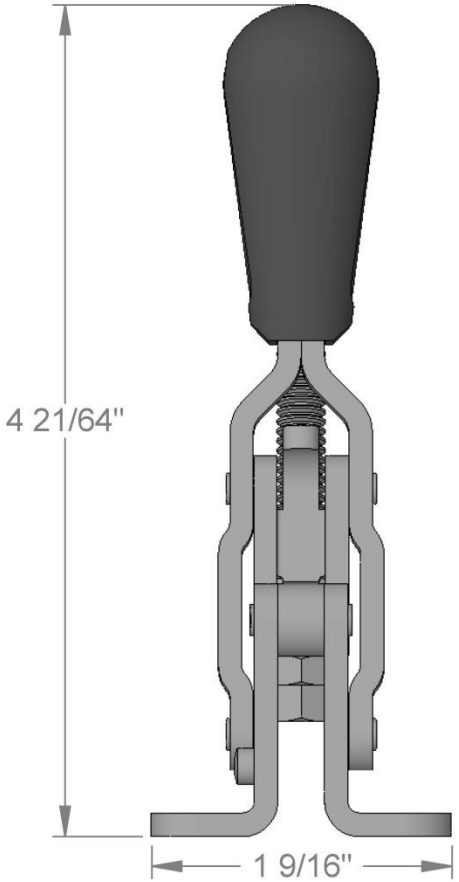

McMASTER-CARR CAD

PART NUMBER **5126A52**

http://www.mcmaster.com

Steel Vertical-Handle Hold-Down Toggle Clamp

Unless otherwise specified, dimensions are in inches. Information in this drawing is provided for reference only.

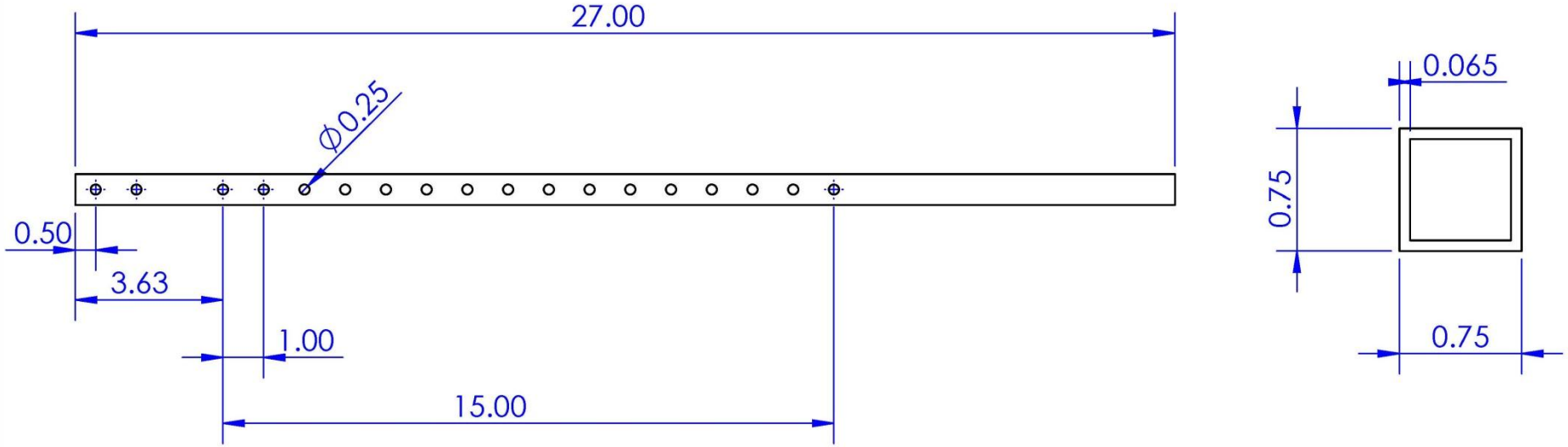

Mechanical Engineering CAL POLY	COMP NAME: REAR GUAGED SUPPORT BOTTOM		COMP #: 26
	SCALE: 1:4	UNITS: INCHES	MATERIAL: STEEL
	DATE: 3/6/12	DRAWN BY: C. DAVIS	GROUP: TEAM ANEMOI
	OTHER: CROSS SECTION 1:1 SCALE		

5 4 3 2 1

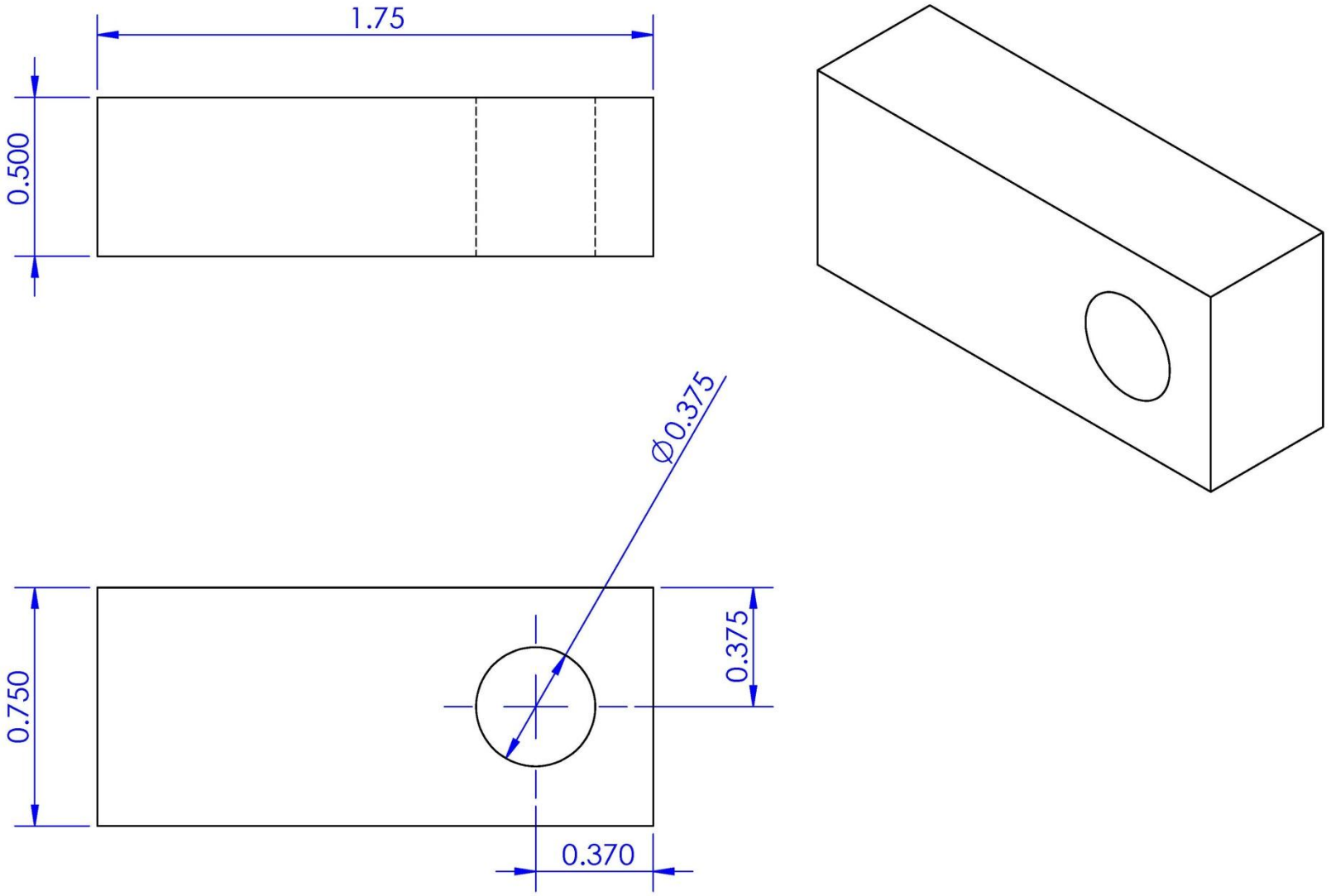

Mechanical Engineering CAL POLY	COMP NAME: BOTTOM PLATE		COMP #: 27
	SCALE: 2:1	UNITS: INCHES	MATERIAL: STEEL
	DATE: 3/6/12	DRAWN BY: C. DAVIS	GROUP: TEAM ANEMOI
	OTHER:		

5 4 3 2 1

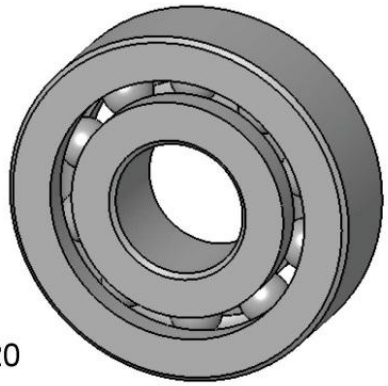

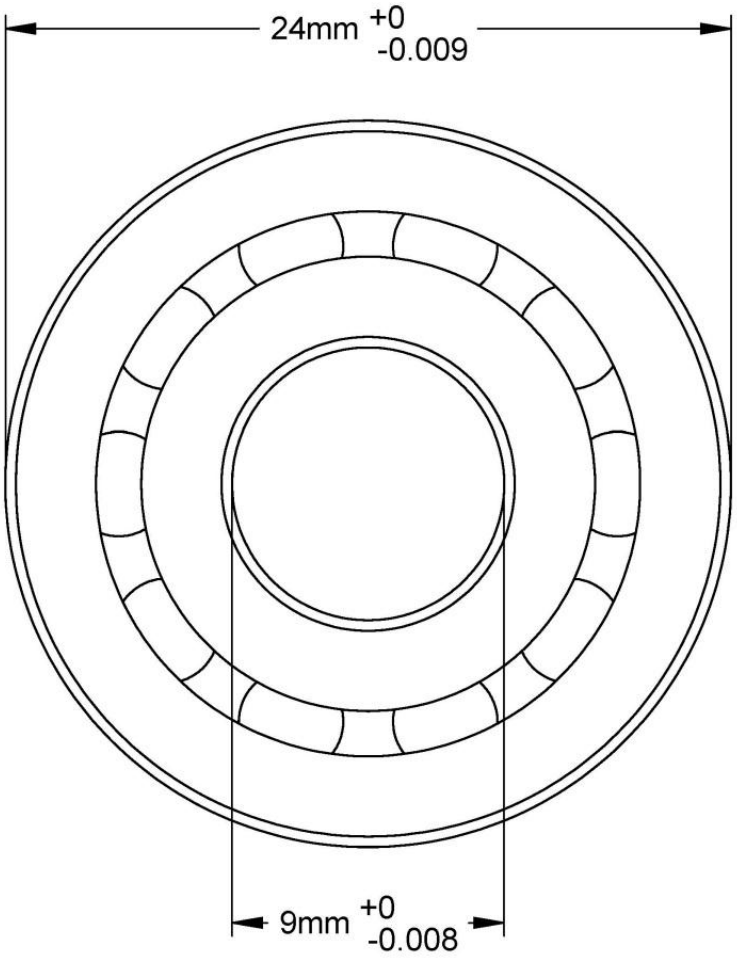

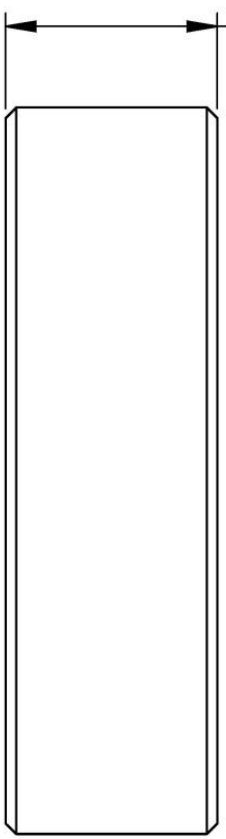

McMASTER-CARR® CAD	PART NUMBER **6153K112**
http://www.mcmaster.com 	Type 440 Stainless Steel Open Ball Bearing

Appendix G — Testing Procedures

This appendix displays all of the testing procedures we have developed for the ATP design verification investigations.

Van Aerodynamics Tuft Test

1. Strap down tuft test rig in desired location.
2. Double-check straps and ensure stability.
3. Establish route where desired speed is safe and acceptable.
4. Accelerate to speed and maintain (via careful pedal work or cruise control).
5. Film tuft behavior with cell phone camera outside of passenger window. (Note: Driver will not operate the camera; he maintains speed and course while other test engineers record video)
6. Record two to three trials of 10-30 second video of tuft behavior at van speeds of 30, 45, and 60 mph.
7. Visually reduce data screenshots using digital photo editing software.

Dropout Strength Test

1. Bolt dropout to test rig, similar to how it is applied on a bicycle.
2. Clamp test apparatus to stationary surface (such as a vise).
3. Insert fork-lengthening rod onto end of assembly
4. Load exercise weights onto rod at known distances (average length) from bolt area
5. Monitor dropout behavior and repeat as necessary

Mounting Test

1. Attach dropout pins of ATP to the dropouts of current and past HPV frames.
2. Confirm pin connection degrees of freedom are maintained
3. Check for locking or other fitting problems throughout range of wheelbases.

Dry Run Test

1. Attach dropout pins of ATP to dropouts of HPV frame.
2. Release front and rear clamps and actuate pitching jack through full range of motion.
3. Stop at intermediate increments, re-clamp roll tube, and check stability.
4. Fully secure front and rear clamps and actuate roll jack through full range of motion.
5. Stop at intermediate increments and check stability.
6. Repeat for past and current HPV frames.

Weigh Station Test

1. Install all scales (front-left, front-right, rear-left, and rear-right) into measurement electronics.
2. Arrange scales at four corners of ATP.
3. Monitor and record weight distribution and total.
4. Check results against specifications.

5. Repeat for different configurations or HPV models.

Maximum Force Test

1. Securely mount ATP and HPV on the roof of the van.
2. Affix a stiff cable to one end of a calibrated weight and ball-bearing pulley scale assembly.
3. Attach the other end of the cable to a fixed structure (such as a wall or pillar).
4. Attach a cable running from the other end of the weight and pulley assembly to the dropout attachment points on the ATP.
5. Tension the cables until they are taught (i.e. not sagging significantly under their own weight).
6. Pull on the center of the strung cable and monitor the response of the scale
7. For scale readings consistent with worst-case load, monitor response of ATP and confirm strength under these conditions

Lab Tension Test

1. Securely mount ATP on vise assembly in the lab.
2. Affix a stiff cable to one end of a calibrated weight and ball-bearing pulley scale assembly.
3. Attach the other end of the cable to a fixed structure (such as a wall or pillar).
4. Attach a cable running from the other end of the weight and pulley assembly to the dropout attachment points on the ATP.
5. Tension the cables until they are taught (i.e. not sagging significantly under their own weight).
6. Pull on the center of the strung cable and monitor the response of the scale
7. For scale readings swept through a known range (0 to 20 lbs., for example), monitor output voltage of strain gauges.
8. Correlate results with orientations and hand calculations to determine voltage-strain relationship.
9. Correlate strain to stress and subsequently lift and drag force using known material and geometric properties.

Appendix H — Schedule of Design Tasks

This appendix gives a rough schedule of the completion of design tasks over the course of this project. This page includes tasks between September and early January. The following page continues the schedule through June.

ID	WBS	Task Name	Duration	Start	Finish	Predecessors
1	**1**	**Meet team**	**6 days**	**Tue 9/27/11**	**Tue 10/4/11**	
2	1.1	Team meal	1 day	Wed 9/28/11	Wed 9/28/11	3
3	1.2	Exchange contact info	1 day	Tue 9/27/11	Tue 9/27/11	4SS
4	1.3	Team building exercises	6 days	Tue 9/27/11	Tue 10/4/11	
5	**2**	**Project proposal**	**17 days**	**Tue 9/27/11**	**Thu 10/20/11**	
6	2.1	Project proposal	0 days	Thu 10/20/11	Thu 10/20/11	
7	2.2	Perform background research	17 days	Tue 9/27/11	Wed 10/19/11	
8	**2.3**	**Develop engineering specifications**	**6 days**	**Tue 10/11/11**	**Tue 10/18/11**	
9	2.3.1	Hand calculations and estimates	6 days	Tue 10/11/11	Tue 10/18/11	
10	2.3.2	Perform QFD	5 days	Tue 10/11/11	Mon 10/17/11	
11	2.4	Develop rough schedule	2 days	Tue 10/18/11	Wed 10/19/11	
12	2.5	Develop management plan	2 days	Tue 10/18/11	Wed 10/19/11	
13	**3**	**Perform background tests/analysis**	**22 days**	**Thu 10/20/11**	**Sun 11/20/11**	
14	3.1	Van flow visualization	10 days	Tue 11/1/11	Sun 11/13/11	
15	3.2	Conceptual model	3 days	Tue 11/1/11	Thu 11/3/11	
16	3.3	Van vibration analysis	6 days	Tue 11/1/11	Tue 11/8/11	
17	3.4	Van CFD	18 days	Thu 10/20/11	Sun 11/13/11	5
18	3.5	Flat ground plane investigation	6 days	Mon 11/14/11	Sun 11/20/11	
19	**4**	**Select best design**	**22 days**	**Thu 10/20/11**	**Fri 11/18/11**	
20	4.1	Generate ideas	14 days	Thu 10/20/11	Tue 11/8/11	5
21	4.2	Evaluate ideas based on background	7 days	Fri 11/4/11	Mon 11/14/11	14SS,15,16SS,20SS
22	4.3	Narrow to < 10 good designs	7 days	Fri 11/4/11	Mon 11/14/11	21SS
23	4.4	Create decision matrix	3 days	Tue 11/15/11	Thu 11/17/11	22
24	4.5	Select best design	1 day	Fri 11/18/11	Fri 11/18/11	23
25	**5**	**Conceptual design review**	**0 days**	**Tue 11/29/11**	**Tue 11/29/11**	
26	5.1	Create initial solid model	6 days	Mon 11/21/11	Mon 11/28/11	24
27	5.2	Write conceptual design report	6 days	Mon 11/21/11	Mon 11/28/11	24
28	**6**	**Finalize design**	**30 days**	**Tue 11/29/11**	**Mon 1/9/12**	
29	6.1	Analyze/size components	30 days	Tue 11/29/11	Mon 1/9/12	24,25SS
30	6.2	Finalize solid model	30 days	Tue 11/29/11	Mon 1/9/12	29SS,26
31	6.3	Create bill of materials	30 days	Tue 11/29/11	Mon 1/9/12	30SS

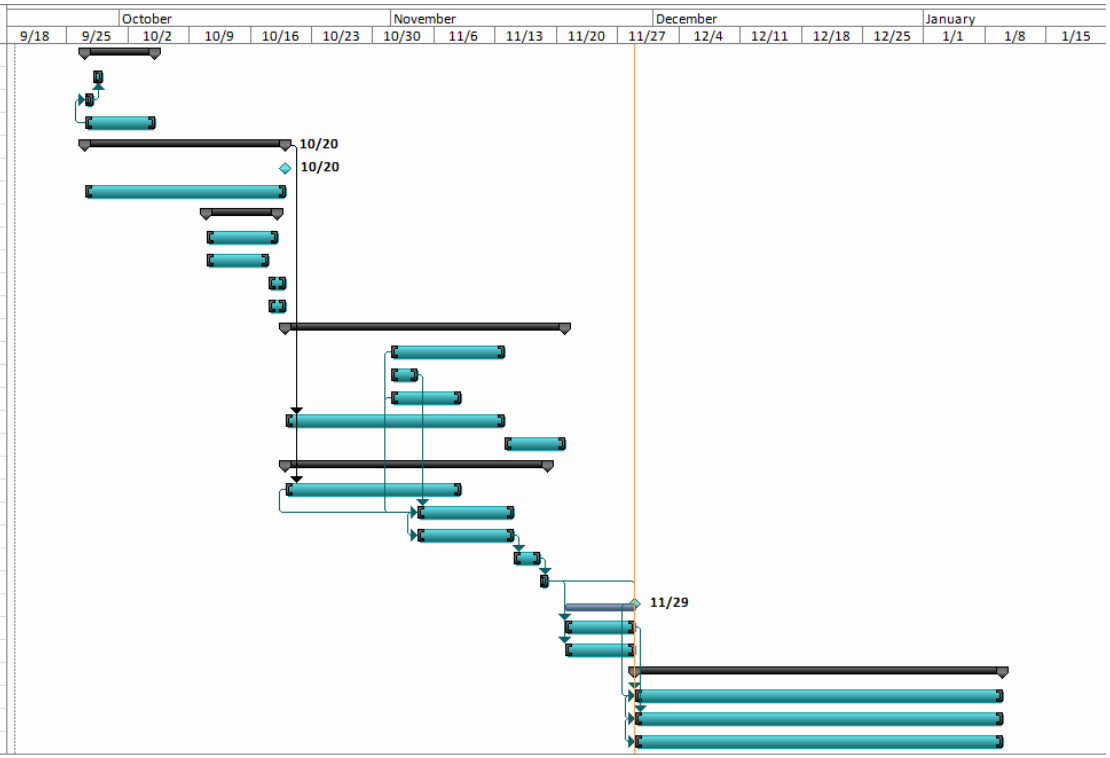

ID	WBS	Task Name	Duration	Start	Finish	Predecessors
32	7	Winter Break	18 days	Sat 12/10/11	Tue 1/3/12	
33	**8**	**Critical design review**	**0 days**	**Thu 2/2/12**	**Thu 2/2/12**	
34	8.1	Finalize design further	14 days	Wed 1/4/12	Mon 1/23/12	32
35	8.2	Write design report	7 days	Tue 1/24/12	Wed 2/1/12	34
36	**9**	**Manufacturing and test review**	**0 days**	**Tue 3/6/12**	**Tue 3/6/12**	
37	9.1	Layout manufacturing plan	10 days	Thu 2/2/12	Wed 2/15/12	33
38	**10**	**Build system**	**42 days**	**Thu 2/16/12**	**Fri 4/13/12**	
39	10.1	Order necessary parts and supplies	6 days	Thu 2/16/12	Thu 2/23/12	37
40	10.2	Machine necessary parts	13 days	Fri 2/24/12	Tue 3/13/12	39
41	**10.3**	**Assemble system**	**36 days**	**Fri 2/24/12**	**Fri 4/13/12**	
42	10.3.1	Assemble system from subsytems	9 days	Tue 4/3/12	Fri 4/13/12	43
43	10.3.2	Assmble subsystems	27 days	Fri 2/24/12	Mon 4/2/12	40SS
44	**11**	**Evaluate system**	**16 days**	**Mon 4/16/12**	**Mon 5/7/12**	
45	11.1	Safety clearance	6 days	Mon 4/16/12	Mon 4/23/12	38
46	**11.2**	**Mount HPV without van**	**3 days**	**Mon 4/16/12**	**Wed 4/18/12**	
47	11.2.1	Stability and static testing	3 days	Mon 4/16/12	Wed 4/18/12	45SS
48	11.3	Gauge calibration	3 days	Mon 4/16/12	Wed 4/18/12	38
49	11.4	Dynamic test on van	5 days	Tue 4/24/12	Mon 4/30/12	45,47
50	11.5	Evaluate and reduce data	2 days	Tue 5/1/12	Wed 5/2/12	47,49
51	11.6	Recommend design modifications	2 days	Fri 5/4/12	Mon 5/7/12	50
52	12	Project update memo	0 days	Mon 3/26/12	Mon 3/26/12	
53	**13**	**Hardware demonstration**	**0 days**	**Mon 5/7/12**	**Mon 5/7/12**	
54	13.1	Make improvements to system	4 days	Tue 5/1/12	Fri 5/4/12	49
55	13.2	Prepare system for demo	2 days	Sat 5/5/12	Sun 5/6/12	54
56	**14**	**Final report presentation**	**21 days**	**Mon 5/7/12**	**Mon 6/4/12**	
57	14.1	Write final report	21 days	Mon 5/7/12	Mon 6/4/12	53
58	14.2	Create final report presentation	18 days	Mon 5/7/12	Wed 5/30/12	57SS
59	14.3	Senior design expo	0 days	Thu 5/31/12	Thu 5/31/12